



Fachhochschule Köln  
Cologne University of Applied Sciences

# Optimization of full-scale Biogas Plants using Nonlinear Model Predictive Control

## Master Thesis

Submitted to the Cologne University of Applied Sciences  
Campus Gummersbach

by  
**André Luis Sousa Brito**

In course:

Master of Automation & IT

Supervised by:

First examiner: Prof. Dr.-Ing. Michael Bongards

Second examiner: Prof. Dr.-Ing. Frithjof Klasen

Gummersbach, March 2011

# Acknowledgement

I am very thankful to Daniel Gaida who offered me advice and immense support to successfully complete my thesis. I also would like to thank Christian Wolf for his constant support and words of encouragement.

I thank Prof. Michael Bongards for providing the environment needed to successfully complete my thesis.

I thank Aldo Javier Sedeño Marquez for the last minute help and advice.

I would like to thank all my professors at the Cologne University of Applied Sciences who contributed with their expertise to my academic and professional instruction.

Lastly, I am grateful to my mother, Alice Maria José Sousa Brito, for her constant support and her concern about every stage of my work. Thanks also to my brother, Alberto Luis Sousa Brito, who has always been my best friend and supporter.

# Table of contents

Abstract .....	v
List of figures .....	vi
List of tables .....	x
List of abbreviations .....	xii
Introduction .....	1
1. Biogas Plants.....	3
1.1 Biogas .....	3
1.1.1 Anaerobic Digestion Process.....	3
1.1.2 Biogas chemical composition.....	5
1.2 Biogas Plant.....	6
1.3 Key aspects in Biogas production.....	6
1.4 Biogas plant control and optimization.....	8
2 Nonlinear Model Predictive Control.....	9
2.1 Linear and Nonlinear Model Predictive Control .....	9
2.2 The Principle of NMPC .....	10
2.3 Mathematical Formulation of State Feedback NMPC.....	12
Problem 1 .....	13
2.4 NMPC Stability .....	13
2.5 NMPC versus MPC .....	14
3 Biogas Toolbox and NMPC implementation.....	15
3.1 Biogas Plant Modeling Toolbox .....	15
3.1.1 Genetic Algorithms .....	16
3.1.2 Particle Swarm Optimization .....	16
3.1.3 Covariance Matrix Adaptation Evolution Strategy .....	17
3.1.4 Differential Evolution.....	17
3.2 Sunderhook Biogas Plant.....	18

3.3	Simulation Model .....	19
3.4	NMPC algorithm principle and implementation .....	22
4	NMPC optimization tool for biogas plants .....	27
4.1	NMPC optimization setup .....	27
4.2	NMPC optimization GUI.....	30
4.3	NMPC algorithm for batch processes.....	37
5	Experimental Results .....	39
5.1	Simulation Scenario & Manipulated variables .....	39
5.2	First Experiment .....	41
5.2.1	Worse Results.....	45
5.2.2	Best Results .....	50
5.2.3	Comparison between Best and Worse results .....	55
5.3	Second Experiment.....	58
5.4	Third Experiment.....	62
5.5	Fourth Experiment .....	68
5.6	Fifth Experiment .....	72
5.6.1	First initial state .....	73
5.6.2	Second initial state.....	78
5.6.3	Third initial state .....	83
5.6.4	Comparison between initial states.....	86
5.7	Sixth Experiment .....	87
6	Conclusion .....	92
	Bibliography .....	94
	Appendix A .....	A-1
	Appendix B.....	B-2
	Appendix C.....	C-3
	Appendix D .....	D-4

# Abstract

Optimal control of biogas plants is an important and complex issue. This is due to the underlying highly nonlinear behavior and complex anaerobic digestion processes, which make almost impossible determining plant's operational state. One approach to address this challenge is the employment of a Nonlinear Model Predictive Control (NMPC) to optimally control the anaerobic digestion process on biogas plants. In this thesis a NMPC algorithm is developed to optimize and control a simulation model of a full-scale biogas plant using the Anaerobic Digestion Model No 1(ADM1). Experiments reveal the feasibility of this approach to optimize the operation of biogas plants and promote their use for environmentally friendly energy production. This thesis demonstrates that by means of the introduced NMPC algorithm it will be possible, in the near future, to optimize full-scale biogas plants using Nonlinear Model Predictive Control.

## List of figures

Figure 1.1: Anaerobic Digestion diagram (Wolf, 2010). ....	4
Figure 1.2: Biogas Plant scheme (Naskeo Environnement, 2009).....	6
Figure 2.1: Principle of model predictive control. ....	11
Figure 3.1: Flow chart of basic genetic algorithm iteration (Nedjah et al., 2006). ....	16
Figure 3.2: Sunderhook Biogas Plant Schematic. ....	18
Figure 3.3: Sunderhook Biogas Plant simulation model. ....	20
Figure 3.4: Sunderhook biogas plant modeling.....	20
Figure 3.5: Digester module ADM1.....	21
Figure 3.6: Basic NMPC control loop.....	22
Figure 3.7: NMPC algorithm flowchart. ....	23
Figure 3.8: NMPC algorithm simulation control overview. ....	25
Figure 4.1 : NMPC optimization tool input data.....	27
Figure 4.2: NMPC GUI. ....	30
Figure 4.3: NMPC GUI – Substrate feed amounts.....	31
Figure 4.4: NMPC GUI – Substrate feed upper and lower bounds modification. ....	31
Figure 4.5: NMPC GUI - Sludge recirculation. ....	32
Figure 4.6: NMPC GUI - NMPC parameters configuration window. ....	33
Figure 4.7: NMPC GUI – Prediction horizon setup.....	34
Figure 4.8: NMPC GUI – Control horizon setup. ....	34
Figure 4.9: NMPC GUI – Optional parameters. ....	35
Figure 4.10: NMPC algorithm command line call. ....	37
Figure 4.11: NMPC results received by e-mail.....	38
Figure 5.1: NMPC System with 4 inputs, 1 output. ....	39
Figure 5.2: NMPC algorithm simulation scenario. ....	40
Figure 5.3: Stepwise control evaluation versus fitness function values (The smaller the value (the colder the color), the better the result). ....	43
Figure 5.4: Stepwise control evaluation versus simulated control duration. The color gradient represents the simulated control duration in hours [h]. ....	44
Figure 5.5: Test n°10 (Worse) - Evolution of fitness function values against maize, manure and manure solids substrate feeds (The smaller the value (the colder the color), the better the substrate mix). ....	46
Figure 5.6: Test n°10 (Worse) - Evolution of cost benefit ratio against maize, manure and manure solids substrate feeds (The smaller the value (the colder the color), the better the substrate mix)....	47

Figure 5.7: Test n°10 (Worse) - Evolution of fitness function values against time and substrate feeds of maize and manure (The smaller the value (the colder the color), the better the substrate mix). ...	48
Figure 5.8: Test n°10 (Worse) - Evolution of cost benefit ratio against time and substrate feeds of maize and bull manure (The smaller the value (the colder the color), the better the substrate mix). 48	
Figure 5.9: Test n°10 (Worse) - Manure stepwise control and biogas production.....	49
Figure 5.10: Test n°10 (Worse) - Manure solids stepwise control and biogas production. ....	49
Figure 5.11: Test n°10 (Worse) - Maize stepwise control and biogas production. ....	50
Figure 5.12: Test n°16 (Best) - Evolution of fitness function values against maize, manure and manure solids substrate feeds (The smaller the value (the colder the color), the better the substrate mix). ..	51
Figure 5.13: Test n°16 (Best) - Evolution of cost benefit ratio against maize, manure and manure solids substrate feeds (The smaller the value (the colder the color), the better the substrate mix)...	52
Figure 5.14: Test n°16 (Best) - Evolution of fitness function values against time and substrate feeds of maize and manure (The smaller the value (the colder the color), the better the substrate mix)...52	
Figure 5.15: Test n°16 (Best) - Evolution of cost benefit ratio against time and substrate feeds of maize and manure (The smaller the value (the colder the color), the better the substrate mix). ....53	
Figure 5.16: Test n°16 (Best) - Manure stepwise control and biogas production. ....53	
Figure 5.17: Test n°16 (Best) - Manure solids stepwise control and biogas production.....54	
Figure 5.18: Test n°16 (Best) - Maize stepwise control and biogas production.....54	
Figure 5.19: Test n°16 (Best) - Evolution of fitness values against maize, manure and manure solids substrate feeds. ....55	
Figure 5.20: Test n°10 (Worse) - Evolution of fitness values against maize, manure and manure solids substrate feeds.....55	
Figure 5.21: Test n°16 (Best) - Evolution of cost benefit ratio against maize, manure and manure solids substrate feeds.....55	
Figure 5.22: Test n°10 (Worse) - Evolution of cost benefit ratio against maize, manure and manure solids substrate feeds.....55	
Figure 5.23: Test n°16 (Best) - Evolution of fitness function values against time and substrate feeds of maize and manure. ....56	
Figure 5.24: Test n°10 (Worse) - Evolution of fitness function values against time and substrate feeds of maize and manure.....56	
Figure 5.25: Test n°16 (Best) - Evolution of cost benefit ratio against time and substrate feeds of maize and manure.....56	
Figure 5.26: Test n°10 (Worse) - Evolution of cost benefit ratio against time and substrate feeds of maize and bull manure. ....56	

Figure 5.27: Test n°16 (Best) - Manure stepwise control and biogas production.....	57
Figure 5.28: Test n°10 (Worse) - Manure stepwise control and biogas production.....	57
Figure 5.29: Test n°10 (Worse) with NMPC optimization of 250 days- Maize stepwise control and biogas production.....	57
Figure 5.30: Test n°16 (Best) - Manure solids stepwise control and biogas production.....	58
Figure 5.31: Test n°10 (Worse) - Manure solids stepwise control and biogas production.....	58
Figure 5.32: Test n°16 (Best) - Maize stepwise control and biogas production.....	58
Figure 5.33: Test n°10 (Worse) - Maize stepwise control and biogas production.....	58
Figure 5.34: Overall fitness values in dependence of “optimization methods” & method configuration (“population size” and “number of generations”). The smaller the fitness value (the colder the color), the better is the result. ....	60
Figure 5.35: Simulated control duration in dependence of “optimization methods” & method configuration (“population size” and “number of generations”). The color gradient represents the simulated control duration in hours [h]. ....	61
Figure 5.36: Overall fitness values in dependence of “optimization methods”, method configuration (“population size” and “number of generations”) and simulated control duration. The color gradient represents the overall fitness values. ....	61
Figure 5.37: Stepwise control evaluation versus fitness function values and fitness trigger active (The smaller the value (the colder the color), the better the result). ....	64
Figure 5.38: Stepwise control evaluation versus simulated control duration and fitness trigger active. The color gradient represents the simulated control duration in hours [h]. ....	64
Figure 5.39: Test n°6 (Best) - Manure solids stepwise control with and without fitness trigger option (Test n°6 set n°1 and Test n°6 set n°3). ....	66
Figure 5.40: Test n°6 (Best) - Manure stepwise control with and without fitness trigger option (Test n°6 set n°1 and Test n°6 set n°3). ....	66
Figure 5.41: Test n°6 (Best) - Maize stepwise control with and without fitness trigger option (Test n°6 set n°1 and Test n°6 set n°3). ....	67
Figure 5.42: Test n°6 (Best) - Biogas production optimization with and without fitness trigger option (Test n°6 set n°1 and Test n°6 set n°3). ....	67
Figure 5.43: Manure solids control strategy & reliability assessment of NMPC optimization. ....	70
Figure 5.44: Manure control strategy & reliability assessment of NMPC optimization.....	70
Figure 5.45: Maize control strategy & reliability assessment of NMPC optimization.....	71
Figure 5.46: Biogas production & reliability assessment of NMPC optimization.....	71
Figure 5.47: Initial state n°1 - Evolution of cost benefit ratio against maize, manure and manure solids substrate feeds (The smaller the value (the colder the color), the better the substrate mix)....	74

Figure 5.48: Initial state n°1 - Evolution of cost benefit ratio against time and substrate feeds of maize and bull manure (The smaller the value (the colder the color), the better the substrate mix). 74
Figure 5.49: Initial state n°1 - Manure stepwise control and biogas production.....75
Figure 5.50: Initial state n°1 - Manure solids stepwise control and biogas production.....75
Figure 5.51: Initial state n°1 - Maize stepwise control and biogas production. ....76
Figure 5.52: Initial state n°1 - NMPC stepwise control with high step size and biogas production.77
Figure 5.53: Initial state n°1 - NMPC stepwise control with high step size and biogas production..78
Figure 5.54: Initial state n°2 – Evolution of cost benefit ratio against maize, manure and manure solids substrate feeds (The smaller the value (the colder the color), the better the substrate mix)....79
Figure 5.55: Initial state n°2 - Evolution of cost benefit ratio against time and substrate feeds of maize and bull manure (The smaller the value (the colder the color), the better the substrate mix).80
Figure 5.56: Initial state n°2 - Manure stepwise control and biogas production.....80
Figure 5.57: Initial state n°2 - Manure solids stepwise control and biogas production.....81
Figure 5.58: Initial state n°2 - Maize stepwise control and biogas production. ....81
Figure 5.59: Initial state n°2 - NMPC stepwise control with high step size and biogas production..82
Figure 5.60: Initial state n°3 - Evolution of cost benefit ratio against time and substrate feeds of maize and bull manure (The smaller the value (the colder the color), the better the substrate mix).84
Figure 5.61: Initial state n°3 - Manure solids stepwise control and biogas production.....84
Figure 5.62: Initial state n°3 - Manure stepwise control and biogas production.....85
Figure 5.63: Initial state n°3 - Maize stepwise control and biogas production. ....85
Figure 5.64: Biogas production and initial states comparison. .....86
Figure 5.65: Manure solids substrate feed “findOptimalEquilibrium” optimization and biogas production.....88
Figure 5.66: Manure substrate feed “findOptimalEquilibrium” optimization and biogas production. ....89
Figure 5.67: Maize substrate feed “findOptimalEquilibrium” optimization and biogas production.89
Figure 5.68: Test n°16 (Best) - Manure solids stepwise control and biogas production.....90
Figure 5.69: Test n°16 (Best) - Manure stepwise control and biogas production. ....90
Figure 5.70: Test n°16 (Best) - Maize stepwise control and biogas production.....91

# List of tables

Table 1.1: Biogas chemical composition for different sources of production (Naskeo Environnement, 2009).....	5
Table 1.2: Physical characteristics (Naskeo Environnement, 2009).....	5
Table 1.3: Potential of methane production per Substrate (Naskeo Environnement, 2009).....	7
Table 2.1: Types of Model Predictive Control (Jaimuokha, 2005).....	14
Table 3.1: Sunderhook Biogas Plant characteristics. ....	19
Table 5.1: NMPC optimization tool settings.....	41
Table 5.2: NMPC optimization - Substrate mixture initial state.....	42
Table 5.3: Test n°10 (Worse) - NMPC optimization tool settings. ....	45
Table 5.4: Test n°16 (Best) - NMPC optimization tool settings.....	50
Table 5.5: NMPC optimization tool settings in dependence of optimization methods.....	59
Table 5.6: NMPC optimization - Substrate mixture initial state.....	59
Table 5.7: NMPC optimization tool settings for fitness trigger option evaluation .....	63
Table 5.8: NMPC optimization & Fitness trigger evaluation - Substrate mixture initial state. ....	63
Table 5.9: Fitness error percentage [%] of NMPC optimization with fitness trigger. ....	65
Table 5.10: NMPC optimization tool settings for reliability assessment.....	68
Table 5.11: Substrate mixture initial state.....	68
Table 5.12: Reliability assessment error of NMPC optimization. ....	69
Table 5.13: Substrate mixture initial state.....	72
Table 5.14: NMPC optimization tool settings for initial states assessment. ....	72
Table 5.15: NMPC optimization with initial state n°1. ....	73
Table 5.16: NMPC optimization with initial state n°2. ....	78
Table 5.17: NMPC optimization with initial state n°3. ....	83
Table 5.18: NMPC optimization tool and findOptimalEquilibrium settings. ....	87
Table 5.19: NMPC optimization and findOptimalEquilibrium - Substrate mixture initial state. ....	88
Table A.1: Control Horizon vs. Prediction Horizon Tests, Step size: 0,01.....	A-1
Table A.2: Control Horizon vs. Prediction Horizon Tests, Step size: 0,025.....	A-1
Table A.3: Control Horizon vs. Prediction Horizon Tests, Step size: 0,05.....	A-1
Table B.1: CMAES optimization method vs. number of generations and population size. ....	B-2
Table B.2: DE optimization method vs. number of generations and population size. ....	B-2
Table B.3: PSO optimization method vs. number of generations and population size. ....	B-2
Table B.4: NMPC optimization - Substrate mixture initial state. ....	B-2

Table C.1: NMPC optimization & Fitness trigger OFF.....	C-3
Table C.2: Control NMPC optimization & Fitness trigger ON.....	C-3
Table C.3: Absolute error [%] of NMPC optimization with fitness trigger.....	C-3
Table C.4: NMPC optimization & Fitness trigger evaluation - Substrate mixture initial state. ....	C-3
Table D.1: Reliability assessment error of NMPC optimization.....	D-4
Table D.2: NMPC optimization tool settings for reliability assessment.....	D-4
Table D.3: NMPC Reliability assessment - Substrate mixture initial state.....	D-4

## List of abbreviations

AD	Anaerobic Digestion
CHP	Combined Heat and Power
CMAES	Covariance Matrix Adaptation Evolution Strategy
DE	Differential Evolution
GA	Genetic Algorithm
GECO-C	Gummersbacher Environmental Computing Center
GUIs	Graphical User Interfaces
MPC	Model Predictive Control
MS	Microsoft
NMPC	Nonlinear Model Predictive Control
PSO	Particle Swarm Optimization Toolbox
QIHNMPG	Quasi-infinite Horizon Approach to NMPC

# Introduction

Efficient energy production is nowadays the key element that drives economies and societies across the globe. This has become more evident since the last quarter of the twentieth century when the worldwide energy demand increased. This fact, in combination with the decline of oil reserves throughout the globe, brought the need for renewable energy production processes that are efficient and environmentally friendly.

For this reason, the biogas production is a feasible solution to fulfill the steadily increasing demand for electric energy and the environmental requirements. The biogas production process or anaerobic digestion is a cleaning system, which transforms biodegradable waste (e.g. biomass, manure, sewage, and municipal waste, green waste and energy crops) into a biofuel that can be used for generation of electric energy and heating. Thus, this process represents a low-cost technology that can be easily installed in a decentralized structure and provide not only treatment of organic waste but also electrical energy to remote areas.

On the other hand, biogas plants are often un-optimized processes due to a lack of interest or the absence of suitable monitoring and control systems. Usually, just biogas production, biogas composition, pH value, redox potential, total solids content and temperature sensors are available (Bastone et al., 2002). In addition, reactors in biogas plants are frequently operating under sub-optimal conditions due to variations in the organic loading composition throughout the anaerobic digestion process, which can be seasonally, monthly, weekly or daily changes (Hartmann & Ahring, 2010). Therefore, this thesis proposes a new approach to optimize and control full-scale biogas plants through the utilization of a state-of-the-art control system technique; namely, Nonlinear Model Predictive Control (NMPC).

The NMPC is a variant of the Model Predictive Control (MPC), which is an advanced control system technique that has been widely employed in process industries since 1980s, e.g., chemical plants and oil refineries.

The main concept of model predictive controllers resides in predicting the current state of the controlled system and, based on these predictions, defining the optimal set of inputs (i.e. manipulated variables) that lead the system its optimal state of operation (i.e. steady state). In addition, these predictions are performed through built-in simulation models that emulate the dynamic behavior of the process. Accordingly, the MPC is composed of a linear model of the process while NMPC consists of a nonlinear model that considers realistic plant behavior with easily incorporation of constraints (e.g. tighter environmental regulations, higher product quality,

etc.). Moreover, NMPC is usually not as fast as a MPC mainly because of its algorithm and model complexity. But, since biogas plants are very slow systems, this restriction is not important for the application in this thesis.

Ergo, in the view of the fact that efficient and green energy production are becoming a major concern due to local and global environmental degradations, NMPC has become a promising solution to produce biogas at highest efficiency while meeting environmental and economical constraints. Additionally, NMPC algorithm can be an effective technology for optimizing biogas plants that utilize broad substrate varieties (i.e. biodegradable matter inlet), given the fact that it was originally developed to control highly complex and multi-variable systems.

Hence, aiming to provide a close-loop control system that is cost-effective in optimizing full-scale biogas plants, this thesis proposes the introduction of a Nonlinear Model Predictive Control algorithm in the Anaerobic Digestion Model No. 1 (ADM1) (Bastone et al., 2002).

In addition, the NMPC algorithm's built-in simulation model consists of a fully calibrated model developed in accordance to theoretical (i.e. ADM1) and empirical observations (e.g. measurement data) of the biogas plant to be controlled.

To conclude, a NMPC algorithm is developed and evaluated in this thesis in a syntactical environment in order to assess its efficiency and reliability. This syntactical environment comprehends two simulation models that are used as the NMPC built-in simulation model (i.e. the prediction model) and the controlled system (i.e. the full-scale biogas plant). Once this NMPC algorithm has proven to be trustworthy for controlling biogas plants in a synthetic environment, the next logical step would be to implement it in the real system.

# 1. Biogas Plants

## 1.1 Biogas

Biogas is a type of biofuel that is produced by micro-organisms from the breakdown of organic matter, e.g. agricultural waste and specially cropped green mass, in the absence of oxygen. The “biogas production process” or anaerobic digestion process (AD) of biodegradable materials can be considered as a cleaning system, i.e. biodegradable waste is converted into a combustible gas that can be used in the co-generation of electricity and heating.

### 1.1.1 Anaerobic Digestion Process

Anaerobic digestion is a natural biological process in which biodegradable material is broken down by microorganisms in the absence of oxygen to produce biogas, which is a renewable energy source. AD also produces a “digestate”, which is a sub-product or residue consisting of high-quality organic compost that can be used to fertilize various kinds of plantations.

This process is carried out mainly by several types of micro-organisms (i.e. anaerobic bacteria) that execute a chain of chemical reactions (see AD diagram shown in Figure 1.1) responsible for the formation of biogas and sludge. These anaerobic bacteria are naturally occurring in nature; these bacteria are commonly found in soils and deep waters, as well as in landfill sites (Renewable Energy Association, 2009).

The AD diagram shown in Figure 1.1 illustrates the four basic steps to anaerobic digestion; they are: Hydrolysis, Acidogenesis, Acetogenesis and Methanogenesis.

### Hydrolysis

Bacterial hydrolysis first breaks down organic macromolecules into simpler elements, consequently allowing solid waste to be liquefied and hydrolyzed in small soluble molecules. Thus, the insoluble organic polymers, such as proteins, fats and carbohydrates, are converted into simpler amino acids, fatty acids and sugars that are more easily digested by other bacteria.

### Acidogenesis

The Acidogenesis process transforms simple molecules (i.e. the previously broken down molecules in the hydrolysis step) into acids of weak molecular weight. Thus, Acidogenic bacteria convert the amino acids, fatty acids and sugars into carbonic acids, alcohols, hydrogen, carbon dioxide and ammonia.

## Acetogenesis

The Acetogenesis process comprehends an additional transformation of the chemical substances before the digester is able to produce methane. Acetogenic bacteria convert the organic acids, obtained in the previous step, into acetic acid, hydrogen, and carbon dioxide.

## Methanogenesis

The Methanogenesis process is responsible for the production of methane. In this last phase the methanogenes bacteria take place converting the hydrogen, acetic acid and carbon dioxide into a mixture of methane, carbon dioxide and other trace elements (e.g. water vapor), called biogas.

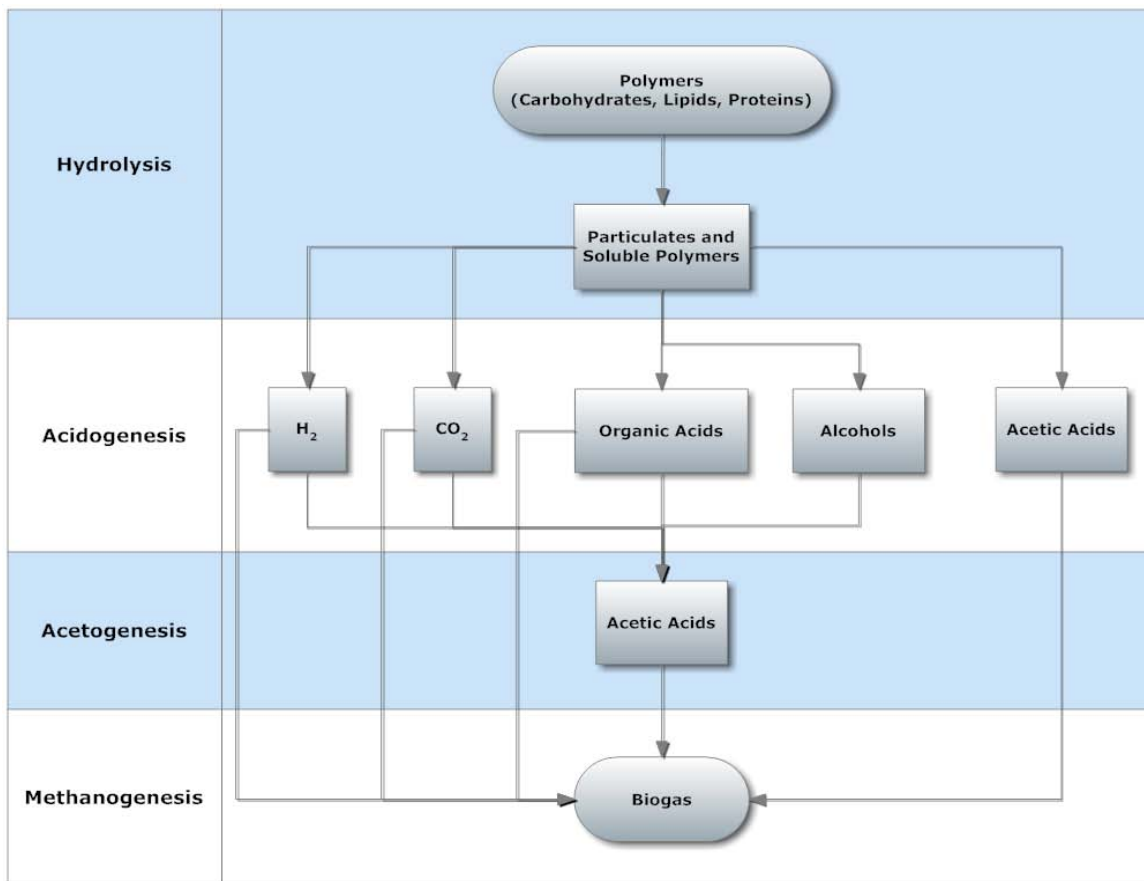


Figure 1.1: Anaerobic Digestion diagram (Wolf, 2010).

Hence, the whole anaerobic digestion process consists of a bacteria community that breaks the organic waste fed into the sealed digester (i.e. absence of oxygen) down into sugars and amino acids. These are then fermented to produce volatile fatty acids and then converted by acetogenic bacteria in to hydrogen, carbon dioxide and acetate. Finally methanogenic bacteria produce biogas, a mixture of carbon dioxide ( $CO_2$ ) and methane ( $CH_4$ ) and other trace elements.

### 1.1.2 Biogas chemical composition

The biogas composition and concentration issued by a fermenter or digester may differ concerning the substrate mixture (i.e. the type of organic matter load) and the feeding rate of the digester. Table 1.1 illustrates how the biogas chemical composition and concentration can vary according to its production process (i.e. type of substrate feed used on the plant).

**Table 1.1: Biogas chemical composition for different sources of production (Naskeo Environnement, 2009).**

Components	Formula	Household waste	Wastewater treatment plants sludge	Agricultural wastes	Waste of Agricultural food industry
Methane % vol	CH <sub>4</sub>	50-60	60-75	60-75	68
Carbon dioxide % vol	CO <sub>2</sub>	38-34	33-19	33-19	26
Nitrogen % vol	N <sub>2</sub>	5-0	1-0	1-0	-
Oxygen % vol	O <sub>2</sub>	1-0	< 0,5	< 0,5	-
Water % vol	H <sub>2</sub> O	6 (at 40 ° C)	6 (at 40 ° C)	6 (at 40 ° C)	6 (at 40 ° C)
Total % vol	-	100	100	100	100
Hydrogen sulfide mg/m <sup>3</sup>	H <sub>2</sub> S	100 - 900	1000 – 4000	3000 – 10000	400
Ammonia mg/m <sup>3</sup>	NH <sub>3</sub>	-	-	50 - 100	-

In sum, the major constituents of biogas are methane (CH<sub>4</sub>, 60 % or more by volume) and carbon dioxide (CO<sub>2</sub>, about 35 %); but small amounts of water vapor, hydrogen sulfide (H<sub>2</sub>S), carbon monoxide (CO), and nitrogen (N<sub>2</sub>) are also present. This composition of biogas varies according to the biological material as can be seen in Table 1.1.

The table below presents the comparison of different gas fuels and their physical properties. It can be seen that natural gas possesses higher concentrations of methane in comparison to other biogas production processes. However, the costs to extract such gas and the rising environmental issues in latest years concerning carbon dioxide concentrations in the atmosphere made the biogas and other renewable energy production processes economically attractive.

**Table 1.2: Physical characteristics (Naskeo Environnement, 2009).**

Types of gas	Biogas 1 Household waste	Biogas 2 Agricultural food industry	Natural gas
Composition	60 % CH <sub>4</sub>	68 % CH4	97,0 % CH <sub>4</sub>
	33 % CO <sub>2</sub>	26 % CO2	2,2 % C <sub>2</sub>
	1 % N <sub>2</sub>	1 % N2	0,3 % C <sub>3</sub>
	0 % O <sub>2</sub>	0 % O2	0,1 % C <sub>4+</sub>
	6 % H <sub>2</sub> O	5 % H2O	0,4 % N <sub>2</sub>
Density	0.93	0.85	0.57
Mass (kg/m3)	1.21	1.11	0.73

## 1.2 Biogas Plant

The construction and configuration of a biogas plant may vary depending on the amount of gas needed, the amount of waste at hand, and whether the digester is designed for batch feeding or continuous feeding. The batch feeding systems use mostly solid wastes that are added to the tank in installments, and continuous feeding models feed mostly liquids to the digester.

A biogas plant may be constructed either above or below ground. An above ground biogas plant is easier to maintain and benefits from solar heating, although its fermentation tanks should withstand the internal pressure of the digester. A below ground biogas plant is a low-cost implementation, however is more difficult to maintain (Kenney, 2010).

Figure 1.2 presents a standard biogas plant schematic that consists of a series of tanks that take different parts in the biogas production (i.e. bio-waste pre-conditioning, anaerobic digester, pasteurization, biogas storage, digestate storage, Combined Heat and Power (CHP) unit). Typically the most important part in the biogas plant is the anaerobic digester vessel, which is responsible for the breakdown of organic matter.

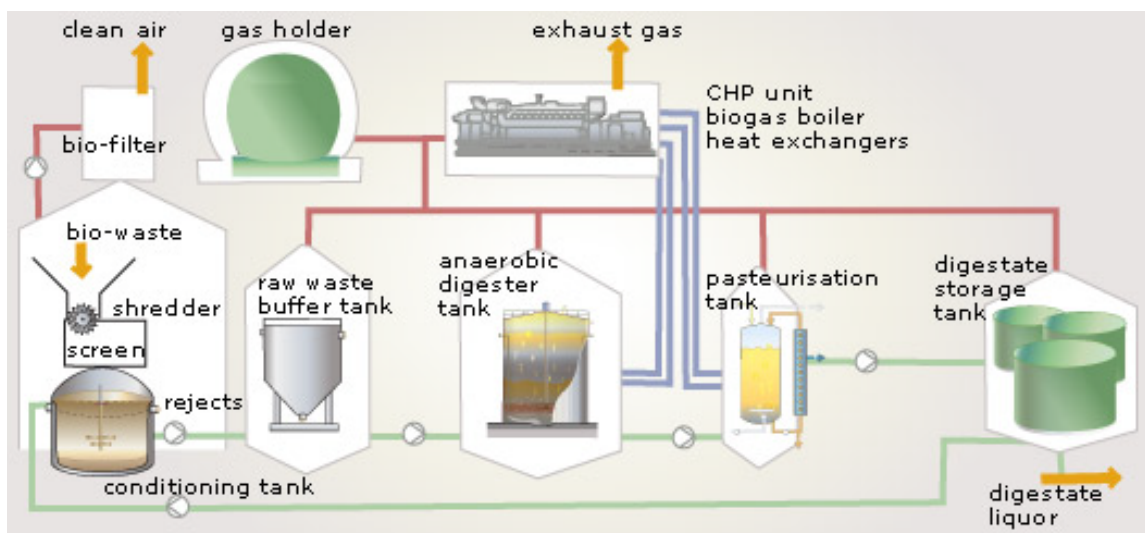


Figure 1.2: Biogas Plant scheme (Naskeo Environnement, 2009).

## 1.3 Key aspects in Biogas production

In order to obtain the optimum biogas production certain key aspects of digestion must be observed. These aspects concern the vessel's organic content, temperature, pH value and operation.

The substrate mixture fed into the digester needs to be fully mixed (i.e. bio-waste pre-conditioning) to allow a uniform fermentation of the substrates by the bacteria inside the vessel. Additionally, the type of substrate feed into the plant has also direct influence on the biogas

production, it is important that the input material is high in organic polymers. Table 1.3 illustrates the most common substrates used in biogas plants and their potential of methane production.

**Table 1.3: Potential of methane production per Substrate (Nasko Environnement, 2009).**

Liquid bovine manure	20
Contents of paunch	30
Bovine manure	40
Potato pulps	50
Brewery waste	75
Shearing of lawn	125
Maize residues	150
Lubricate from slaughter-house	180
Molasses	230
Used grease	250
Cereal waste	300

Another key factor in biogas production is the warming of the digester content that facilitates fast decomposition with optimal gas production; given that the digester's bacteria function at optimum temperature ranges in between 29°C and 41°C (Kenney, 2010).

Furthermore, the temperature is a critical asset in the anaerobic digestion; a 5 °C fluctuation in the temperature can inhibit digestion by causing the accumulation of acids resulting in digester failure. Thus, the temperature must be kept constant to allow a complete digestion (BioGeoPerm, 2008).

The pH value can also cause failure in the digester by increase of acidity; hence, the pH value must be kept in a range of 6.5 to 7.5. Movement to either side of this range quickly affects the methanogenesis metabolic rates and slows or stops methane production (Clisso, 2010).

Finally, the slurry within the tank must also be frequently stirred to prevent a hard crust from forming on top of the waste. A crust can trap the gases within the slurry and impede the machinery's ability to harness the gases. The carbon dioxide is also used in the process in an attempt to neutralize the slurry (Kenney, 2010).

Consequently, not only is it important that the input material be high in organic polymers but the vessel's temperature must be kept at a constant temperature and constant pH in order to promote maximum digestion.

The biogas turns waste into a resource, providing a biofuel that can be used instead of fossil fuels without exhausting greenhouse gases into the air, since it comes from biomass. Conversely, the methane has a global warming potential 22 times larger than that of CO<sub>2</sub>; and as a result the methane produced by waste in landfill sites could increase the global warming effects if the

biological waste were not harvest in biogas plants and therefore, preventing climate change (Kangmin & Ho, 2006). These biogas plants also contribute to safe-keeping and clean environment by preventing bad odor and contamination of the underground.

In addition, biogas plants could deliver a badly needed means of energy self-sufficiency to rural areas; where the biofuel can be used to produce electrical power, heating, oven cooking fuel and also fertilizer from the leftover of the anaerobic digestion.

Furthermore, the biogas could be used as fuel for vehicles and also to prolong storage of fruit and grain when exposed to an environment rich in methane and carbon dioxide that inhibit metabolism and kill harmful insects, mould, and bacteria that cause diseases (Kangmin & Ho, 2006).

## 1.4 Biogas plant control and optimization

In the view of the fact that biogas plants are highly complex systems, many researches have been done to optimally control such nonlinear and multi-variable system.

One approach is the employment of powerful optimization tools to find optimal and constant substrate mixtures for long-term optimal steady-state operation of full-scale biogas plants (Wolf, 2009). Although this approach yields very good results, it only implements an open loop control, in which further influences and disturbances over the anaerobic digestion process are disregarded, e.g., the variation of the process temperature throughout the control implementation. This in combination with the fact that most biogas plants are manually operated because of a lack of online-measurements and limited knowledge about the anaerobic digestion process makes it necessary to develop new optimization and control strategies.

Therefore, this thesis proposes a closed loop optimal control to consider modeling mismatch between the biogas plant model and the real plant and further disturbances. In addition, given the highly nonlinear behavior of anaerobic digestion processes and the necessity of meeting environmental constraints, this thesis proposes the introduction of Nonlinear Model Predictive Control (NMPC) into the biogas plants control and optimization challenge.

This advanced control technique has the advantage of been able to control nonlinear and multi-variable systems with easy incorporation of constraints. Additionally, its linear application the Model Predictive Control (MPC) is already largely employed in process industries since 1980s. Consequently, NMPC can be an outstanding technology for optimally control full-scale biogas plants. The next chapter introduces the NMPC technology and its mathematical formulations.

## 2 Nonlinear Model Predictive Control

### 2.1 Linear and Nonlinear Model Predictive Control

Model Predictive Control, or MPC, refers to a control system technique that utilizes state-of-the-art computer control algorithms to solve an on-line optimization problem. This optimization problem is formulated from a simulation model that emulates the behavior of the plant (i.e. controlled system) and real-time process measurements to predict the system's future response; and therefore, obtain control values for process inputs prior to any significant change in the states of plant.

Since MPC consists of an online optimization the prediction and control of the plant occurs at all times in a continuous iteration loop; for this reason MPC is also referred as “*moving horizon control*” or “*receding horizon control*”. Accordingly, at each control interval, the optimization algorithm attempts to determine the plant dynamics by computing its measurements through the simulation model and consequently define and apply a sequence of manipulated variable adjustments that optimize the future plant behavior (Maciejowski & Marian, 2002). This optimization procedure in which the system behavior is predicted according to its measurements over a certain time is known as “*prediction horizon*”. While, the time period in which the optimal control inputs are applied in the controlled system is known as “*control horizon*”.

Nevertheless, the latest sequence of control input values satisfy control specifications and constraints inherited by the plant. Once the first control input in the sequence is applied to the plant, the entire calculation is repeated at subsequent control intervals (Tricaud & Chen, 2008).

MPC technology was originally developed for advanced process control (e.g. power plants and petroleum refinery applications) due to the fact it allows an easy incorporation of constraints; which is a decisive advantage for industrial applications when compared to other methods. However, from a theoretical perspective, the major issue consists in ensuring stability for a finite horizon (Magni et al., 2009) (Kouvaritakis & Cannon, 2001).

Given this crucial benefit in the incorporation of constraints, MPC become an attractive feedback strategy for linear processes; that can be found in a wide variety of manufacturing environments including chemicals, food processing, automotive, aerospace, metallurgy and pulp and paper (Kouvaritakis & Cannon, 2001).

On the other hand, when a realistic model of the plant is considered, the nonlinearities inherent to the process cannot be avoided and the quality of linear MPC diminishes because of the incapability of the linear model to describe the process dynamics; the closed-loop system becomes

nonlinear due to the presence of constraints (Tricaud & Chen, 2008) (Findeisen & Allgöwer, 2002). Additionally, the higher product quality specifications and increasing productivity demands, tighter environmental regulations and demanding economical considerations require systems to operate over a wide range of operating conditions and often near the boundary of the admissible region; hence, a nonlinear model must be employed due to its complexity (Findeisen et al., 2003).

As a result, the Nonlinear Model Predictive Control (NMPC) was developed to take into account the influence of nonlinearities in the plant's dynamic model and for the cases in which the nonlinear behavior is of important consideration for controlling the system (e.g. biological systems such as biogas plants).

## 2.2 The Principle of NMPC

NMPC is characterized for the utilization of more realistic system models being implemented for prediction and optimization of highly nonlinear systems. This implementation increases significantly the complexity of the optimal control problem and its computational requirements; however, this is achievable nowadays due to the increase of hardware's calculation speed (Rossiter, 2004).

Figure 2.1 illustrates the basic principle behind model predictive control implementation; where measurements obtained at time  $t$  are used by the controller to predict the system's dynamic behavior (i.e. states of the system  $\bar{x}$ ) over a prediction horizon  $T_p$  in the future according to an optimal input sequence that satisfies constraints inherent to the system. Such input sequence is predetermined by optimization algorithms that try to minimize an objective function and consequently improve the open-loop performance over a control horizon ( $T_c \leq T_p$ ).

One might consider in use prediction models to solve the whole optimization problem over the infinite horizon (i.e. open-loop control problem) by applying the predicted input signals found at  $t = 0$  to the system for all  $t \geq 0$ . However, such implementation could be unsuccessful since the actual system behavior is different from the predicted one due to measurement disturbances, model-plant mismatch and the finite prediction horizon.

Therefore, in order to avoid such influences over model predictive control systems a feedback is incorporated in the finite horizon control to apply the optimal open-loop input only until the next sampling instant. In principle the sampling time or time between each new optimization can vary; although the sampling time is considered to be fixed for simplification reasons.

Thus, the optimal control problem is re-evaluated after the constant sampling time  $\delta$ ; and at time  $t + \delta$ , the whole procedure (prediction and optimization) is repeated in accordance to the

current state measurements of the system. Consequently, moving the control and prediction horizons forward based on a piecewise constant input control; with  $\frac{T_c}{\delta}$  decisions over the control horizon (Findeisen et al., 2003).

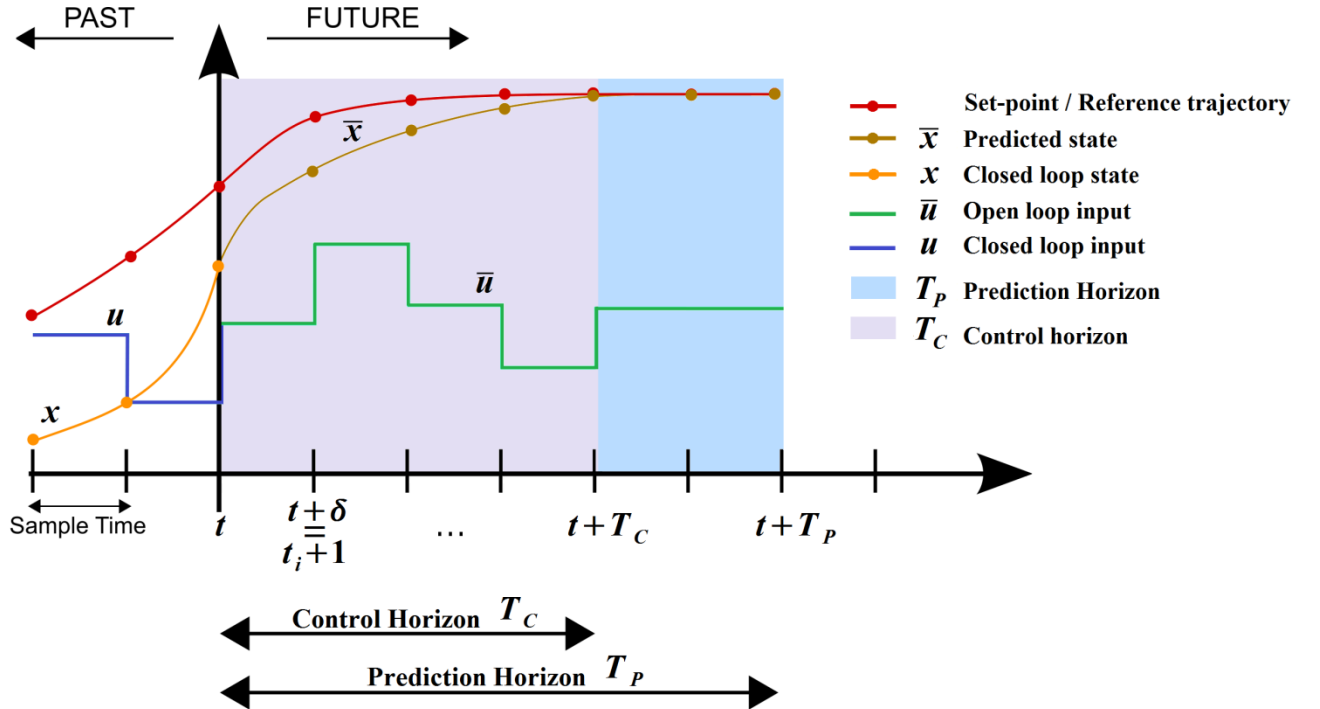


Figure 2.1: Principle of model predictive control.

Finally, founded on the figure presented above a standard NMPC scheme works as follows:

- 1) Obtain estimates of the states of the system  $x(t)$ .
- 2) Calculate a constraint-conforming optimal input  $\{\bar{u}(t), \bar{u}(t + \delta), \bar{u}(t + 2\delta), \dots, \bar{u}(t + T_p)\}$  minimizing the desired cost function  $F(\bar{x}(\tau), \bar{u}(\tau))$  over the prediction horizon  $(t + T_p)$  using the system model and the current state estimate  $x(t)$ .
- 3) Implement the first part of the optimal input until the next sampling instant  $\bar{u}(t + \delta)$ .
- 4) Continue with item 1.

To summarize, the whole NMPC optimization concerns a “*finite horizon optimal control problem*” that is subjected to more realistic system dynamics, inputs and state constraints in a nonstop online optimization loop that performs a global or local optimization of some cost function that describes the system’s encoded behavior (Sprinkle et al., 2004). The basic formulation of a NMPC problem is shown in the next section.

## 2.3 Mathematical Formulation of State Feedback NMPC

Consider the stabilization of time-invariant nonlinear systems of the form

$$\dot{\mathbf{x}}(t) = f(\mathbf{x}(t), \mathbf{u}(t)), \quad \mathbf{x}(0) = \mathbf{x}_0 \quad (1)$$

subject to input and state constraints of the form:

$$\mathbf{u}(t) \in \mathcal{U}, \quad \forall t \geq 0 \quad (2)$$

$$\mathbf{x}(t) \in \mathcal{X}, \quad \forall t \geq 0 \quad (3)$$

where  $\mathbf{x}(t) \in \mathcal{X} \subseteq \mathbb{R}^n$  and  $\mathbf{u}(t) \in \mathcal{U} \subseteq \mathbb{R}^m$  denotes the vector of states and inputs of the controlled system at time  $t$ , respectively. The set of feasible input values is denoted by  $\mathcal{U}$ ; within the maximal number of inputs  $m$  in the space  $\mathbb{R}^m$ . And, the set of feasible states is denoted by  $\mathcal{X}$ ; within the maximal number of states  $n$  in the space  $\mathbb{R}^n$ .

With respect to the vector field  $f : \mathbb{R}^n \times \mathbb{R}^m \rightarrow \mathbb{R}^n$  we assume that it is locally Lipschitz continuous<sup>1</sup> in the region of interest (i.e. the region of attraction) and satisfies  $f(0, 0) = 0$ . Hence, the system represented in equation (1) is assumed to have a unique continuous solution for any initial condition in the region of interest and any piecewise continuous and right continuous input function  $\bar{\mathbf{u}}(\cdot) : [0, T_p] \rightarrow \mathcal{U}$ . Furthermore, the set  $\mathcal{U} \subset \mathbb{R}^m$  is compact<sup>2</sup>,  $\mathcal{X} \subseteq \mathbb{R}^n$  is connected<sup>3</sup>, and  $(0, 0) \in \mathcal{X} \times \mathcal{U}$ . Typically  $\mathcal{U}$  and  $\mathcal{X}$  are (convex) box constraints of the form:

$$\mathcal{U} := \{\mathbf{u} \in \mathbb{R}^m \mid \mathbf{u}_{\min} \leq \mathbf{u} \leq \mathbf{u}_{\max}\}, \quad (4)$$

$$\mathcal{X} := \{\mathbf{x} \in \mathbb{R}^n \mid \mathbf{x}_{\min} \leq \mathbf{x} \leq \mathbf{x}_{\max}\}. \quad (5)$$

with the constant vectors  $\mathbf{u}_{\min}, \mathbf{u}_{\max} \in \mathbb{R}^m$  and  $\mathbf{x}_{\min}, \mathbf{x}_{\max} \in \mathbb{R}^n$ .

In sampled-data NMPC an open-loop optimal control problem is solved at discrete sampling instants  $t_i$  based on the current state information  $\mathbf{x}(t_i)$ . Since we consider a constant sampling time  $\delta$ , the sampling instants  $t_i$  are given by  $t_i = i \cdot \delta$ ,  $i = 0, 1, 2, \dots$ . When the time  $t$  and  $t_i$  occurs in the same setting,  $t_i$  should be taken as the closest previous sampling instant  $t_i < t$ . The predicted variables of the NMPC are denoted as internal variables in the controller by  $\bar{\mathbf{x}}$  (i.e. predicted states) and  $\bar{\mathbf{u}}$  (i.e. predicted inputs).

<sup>1</sup> A function is Lipschitz continuous if it satisfies the Lipschitz Condition for a finite constant  $k$ ; this means that the slope is never outside the range  $(-k, k)$ . In other words, the Lipschitz continuity is a smoothness condition (continuous but not differentiable everywhere).

<sup>2</sup> The compact space is a topological space that resembles a closed and bounded subset of Euclidean space  $\mathbb{R}^n$ , which is “small” in a certain sense and “contains” all its limit points (i.e. compact set).

<sup>3</sup> The connected space is a topological space which cannot be written as the disjoint union of two or more nonempty open spaces.

Hence, the finite horizon open-loop optimal control problem described above is mathematically formulated as follows:

**Problem 1 Find**

$$\min_{\bar{u}(\cdot)} J(x(t), \bar{u}(\cdot); T_c, T_p) \quad (6)$$

with

$$J(x(t), \bar{u}(\cdot); T_c, T_p) := \int_t^{t+T_p} F(\bar{x}(\tau), \bar{u}(\tau)) d\tau \quad (7)$$

subject to:

$$\dot{\bar{x}}(\tau) = f(\bar{x}(\tau), \bar{u}(\tau)), \bar{x}(t) = x(t) \quad (8)$$

$$\bar{u}(\tau) \in \mathcal{U}, \forall \tau \in [t, t + T_c] \quad (9)$$

$$\bar{u}(\tau) = \bar{u}(t + T_c), \forall \tau \in [t + T_c, t + T_p] \quad (10)$$

$$\bar{x}(\tau) \in \mathcal{X}, \forall \tau \in [t, t + T_p] \quad (11)$$

where  $T_p$  and  $T_c$  are the prediction and the control horizon with  $T_c \leq T_p$ .

The predicted state solution  $\bar{x}(\cdot)$ , equation (8), is given by the input  $\bar{u}(\cdot): [0, T_p] \rightarrow \mathcal{U}$  and the initial condition  $x(t)$ . Thus, the NMPC formulation takes into account the actual state of the system to determine its future state.

The predicted values  $\bar{x}(\cdot)$  are often not the same as the actual closed-loop values (i.e. the real system behavior) since the prediction is a nominal undisturbed case; however this drawback is corrected by the NMPC algorithm that recalculates the optimal input  $\bar{u}(\cdot)$  over a moving finite horizon at every sampling instance. Furthermore, equation (10) implies that beyond the control horizon the predicted input  $\bar{u}(\cdot)$  is constant and is equivalent to the last step of the control horizon.

## 2.4 NMPC Stability

The finite horizon NMPC strategy could lead to issues in stability and robustness; since the predicted open-loop and its resulting closed-loop behavior are in general different.

Such differences induce uncertainties in the NMPC controller performance what can affect its robust stability, sensitivity to plant-model mismatch, and the ability to handle disturbances from process data.

Ideally, the robustness and stability of NMPC algorithms could be achieved with algorithms including the terminal state constraints or infinite prediction horizon; which is required by control theory for nominal stability. However, these algorithms are not currently available or they cannot be easily applied in practical solutions (Kouvaritakis & Cannon, 2001).

Accordingly, NMPC algorithms with closed-loop stability rely on the infinite horizon approximation scheme; where the prediction horizon is set long enough to effectively approximate an infinite horizon (e.g. quasi-infinite horizon approach to NMPC or QIHNMPC). Such approach can achieve guaranteed closed loop stability while being computationally feasible (Kouvaritakis & Cannon, 2001).

A NMPC strategy that achieves closed-loop stability independent of the choice of the performance parameters is usually referred to a NMPC approach with guaranteed stability (Findeisen & Allgöwer, 2002).

## 2.5 NMPC versus MPC

In general, the Linear MPC refers to a family of MPC schemes in which linear models are used to predict the system dynamics and considers linear constraints on the states and inputs and a quadratic cost function; while, the NMPC refers to MPC schemes that are based on nonlinear models and/or consider non-quadratic cost-functional and general nonlinear constraints on the states and inputs (Findeisen et al., 2003). The Table 2.1 presents the main differences between the Linear MPC and the Nonlinear MPC.

**Table 2.1: Types of Model Predictive Control (Jaimuokha, 2005).**

Characteristics	Linear MPC	Nonlinear MPC
Modeling	Linear Model: $\dot{\mathbf{x}} = \mathbf{A}\mathbf{x} + \mathbf{B}\mathbf{u}$	Nonlinear Model $\dot{\mathbf{x}} = \mathbf{f}(\mathbf{x}, \mathbf{u})$
Formulation	Quadratic cost function: $\mathbf{F} = \mathbf{x}^T \mathbf{Q} \mathbf{x} + \mathbf{u}^T \mathbf{R} \mathbf{u}$	Cost function can be non-quadratic: $\mathbf{F}(\mathbf{x}, \mathbf{u})$
Constraints	Linear constraints: $\mathbf{Hx} + \mathbf{Gu} < 0$	Nonlinear constraints: $\mathbf{h}(\mathbf{x}, \mathbf{u}) < 0$
Programming	Quadratic program	Nonlinear program

### 3 Biogas Toolbox and NMPC implementation

This chapter provides an overview of the “Biogas Plant Modeling Toolbox” developed in MATLAB/Simulink by the Gummersbacher Environmental Computing Center GECOC in cooperation with the PlanET Biogastechnik GmbH. Followed by a succinct insight of the Sunderhook biogas plant, object of study in this thesis, and the subsequent description of its simulation model. Moreover, this chapter will introduce the Nonlinear Model Predictive Control implementation for biogas plants, establishing a link between the theoretical and practical implementation for the optimization of full-scale biogas plants.

#### 3.1 Biogas Plant Modeling Toolbox

As mentioned before, the “Biogas Plant Modeling Toolbox” consists of a toolbox developed for the MATLAB/Simulink simulation environment in a research project developed by the Gummersbacher Environmental Computing Center GECO-C in cooperation with PlanET Biogastechnik GmbH.

The purpose of this toolbox is to provide well-structured and reliable algorithms for modeling, simulation, optimization and control of biogas plants. The Biogas Plant Modeling Toolbox allows the uncomplicated modeling of different biogas plants configurations with the specification of its detailed physical and chemical characteristics through graphical user interfaces (GUIs). Therefore, simulation models can be easily created by adding modules that can be fully configured in accordance to real systems; these modules concern digesters, cogeneration units, pumps, heating systems, sensors (i.e. data export) and energy analysis.

Consequently, this toolbox can be used to improve biogas production and define new control strategies by means of simulating various scenarios of study (i.e. fully calibrated models) with different optimization algorithms through the evaluation of inlet rates of substrates fed into the digesters and the type of substrates used.

Thus, the “Biogas Plant Modeling Toolbox” provides a generic optimization scheme to easily apply and adapt various optimization algorithms. The optimization algorithms utilized in this thesis are described in the following sections.

### 3.1.1 Genetic Algorithms

The genetic algorithm (GA) optimization tool is part of MATLAB's Genetic Algorithm and Direct Toolbox. This toolbox provides methods that search for global solutions to solve multiple maxima, multiple minima, and nonsmooth optimization problems.

Genetic algorithms (GAs) are heuristic global search and optimization methods that are based in solvers mimicking the principles of biological evolution. In essence, the algorithm reproduces the survival of the fittest to produce successively better approximations to a solution in a repetitive iteration loop (i.e. each iteration is known as a generation); and at each iteration, a new set of approximations is created by the process of selecting individuals (i.e. populations) according to their level of fitness and reproducing them using operators borrowed from natural genetics (e.g. inheritance, mutation, selection, and crossover.). Genetic algorithm also improves the likelihood of finding a global solution due to its random nature (Chipperfield & Fleming, 1995) (MathWorks, 2011). In Figure 3.1 a typical flowchart of a Genetic Algorithm (GA) is presented.

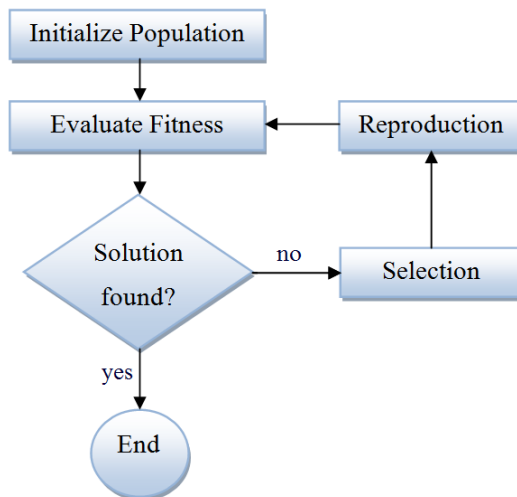


Figure 3.1: Flow chart of basic genetic algorithm iteration (Nedjah et al., 2006).

### 3.1.2 Particle Swarm Optimization

The Particle Swarm Optimization Toolbox (PSO) utilized in this thesis was developed by Brian Birge for MATLAB's computational environment (Birge, 2006); based in the PSO stochastic optimization method proposed by Dr. Eberhart and Dr. Kennedy in 1995.

The general purpose of this optimization method is to maintain a swarm of particles that move around in a search-space influenced by the improvements discovered by the other particles according a fitness function (Pedersen, 2010). Each individual in this particle swarm is defined by n-dimensional vectors containing its position  $\mathbf{p}_i$ , the previous best position  $\mathbf{p}_{best,i}$ , and the velocity  $\mathbf{v}_i$ . Thus, the PSO algorithm utilizes the information of each individual current and best

location in combination to the best positions of other members in the particle swarm to eventually get closer to an optimum of the fitness function (Poli et al., 2007).

The advantage of this optimization method is that it does not require the gradient of the problem to be optimized. Therefore, PSO can be readily employed for a wide range of application such as Communication Networks, Control Systems, Engines and Motors design, Prediction and forecasting, Power systems and plants, Robotics, Financial, etc (Poli, 2007).

### 3.1.3 Covariance Matrix Adaptation Evolution Strategy

The Covariance Matrix Adaptation Evolution Strategy (CMAES) toolbox utilized in this thesis was developed by Nikolaus Hansen for MATLAB's computational environment (Hansen, 2007).

The CMAES optimization method belongs to the evolutionary strategy (ES) class of algorithms. This optimization method is based in employing the full covariance matrix<sup>4</sup> of a normal search distribution to the given objective function; such implementation allows the evaluation of pairwise dependencies between the variables described by this matrix inside an EA distribution (Auger & Hansen, 2005) (Hansen et al., 2009).

CMAES is characterized for being a non-elitist, continuous domain evolutionary algorithm based in the ranking between candidate solutions; which is responsible for the sample distribution learning. Therefore, CMAES brings additional robustness in a noisy environment given that neither derivatives nor function values are necessary for the method. Furthermore, CMAES functions independently of the specified population size; this allows fast adaptation for online optimization applications since the population size is small by default (Hansen et al., 2009).

### 3.1.4 Differential Evolution

The Differential Evolution (DE) toolbox utilized in this thesis was developed by Kenneth Price and Rainer Storn for MATLAB's computational environment (Price & Storn, 2005).

The Differential Evolution (DE) optimization method is another evolutionary strategy (ES) algorithms; which is based in optimizing a problem without using its gradient (i.e. DE does not require for the optimization problem to be differentiable). The main principle of this method is to optimize a problem by iteratively exploring the search space to improve a candidate solution with regard to given real-valued parameters and very large sets of candidate solutions (Pedersen, 2010) (Jia et al., 2010).

<sup>4</sup> A Covariance matrix is a matrix that describes the pairwise dependencies between variables inside vectors; therefore, the element  $M_{ij}$  of this matrix is the covariance (i.e. a measure of how much two variables change together) between the  $i^{th}$  and  $j^{th}$  elements of a vector.

The advantages of DE are its simple structure, ease of use, speed, robustness and capacity to explore the search space to locate the region of global minimum; however, it is slow at the exploitation of the solutions. Some applications of this method are: data mining, neural network training, pattern recognition, digital filter design, etc (Jia et al., 2010).

## 3.2 Sunderhook Biogas Plant

The Sunderhook biogas plant, object of study in this thesis, is a plant localized at the address: Sunderhook 8, 48599 Gronau (North Rhine-Westphalia), Germany. A schematic of the Sunderhook biogas plant is provided in Figure 3.2. In addition, the main characteristics (e.g. types of substrates, electrical power and gas production) of the Sunderhook biogas plant are shown in

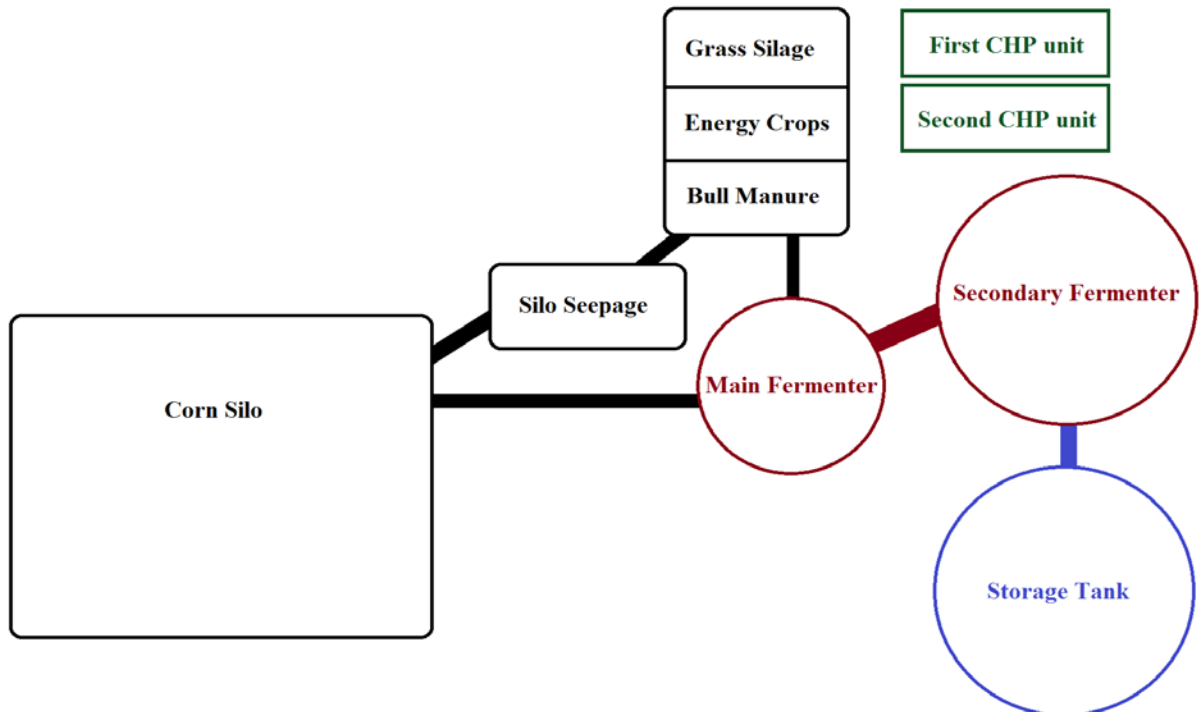


Figure 3.2: Sunderhook Biogas Plant Schematic.

The plant shown in Figure 3.2 comprises two fermenters (i.e. Main fermenter and Secondary fermenter), a storage tank, two CHP units and five storage silos containing each type of substrate used. Every structure shown in this scheme represents its size accordingly to their size in relation to the other structures at the real plant; however the picture is not presented in real-scale. In addition, the main fermenter is smaller in relation to the secondary fermenter only regarding to its diameter; the main fermenter is higher in height. The substrate silos are different in consequence to their quantitative utilization in the fermentation process; therefore, the maize silo is bigger in relation to the others.

**Table 3.1: Sunderhook Biogas Plant characteristics.**

Properties	Sunderhook Biogas Plant
Used substrates	Maize Grass silage Silo seepage Energy crops Manure
Fermenter volume	Main fermenter: 3180 m <sup>3</sup> Secondary fermenter: 3180 m <sup>3</sup>
Electric power	750 kW
Location	Gronau-Epe (NRW - Germany)

The whole gas production process in this plant is done with a WinCC-based control system; where the process variables measurements (e.g. methane concentration CH<sub>4</sub> [%]) are recorded in MS Access database and provided through online remote access. These measurements are used not only for controlling biogas production but also for its further optimization.

The measured process variables are: gas volume; gas composition (e.g. CH<sub>4</sub> [%], H<sub>2</sub> [ppm], H<sub>2</sub>S [ppm] and O<sub>2</sub> [%]); temperature of the main and secondary fermenters; the gas temperatures at the inlet, after the scrubber and after re-heater; the amount of electricity produced by the two CHP units; overall power consumption of the system; pH values, dry matter concentrations and the operational work time of pumps and transport equipments (e.g. transport of substrates and digestate discard). These measurements are taken in the time stamps of two hours since the whole digestion process is a very slow system (MOBIO final report, 2010).

Furthermore, these process measurements are of great importance to simulate, calibrate and validate the Sunderhook simulation model; and also, define new control strategies for the production process. The next section presents the Sunderhook Biogas Plant Simulation Model.

### 3.3 Simulation Model

This section will present a brief introduction to the Sunderhook Biogas Plant Model shown in Figure 3.3; which was modeled with the “Biogas Plant Modeling Toolbox” in MATLAB/Simulink simulation environment.

The simulation model presented in Figure 3.3 is an abstraction of the real biogas production process that occurs at the Sunderhook plant; this model was developed in accordance to the plant’s structure (i.e. Figure 3.2).

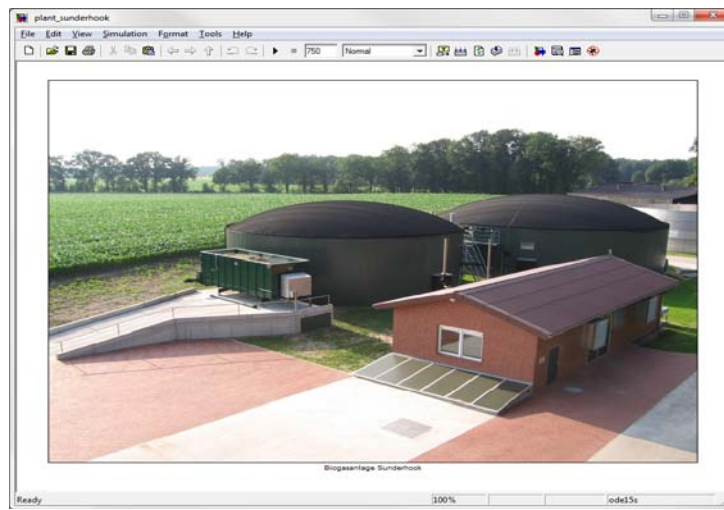


Figure 3.3: Sunderhook Biogas Plant simulation model.

Moreover, this simulation model basically consists of separate units that take charge in different parts of the biogas production process; such as: substrate inlet, anaerobic digestion, pumping, heating systems, energy production, sensors and energy analysis (e.g. see Figure 3.4).

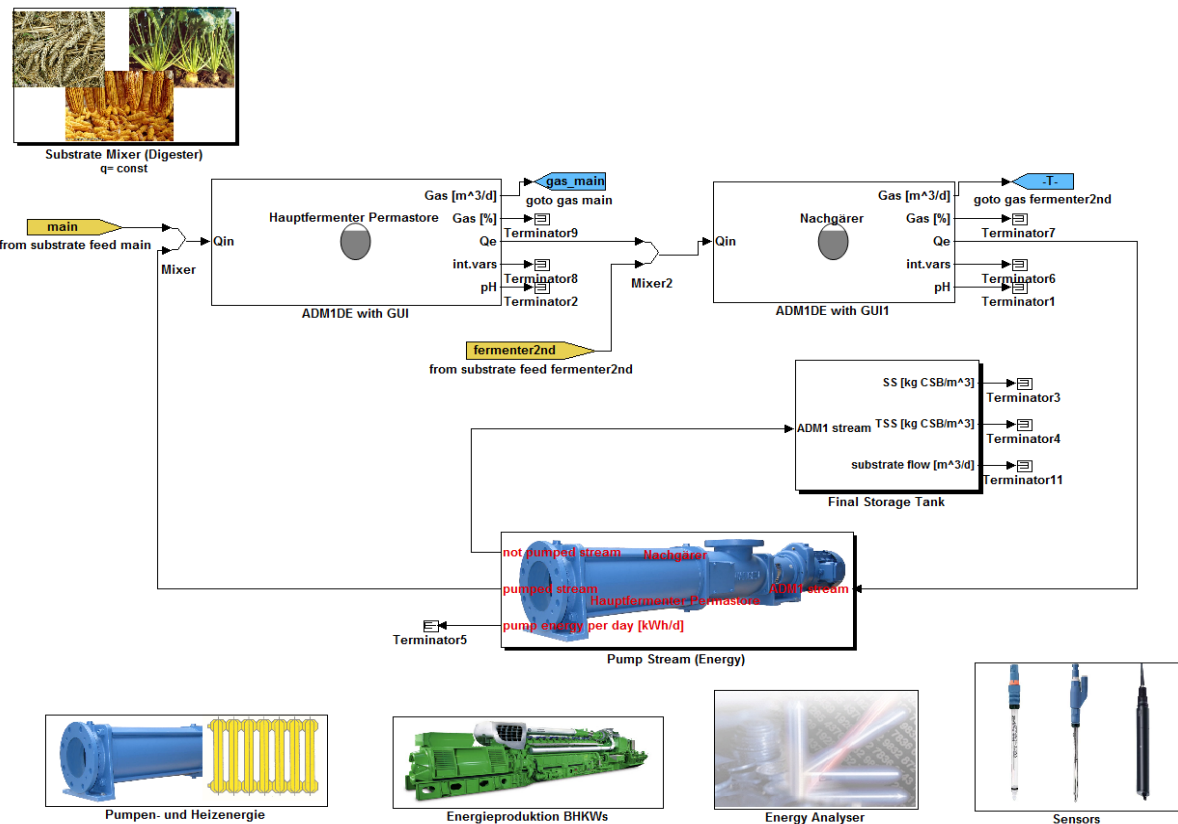


Figure 3.4: Sunderhook biogas plant modeling.

Furthermore, the simulation model is calibrated and validated in accordance to its measurement data. Calibrated models are of crucial importance in order to obtain feasible simulation results that correlate to the actual behavior of the modeled system; in this case a biogas plant. The “Biogas Plant Modeling Toolbox” permits the calibration and validation of simulation

models based on their simulation results and input data (i.e. virtual and real measured values such as pH value, biogas flow, methane, etc). Therefore, the highly nonlinear behaviors of the biological processes that occur inside the digester are correctly emulated by this simulation model; and also, avoids further propagation of errors when predicting or simulating the plant.

The simulation model design shown in Figure 3.4 is composed by blocks representing each process of the biogas production chain. These blocks consist of two digesters, pumping and heating systems, energy production (i.e. CHP units), sensors, energy analysis, storage tank and the substrate mixture preparation.

The “Substrate Mixture” block is responsible for selecting the type of substrates (e.g. const, user) used by the simulation model and create the substrate mixture for each substrate.

The fermenter or digester modules are based on the Anaerobic Digestion Model No. 1 (ADM1) (Batstone et al., 2002), which brings in the mathematical formulation to describe the anaerobic digestion process. Such formulation makes possible to simulate biogas production and plant behavior according to plant’s measurements. These blocks simulate ideally mixed reactors at a constant temperature of 41°C (i.e. the bacterial optimal temperature range for methane production). The digester module has five outputs: biogas amount in  $\text{m}^3/\text{d}$  (1), biogas concentrations in percentage (2), digestate or fertilizer flow (3), internal variables (4) and pH value that are calculated according to the ADM1 formulation (e.g. see Figure 3.5).



**Figure 3.5: Digester module ADM1**

The remaining modules are responsible for the simulation’s energy balance, where both the energy consumption for pumping and heating, and the fermenter energy production from the CHP units are evaluated according to cost-effective boundaries. Hence, the digester operational and heating costs must be compensated by the energy and biofuel production. This production is influenced by a range of factors such as types of substrate involved in the digestion as seen in the (e.g. see Table 1.3), vessels temperature, substrate feed rate, etc.

The next section will introduce the nonlinear model predictive control (NMPC) implementation in the simulation model application (i.e. biogas plant model).

### 3.4 NMPC algorithm principle and implementation

The basic structure of a NMPC control loop is illustrated in Figure 3.6, where a NMPC controller based on estimated states  $\hat{x}$  from the controlled system (i.e. full-scale biogas plant) defines optimal input  $u$  that forces the system to its steady state of operation. This optimal input  $u$  is defined through the dynamic optimization of a built-in simulation model that emulates the nonlinear behavior of the controlled system in accordance to a certain cost function and predefined constraints (e.g. see Figure 3.6).

Furthermore, as can be seen in Figure 3.6 the NMPC controller implements a closed-loop control system, where the optimal inputs are incessantly predicted and employed at the plant in accordance to its current state of operation.

Such online configuration was not fully implemented in a real system since the main objective of this thesis is to evaluate the proposed NMPC algorithm efficiency and reliability for controlling biogas plants. Thus, the controlled system (i.e. biogas plant in Figure 3.6) was replaced by a fully calibrated biogas plant model based in the ADM1 and real measurements from the Sunderhook biogas plant (e.g. see section 3.2).

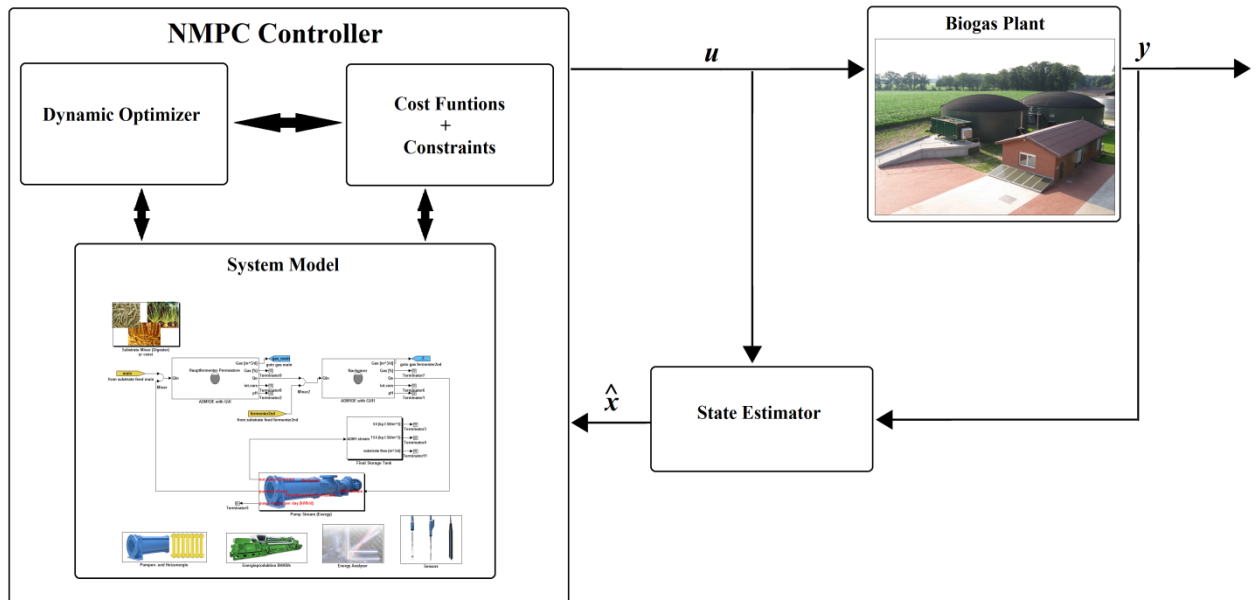
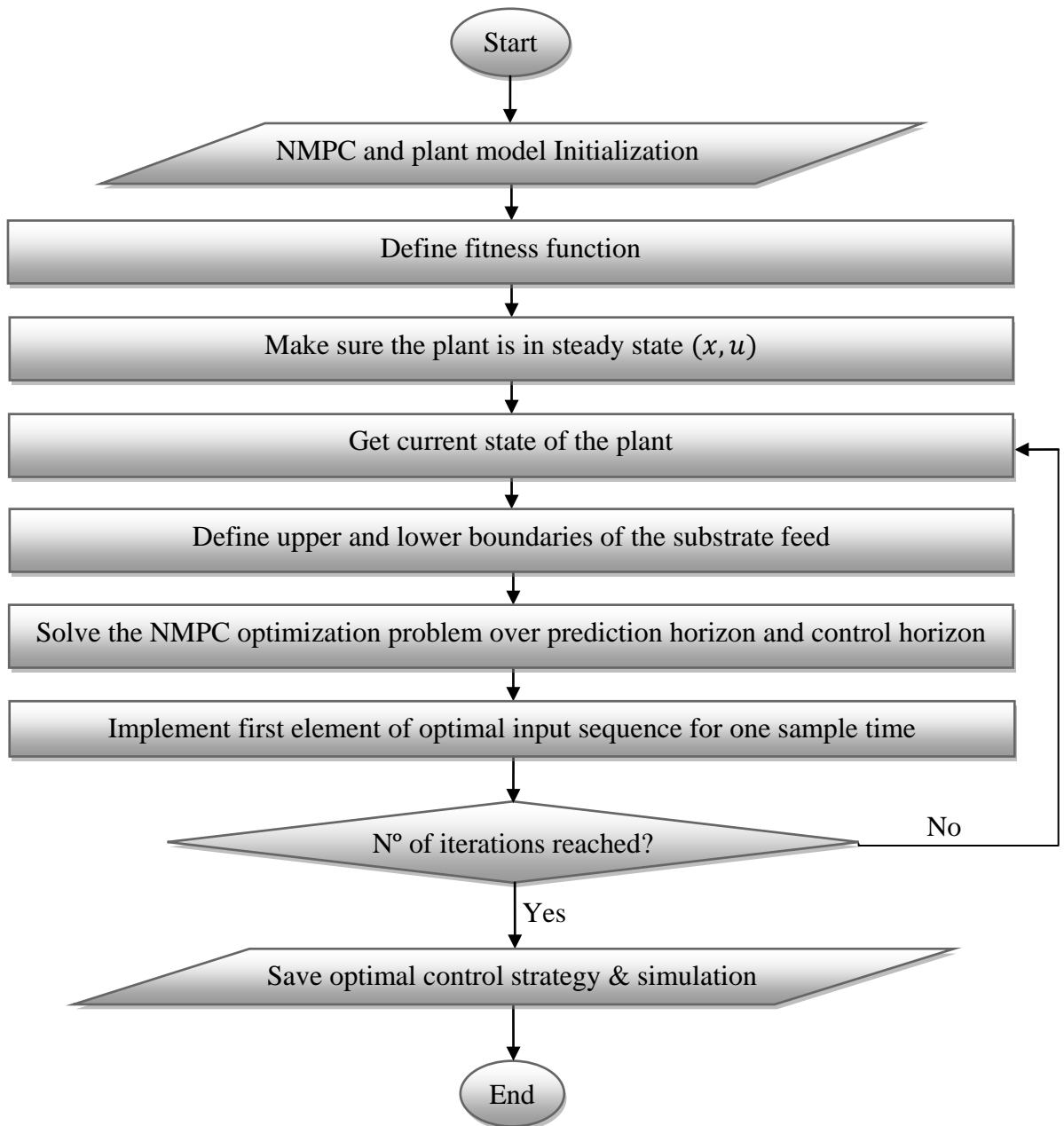


Figure 3.6: Basic NMPC control loop.

Therefore, once the NMPC algorithm has proven to be trustworthy for controlling biogas plants in a synthetic environment, the next logical step would be to implement it in the real system. In addition, the state estimator is unnecessary at this stage given that the plant states can be extracted directly from the simulation models; however, in future on-line implementations the state estimator will be indispensable.

Moreover, the NMPC algorithm can be used to determine an optimal control strategy (i.e. substrate mixture inlet sequence) for the real biogas plant, which leads the real system to an optimal operating point by satisfying various practical constraints.

Figure 3.7 illustrates the NMPC algorithm proposed in this thesis; where the on-line optimization is replaced by an iteration loop that repeats the procedures of prediction and control



horizon for a user defined number of days.

**Figure 3.7: NMPC algorithm flowchart.**

The NMPC algorithm starts by initializing the data from the Sunderhook plant (e.g. substrates flows, initial states, etc.) in order to provide the plant's operational states for the simulation model. Subsequently, this data is used to determine the plant's steady state. The steady

state is a condition in which the plant reached its undisturbed state; in other words, its dynamic equilibrium. The steady state definition is crucial to obtain reliable simulation results that were not influenced by other disturbances or variables. Thus, a simulation model of the plant is ran for an amount of 750 days at constant substrate feed with the purpose of obtaining the steady state of the Sunderhook biogas plant; which is used in the next simulation step as the plant's initial state.

The next steps concern the inner core of the NMPC algorithm, the prediction and control horizons. During the prediction horizon a simulation model of the biogas plant has its optimized inputs parameters (i.e. substrate feed rates) according to optimization algorithms, such as Covariance Matrix Adaptation Evolution Strategy. These optimization algorithms search within a predefined bounded search space for the best substrate feed rates that would result in maximal biogas production with reduced operational costs. Usually, these algorithms make use of a function that numerically describes such relationships; for example, it weights the heating costs of the digester during the biogas production, the digester pH values and many other important process values and restrictions. This function is known as fitness function.

Concerning the NMPC formulation described in section 2.3, the fitness function is the cost function  $J$  in equation (7) that describes the behavior of the controlled system according to its current states and predicted optimal input values over the prediction horizon, i.e.,  $J(\bar{\mathbf{x}}(t), \bar{\mathbf{u}}(\cdot); T_c, T_p)$ .

Although the cost function in equation (7) comprises the NMPC optimization problem in the original formulation (i.e. section 2.3), the cost function  $J$  is replaced here by the fitness function  $F$ . Such replacement is due to the NMPC algorithm's center of attention, where the interest is only at final optimal state and not in the entire way to reach the steady state represented by the integral  $\int_t^{t+T_p} F(\bar{\mathbf{x}}(\tau), \bar{\mathbf{u}}(\tau)) d\tau$ . Hence, the fitness function  $F$  is calculated at predicted final state  $\bar{\mathbf{x}}(t + T_p)$  and initial input  $\bar{\mathbf{u}}(t + T_p)$  in every iteration loop; and it follows that  $F(\bar{\mathbf{x}}(t + T_p), \bar{\mathbf{u}}(t + T_p))$ .

Finally, the fitness function  $F(\bar{\mathbf{x}}(t + T_p), \bar{\mathbf{u}}(t + T_p))$  considers economical and ecological characteristics inherent to the system process for optimum biogas production. The fitness function formulation frequently is in quadratic form  $\mathbf{F} = \mathbf{x}^T Q \mathbf{x} + \mathbf{u}^T R \mathbf{u}$ ; with weightings  $Q \geq 0$  and  $R > 0$ .

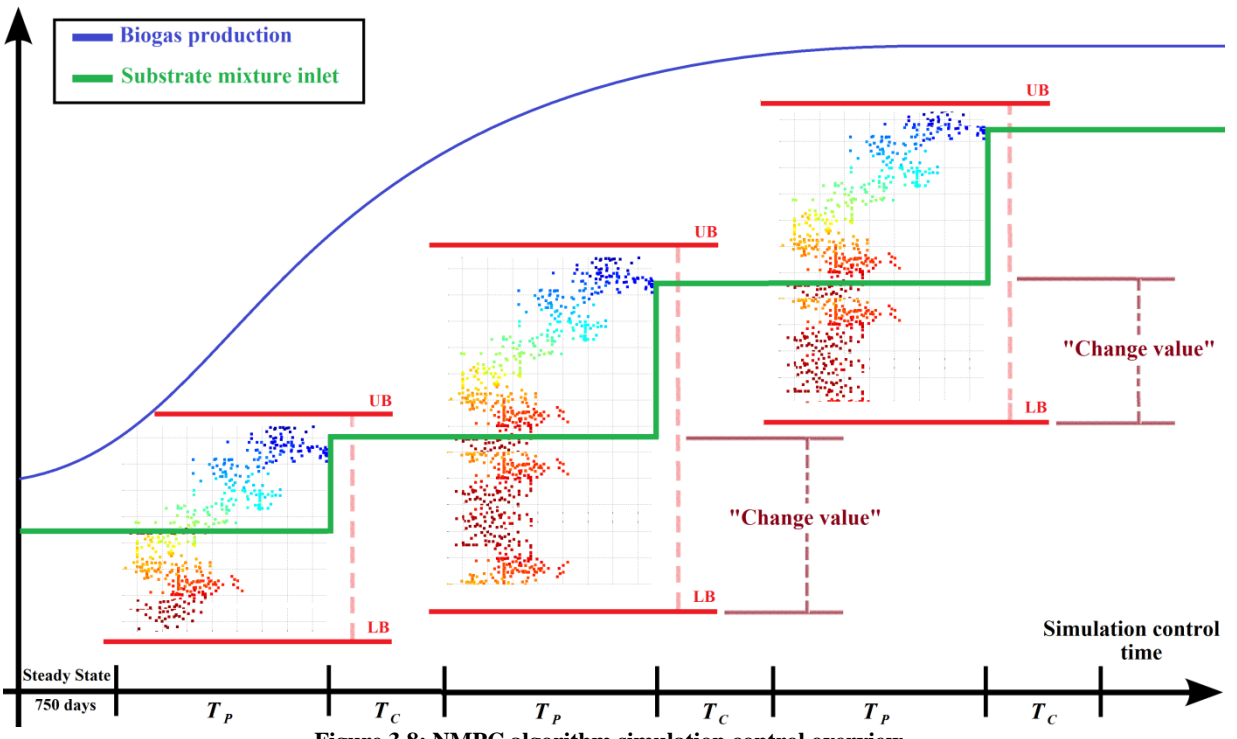
Once the prediction horizon calculation is completed and a feasible solution (i.e. set of plant's inputs) is found according to the fitness function  $F$  evaluated at  $(\bar{\mathbf{x}}(t + T_p), \bar{\mathbf{u}}(t + T_p))$ , this optimal set of inputs is applied to the simulation model during the control horizon.

At this stage, the biogas simulation model is simulated at its last known state prior to the prediction horizon (i.e. the actual initial state at  $\bar{\mathbf{x}}(t)$ ); in other words, the predicted state at the end of the prediction horizon  $\bar{\mathbf{x}}(t + T_p)$  is not taken into account. Therefore, the control horizon utilizes

solely the optimal control inputs  $\bar{u}(t + T_p)$  defined during the prediction horizon to correctly predict the final states of the plant  $\bar{x}(t + T_c)$  at each control iteration loop ( $t + T_c$ ). Furthermore, the optimal control inputs  $\bar{u}(t + T_p)$  are constants during the whole prediction horizon simulation only changing at every optimization iteration loop, i.e.,  $\bar{u}(t + T_p) | u(\tau) = \text{const } \forall \tau \in [t, t + T_c]$ .

This cycle of prediction and control horizons are repeated in accordance with a user-defined variable, number of iterations  $N$ , to emulate an NMPC on-line optimization as shown in Figure 3.6.

Accordingly, the whole “NMPC algorithm simulation control” can be depicted as shown in Figure 3.8, where the steady state calculation and the cycle of prediction and control horizons are illustrated.



In addition, the substrate feed over prediction horizon  $T_P$  shown in Figure 3.8 is limited by an upper and lower bound, which defines the permitted search space to be utilized by the optimization method. In this case, the best input data (i.e. substrate mixture inlet that leads the system to an optimal operation point) is searched throughout this bounded space and, once it is found, is implemented in the control horizon  $T_C$  (e.g. see Figure 3.8). This search is represented by the colored points in Figure 3.8.

Moreover, the sampling time constant  $\delta$  (e.g. see section 2.2) is the “control horizon” duration  $T_C$  throughout the NMPC stepwise control (i.e.  $\delta = T_C$ ).

Therefore, once the optimal input sequence is implemented, the second cycle begins and the upper and lower bounds are incremented according to the “change value” a user-defined variable, which moves the search space to achieve an optimal system response (e.g. biogas production).

Ultimately, when the  $N$  number of iterations is reached, the NMPC algorithm saves the previously defined optimal control inputs at all steps (e.g. control horizon  $T_C$  step sizes) and all relevant simulation results.

These simulation data are then used to define a sequence of control inputs (i.e. NMPC stepwise control) that lead the system from its initial state to the calculated optimal state, where the biogas production is maximized and the system’s operational costs are minimized. Moreover, the NMPC stepwise control for biogas plants is the combination of all step sizes that were carried out during the control horizon  $T_C$  (e.g. see Figure 3.8).

The next chapter presents the proposed “NMPC optimization tool” developed in accordance to the NMPC algorithm principle explained in this section.

## 4 NMPC optimization tool for biogas plants

This chapter presents the proposed “NMPC optimization tool” developed to optimize full-scale biogas plants. Firstly, the NMPC optimization setup is presented including its required input data, optimization problem definition, and returned outputs data. Secondly, a complete description of the graphical user interface (GUI) developed to ease the NMPC algorithm usage is presented. Lastly, this chapter concludes with a brief description of the NMPC algorithm for the optimization of batch processes and other advanced options.

### 4.1 NMPC optimization setup

Figure 4.1 shows the required input data for the “NMPC optimization tool”. These input data concerns the biogas plant model (e.g. `plant_sunderhook.mdl`<sup>5</sup>), the sludge flow between fermenters (e.g. `volumeflow_fermenter2nd_main_const.mat`), and the substrate inlet rate (e.g. `volumeflow_maize1_const.mat`<sup>6</sup>). Additionally, the fitness function internal parameters are defined in the “`fitness_params_sunderhook.mat`” file.

	Name	Type
	<code>plant_sunderhook.mdl</code>	Simulink Model File
	<code>volumeflow_stiffmanure_const.mat</code>	MAT File
	<code>volumeflow_silojuice_const.mat</code>	MAT File
	<code>volumeflow_oat_const.mat</code>	MAT File
	<code>volumeflow_maize1_const.mat</code>	MAT File
	<code>volumeflow_greenrye_const.mat</code>	MAT File
	<code>volumeflow_grass_const.mat</code>	MAT File
	<code>volumeflow_fermenter2nd_main_const.mat</code>	MAT File
	<code>volumeflow_bullmanure_const.mat</code>	MAT File
	<code>substrate_network_min_sunderhook.mat</code>	MAT File
	<code>substrate_network_max_sunderhook.mat</code>	MAT File
	<code>plant_network_min_sunderhook.mat</code>	MAT File
	<code>plant_network_max_sunderhook.mat</code>	MAT File
	<code>initstate_sunderhook.mat</code>	MAT File
	<code>fitness_params_sunderhook.mat</code>	MAT File
	<code>digester_state_min_sunderhook.mat</code>	MAT File
	<code>digester_state_max_sunderhook.mat</code>	MAT File

Figure 4.1 : NMPC optimization tool input data.

<sup>5</sup> MDL-file format comprises a simulation model created with Simulink Simulation and Model-Based Design software; contains the block diagram and block properties of the simulation.

<sup>6</sup> MAT-file format comprises a binary data container used by MATLAB; may include arrays, variables, functions, and other types of data.

In addition, sludge flow between fermenters and the substrate feeds are delimited by upper and lower boundaries. The upper and lower boundaries of the sludge flow between fermenters are defined by the files “plant\_network\_max\_sunderhook.mat” and “plant\_network\_min\_sunderhook.mat”, respectively; while the upper and lower boundaries of the substrate mixture inlet at the reactor are defined by the “substrate\_network\_max\_sunderhook.mat” and the “substrate\_network\_min\_sunderhook.mat”, respectively.

Furthermore, the NMPC algorithm defines the initial state of the system out of the “digester\_state\_min\_sunderhook.mat” and “digester\_state\_min\_sunderhook.mat files”. Once defined, this initial state is saved in the “initstate\_sunderhook.mat”; where it can be used later by the NMPC algorithm for defining the steady state of the system as previously explained in chapter 3 section 3.4.

Moreover, all remaining files concern the substrate feeds at the reaction before the NMPC optimization starts. These files can be in two forms: constant or user defined. If the file is constant (e.g. volumeflow\_substrate\_const.mat) it contains a vector with a constant volume flow that remain constant throughout the time (e.g. ten days with  $30\text{m}^3/\text{d}$ ). In the case it is user defined e.g. volumeflow\_substrate\_user.mat), it consists of a sequence of substrate feeds defined by the user (e.g. ten days with  $30\text{m}^3/\text{d}$  followed by twenty days with  $15\text{m}^3/\text{d}$ ).

Since all the input data files described above are required by the NMPC algorithm in order to launch the NMPC optimization, they must be created and correctly configured. Thus, the input data can be either manually generated in MATLAB's command line or defined through the utilization of graphical user interfaces provided by the "Biogas Plant Modeling Toolbox"<sup>7</sup>. In view of the fact that "NMPC optimization tool" utilizes this toolboxes modeling environment, this initial configuration is relatively simple and comprises the following steps:

- 1) Plant modeling and systems configuration (digester, CHP)
    - a. MATLAB call: “gui\_plant()”
      - i. Generates: plant\_sunderhook.mdl
  - 2) Reactors linking definition
    - a. MATLAB call: “gui\_plant\_network()”
      - i. Generates: plant\_network\_max\_sunderhook.mat,  
plant\_network\_min\_sun-derhook.mat.

<sup>7</sup> MATLAB/Simulink toolbox developed by the Gummersbacher Environmental Computing Center GECO-C in cooperation with PlanET Biogastechnik GmbH.

- 3) Substrates chemical and physical characteristics definition
  - a. MATLAB call: “gui\_substrate()”
    - i. Generates: substrate\_sunderhook.mat.
- 4) Substrate feed distribution between reactors
  - a. MATLAB call: “gui\_substrate\_network()”
    - i. Generates: substrate\_network\_max\_sunderhook.mat,  
substrate\_network\_min\_sunderhook.mat.
- 5) Substrates inlet rate definition
  - a. MATLAB call: “set\_input\_stream()”
    - i. Generates: volumeflow\_maize1\_user.mat,  
volumeflow\_bullmanure\_const.mat, etc.
- 6) Initial state definition
  - a. MATLAB call: “createinitstatefile()”
    - i. Generates: initstate\_sunderhook.mat.

Once the optimization problem is configured (e.g. biogas plant model) and the simulation input data is defined the “NMPC optimization tool” can be executed. This can be performed in two ways; the first is a direct command line call (e.g. “nonlinearMPC()”) and the second is through the NMPC optimization tool graphical user interface. These two possibilities will be further explained in the following sections.

Finally, once the NMPC optimization is completed the final results are saved in the user defined files (e.g. volumeflow\_maize1\_user.mat), which comprise the stepwise control for the specific substrate feed (i.e. the maize substrate in this case). Therefore, the combinations of each stepwise control compose the NMPC control strategy. Additionally, the NMPC algorithm saves the final state of the biogas plant and the overall optimization parameters (e.g. cost benefit ratio, fitness values, energy consumption, etc.).

## 4.2 NMPC optimization GUI

For the purpose of providing a straightforward approach to configure and execute the developed NMPC optimization tool, a graphical user interface (GUI) was developed (e.g. see Figure 4.2). This NMPC GUI enables quick changes in the biogas plant optimization scenario; allowing as well the specification of its detailed NMPC optimization parameter settings (e.g. number of iterations, optimization method, control horizon time, prediction horizon time, etc.). Hence, allowing the uncomplicated definition of different possible scenarios for biogas plant optimization.

Figure 4.2 presents the NMPC GUI main window, which is composed of three configuration stages depicted in the numbered red boxes one through three.

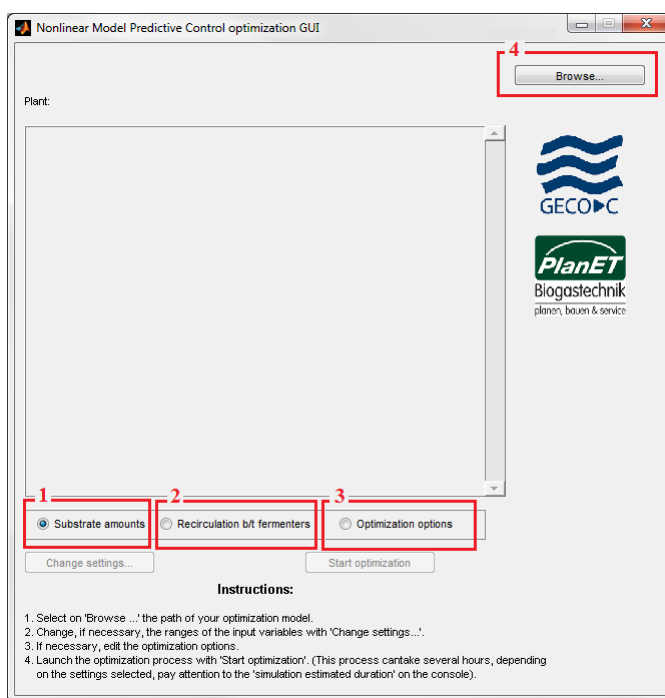


**Figure 4.2: NMPC GUI.**

As described in the previous section, the “NMPC optimization tool” requires a conjunction of input data (e.g. biogas plant model, substrate inlet rate, etc.) that is contained in a specific folder. This folder path must be given to the NMPC GUI in order to start the NMPC algorithm configuration and the subsequent optimization. Thus, the red box n°4 shown in Figure 4.2 highlights the browse button, which is used to select the “optimization model folder” containing the biogas plant model and its substrate amounts

Once the folder is selected, the GUI automatically loads and displays all substrates feeds utilized in the plant and their respective maximum and minimum values; as respectively shown by the red box n°1 and red box n°2 in Figure 4.3.

In addition, the green marked substrate feeds indicates which substrates are to be utilized in the NMPC optimization (e.g. Bullengülle (Bull manure) in Figure 4.3). This is defined by their upper and lower bounds, which specify the NMPC search space scenario. In the case that the substrate feed is constant and/or not used, there is only one value shown (e.g. Grünroggen (Green rye) in Figure 4.3).

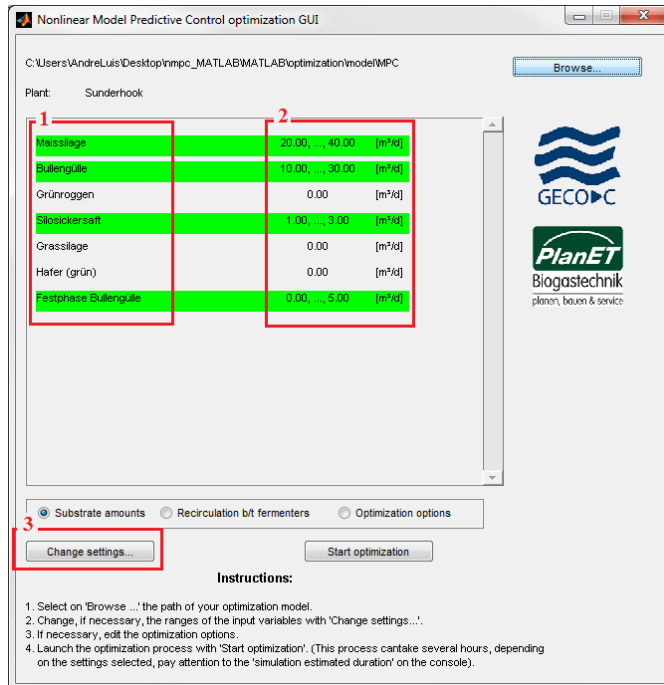


Figure 4.3: NMPC GUI – Substrate feed amounts.

Furthermore, the substrates feed upper and lower bounds (e.g. see red box n°2 in Figure 4.3) can be modified by clicking in the “change settings” button, which is highlighted by the red box n°3 in Figure 4.3. Figure 4.4 portrays the new opened interface when the “change settings” button is clicked, where the substrates maximum and minimum values can be modified.

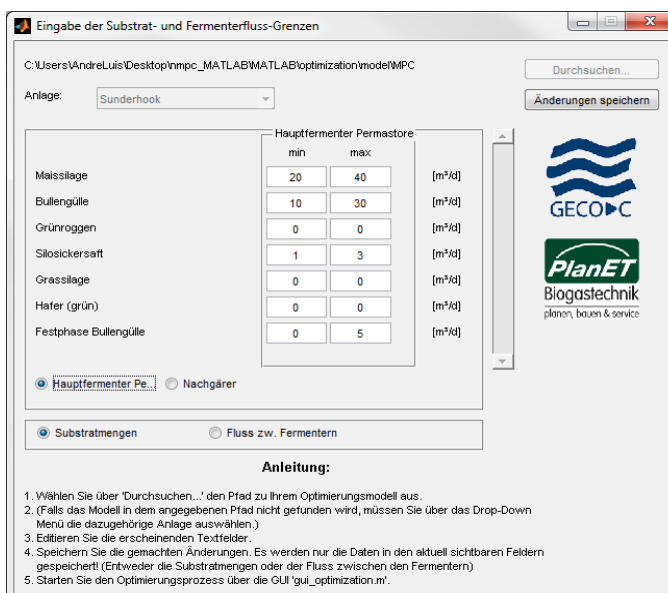


Figure 4.4: NMPC GUI – Substrate feed upper and lower bounds modification.

Figure 4.5 shows second state in the NMPC configuration; which is accessed by selecting the radio button shown by red box n°4 in Figure 4.5. In this stage the recirculation between fermenters is defined. This recirculation concerns the sludge feeding among reactors, which is imperative in the biogas production process to maintain a well balanced substrate mixture.

Furthermore, the proposed scenario of study (i.e. NMPC optimization of the Sunderhook biogas plant) is composed just one sludge recirculation between the main and the secondary reactors. This highlighted by the red box n°1 in Figure 4.5. Additionally, the sludge recirculation between fermenters is chosen to be a constant volume flow (e.g. see red box n°2 in Figure 4.5).

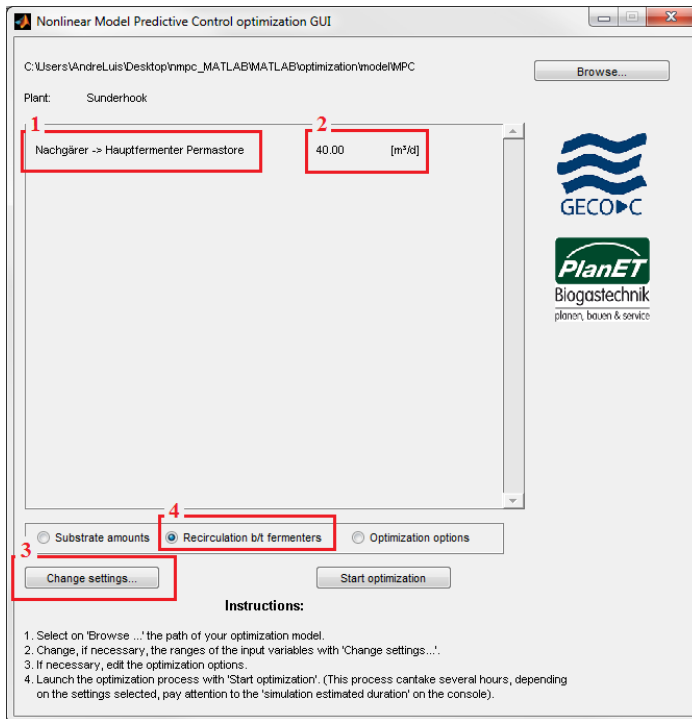


Figure 4.5: NMPC GUI - Sludge recirculation.

Moreover, the upper and lower bounds for the sludge recirculation can be modified by on the “change settings” button, which is highlighted by the red box n°3 in Figure 4.5. Afterwards, the interface shown in Figure 4.4 is opened to allow the modification of maximum and minimum sludge recirculation values.

Once the “optimization model folder” path is set and the substrates search space (i.e. upper and lower bounds) are defined, the NMPC algorithm can be configured. Figure 4.6 illustrates the “NMPC algorithm configuration window” in which the MPC optimization parameters can be configured. This window is shown when the “Optimization options” radio button is checked, as highlighted by the red box n°4 in Figure 4.6.

The opened “NMPC algorithm configuration window” in the NMPC GUI provides a default configuration for the NMPC optimization as can be observed in Figure 4.6; however, is also possible to modify these values according to different optimization scenarios.

Furthermore, the NMPC parameters shown in Figure 4.6 can be classified in three different categories: “NMPC prediction horizon options”, “NMPC control horizon options” and the “optional parameters”.

The “NMPC prediction horizon options” is highlighted by red box n°1 in Figure 4.6. This first category of parameters concerns only the input variables that take place in the NMPC algorithm’s “prediction horizon time”. Thus, it consists of: “optimization method”, “population size”, “number of generations” and the “prediction horizon time”.

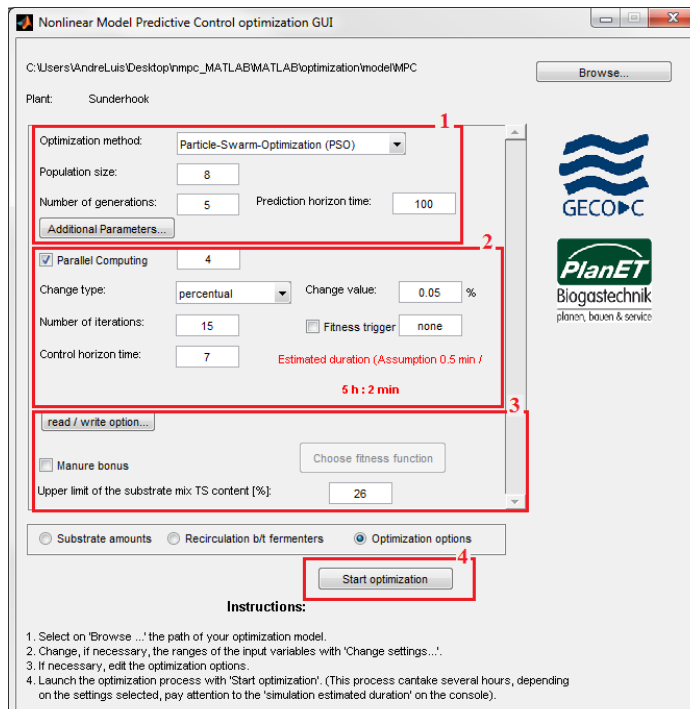


Figure 4.6: NMPC GUI - NMPC parameters configuration window.

Moreover, the “NMPC control horizon options” concerns only the input variables that take place in the NMPC algorithm’s “control horizon time”, which is highlighted by the red box n°2 in Figure 4.6. Thus, it consists of: “change type”, “change value”, “number of iterations”, “fitness trigger” and the “control horizon time”.

Lastly, the “optional parameters” which is highlighted by the red box n°3 in Figure 4.6 concerns further configuration parameters (e.g. Manure bonus, fitness function selection, etc.).

Figure 4.7 presents the six possible “optimization methods” that can be chosen for the NMPC optimization algorithm (e.g. Differential Evolution (DE)); and also, the further specification of its “population size” and “number of generations” (e.g. eight and five in Figure 4.6, respectively).

In addition, the “prediction horizon time” indicates for how long the optimization method will run to find the best possible outcome according to the defined fitness function and the substrate mixture inlet.

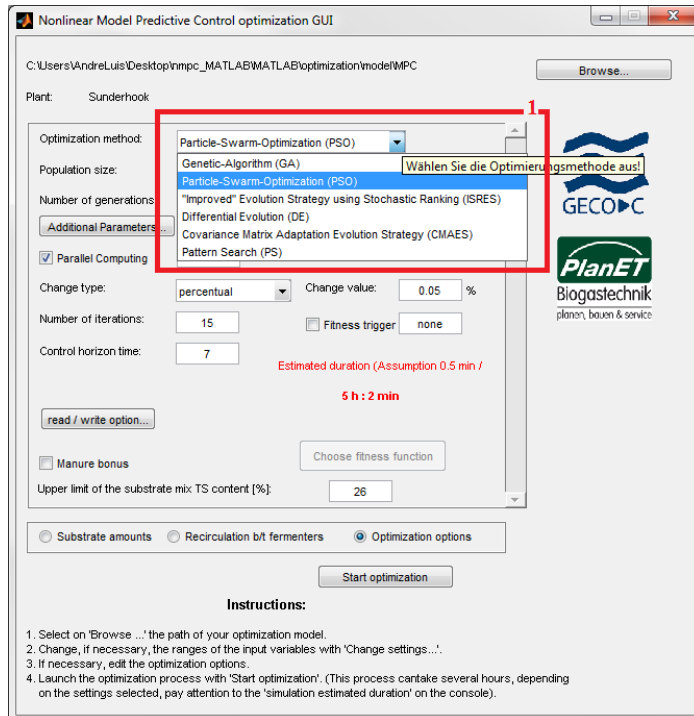


Figure 4.7: NMPC GUI – Prediction horizon setup.

The “change type” parameter (e.g. see red box n°1 in Figure 4.8) must be configured in combination with the “change value” parameter (e.g. see red box n°2 in Figure 4.8). These two values will define the step size throughout the NMPC optimization, as previously explained in the section 3.4. Thus, the “change type” defines the step size dimension; either in percentage [%] or absolute [m<sup>3</sup>/day]. While the “change value” parameter is the step size value (e.g. see Figure 4.8).

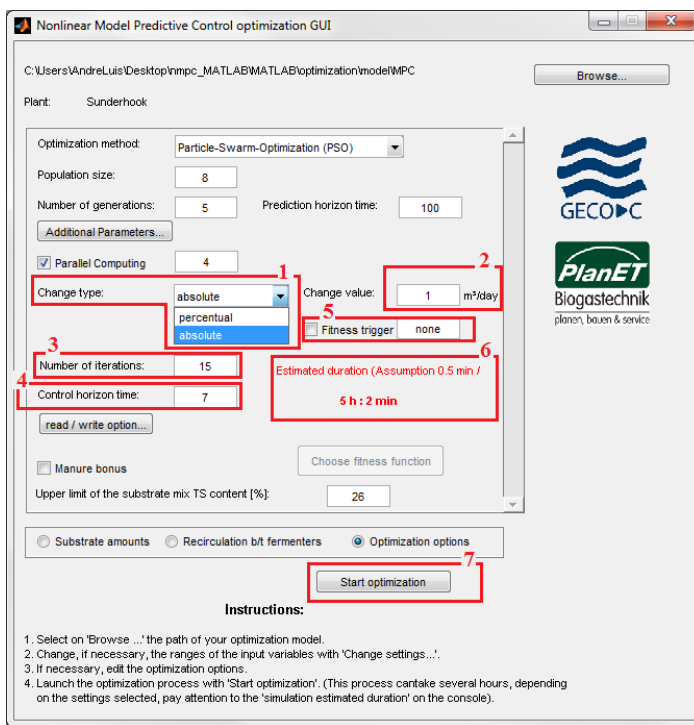


Figure 4.8: NMPC GUI – Control horizon setup.

Therefore, the resulting step size is a constant increment of ten meter cubic per day (i.e. “change type”= ‘absolute’ and “change value”=10) during the NMPC optimization or a ten percent increment over previous utilized step (i.e. “change type”= ‘percentual’ and “change value”=10). This step size actually moves the upper and lower boundaries of the substrates feeds throughout the NMPC optimization as explained in chapter 3 section 3.4. Thus, it can be translated into the following equations:

$$UB = \text{"current substrate feed"} * (1 + \text{"change value"}) \quad (12)$$

$$LB = \text{"current substrate feed"} * (1 - \text{"change value"}) \quad (13)$$

Furthermore, the “number of iterations” highlighted by the red box n°3 in Figure 4.8 defines the number of iteration loops that repeats the procedures of prediction and control horizon as described in the section 3.4. Accordingly, the red box n°4 in Figure 4.8 presents the “control horizon time” parameter, which indicates for how long the “predicted optimal inputs” will be applied in the biogas simulation model during the control simulation.

Moreover, the “fitness trigger” can be utilized to further enhance the NMPC algorithm response (e.g. see red box n°5 in Figure 4.8). This option is a special feature in the “NMPC control horizon options” and, if selected, takes action when a fitness function value has not improved in the last five NMPC iterations. This action consists of increasing (i.e. +Inf), decreasing (i.e. -Inf) or adding by a constant the step size value. In addition, the “fitness trigger” option will be explained in more detail in section 5.4, where the NMPC algorithm is evaluated.

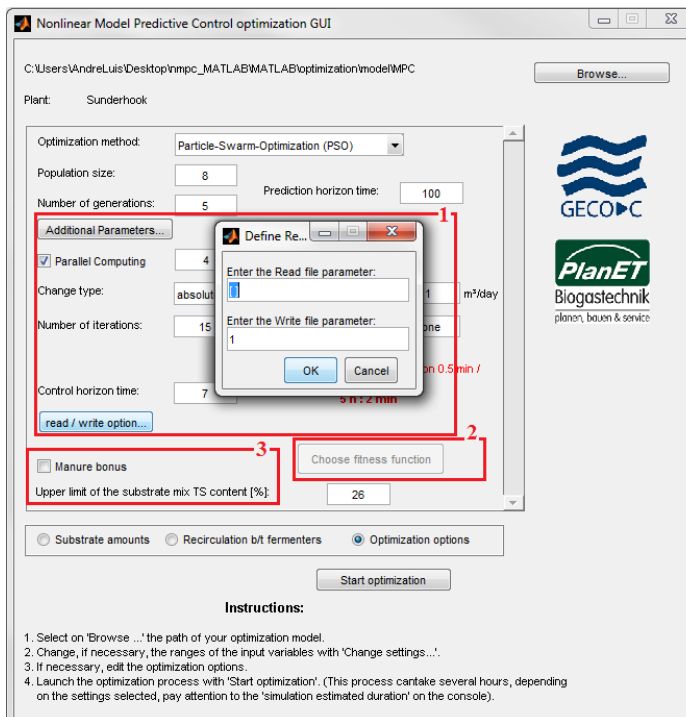


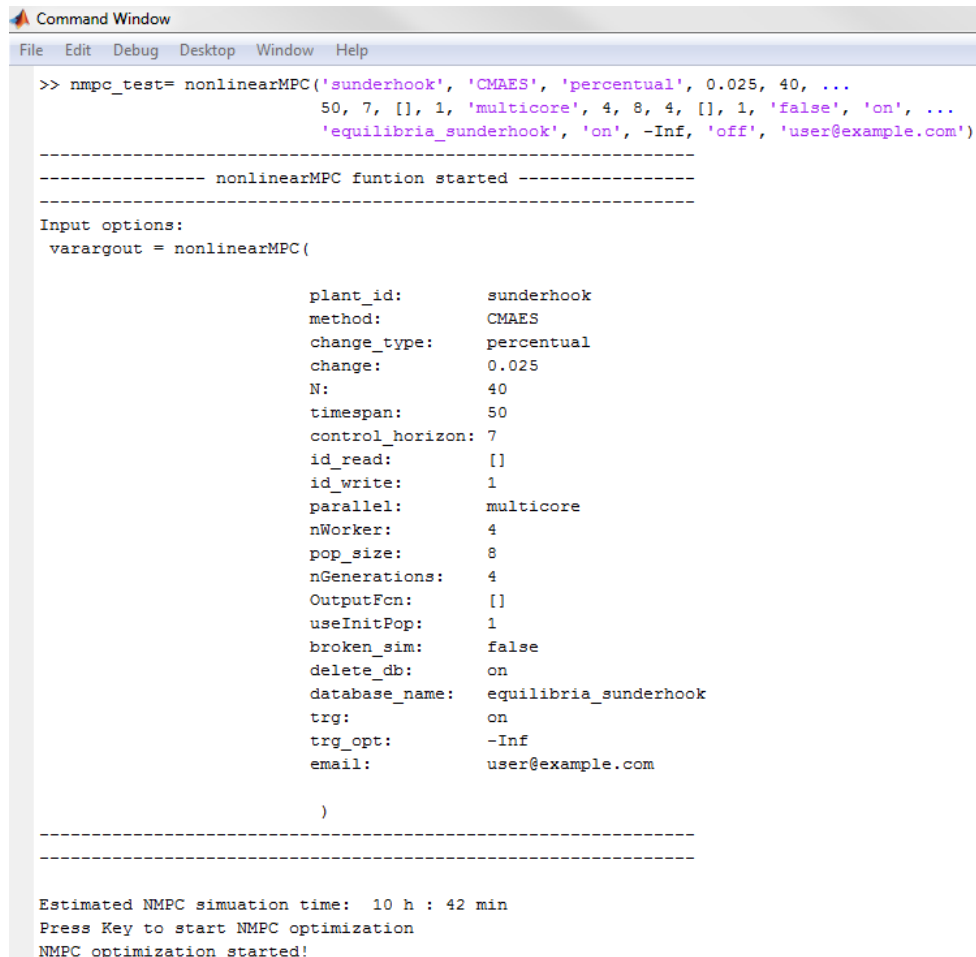
Figure 4.9: NMPC GUI – Optional parameters.

As mentioned before, the NMPC GUI provides further options such as the “manure bonus”, “fitness function selection” and “read/write option” (e.g. see Figure 4.9). The manure bonus, highlighted by red box n°3 in Figure 4.9, concerns a government incentive issued by Renewable Energy Sources Act (EEG) in Germany. The “fitness function selection” (e.g. red box n°2 in Figure 4.9) concerns the definition of the fitness function to be used in the NMPC optimization. The “read/write option”, shown by red box n°1 in Figure 4.9, defines the result’s name (e.g. if write= 1 then implies: volumeflow\_substrate\_user\_1.mat); and also, it defines from which file names the NMPC input data is loaded (e.g. if read= ‘empty’ then implies: volumeflow\_substrate\_user.mat)

Finally, once all parameters are set, the NMPC optimization can be started by clicking on the button “Start optimization” (e.g. see red box n°7 in Figure 4.8). In addition, the overall NMPC parameter configuration will have direct influence over the final simulation time. Therefore, in order to provide an accurate anticipation of the required simulation time, the NMPC GUI updates the estimated simulation time after every alteration in the NMPC parameters (e.g. red box n°6 in Figure 4.8).

## 4.3 NMPC algorithm for batch processes

The NMPC algorithm can also be called directly from the MATLAB's command line, as shown in Figure 4.10. This is mostly useful for batch processes' optimization, which allows the rapidly configuration and testing of various optimization scenarios in a sequential manner (i.e. many NMPC optimizations executed one after the other).



The screenshot shows the MATLAB Command Window with the title 'Command Window'. The window displays the following code and output:

```

>> nmpc_test= nonlinearMPC('sunderhook', 'CMAES', 'percentual', 0.025, 40, ...
    50, 7, [], 1, 'multicore', 4, 8, 4, [], 1, 'false', 'on', ...
    'equilibria_sunderhook', 'on', -Inf, 'off', 'user@example.com')
-----
----- nonlinearMPC funtion started -----
-----
Input options:
varargout = nonlinearMPC(
    plant_id:        sunderhook
    method:          CMAES
    change_type:     percentual
    change:          0.025
    N:               40
    timespan:        50
    control_horizon: 7
    id_read:         []
    id_write:        1
    parallel:        multicore
    nWorker:         4
    pop_size:        8
    nGenerations:   4
    OutputFcn:       []
    useInitPop:      1
    broken_sim:     false
    delete_db:       on
    database_name:  equilibria_sunderhook
    trg:             on
    trg_opt:         -Inf
    email:           user@example.com
)
-----
-----
Estimated NMPC simuation time: 10 h : 42 min
Press Key to start NMPC optimization
NMPC optimization started!

```

Figure 4.10: NMPC algorithm command line call.

Obviously, a deep understanding of the NMPC algorithm is required in order to correctly configure it. Thus, the proposed NMPC algorithm is provided with a full documentation of each parameter option; although these features are basically the same as the ones used in the NMPC GUI plus further advanced options (e.g. “e-mail option”).

Moreover, in order to obtain the batch process results in a practical manner (i.e. batch processes' optimization may require longer simulation times) a further option was created; it consists of sending the whole NMPC optimization data per e-mail as shown in Figure 4.11. This option is configured by simply stating the desired e-mail recipient (e.g. “user@domain.com”) in the

last NMPC function parameter, and once the NMPC simulation run is finished an e-mail will be sent with the simulation results.

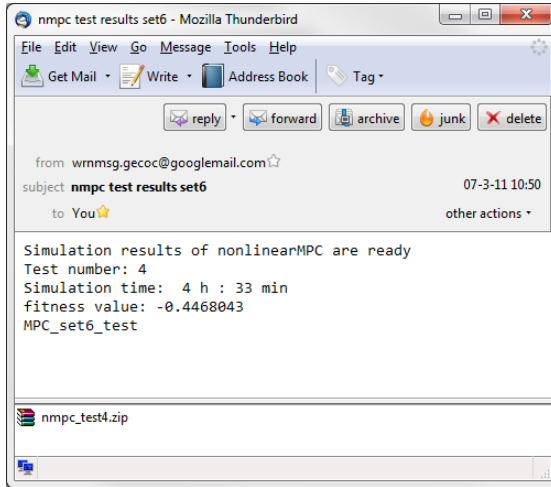


Figure 4.11: NMPC results received by e-mail.

To conclude, depending on the user's requirement, the NMPC optimization can be performed through a graphical user interface (i.e. NMPC GUI) or the command line function call (i.e. “nonlinearMPC()”).

The previously described NMPC algorithm is evaluated in the next chapter by comparing various simulation results obtained from different test scenarios.

# 5 Experimental Results

This chapter presents different tests performed with the Nonlinear Model Predictive Control algorithm proposed in this thesis and their data results analysis.

## 5.1 Simulation Scenario & Manipulated variables

Essentially the NMPC system can be seen as a black box, in which a nonlinear system is controlled through the prediction of how the system will react to an optimal set of inputs. Such optimal set of input variables should eventually, in a closed-loop control, lead the system to an optimal steady state according to its fitness function  $F$  and the NMPC algorithm implementation.

Therefore, the multi-input single-output system shown in the Figure 5.1 represents the main core of an NMPC system; where manipulated variables are used to control a nonlinear system and its output response based on the system's predicted behavior. In addition, the nonlinear system employed in this thesis concerns a fully calibrated biogas plant model based on the ADM1 as exposed in section 3.3.

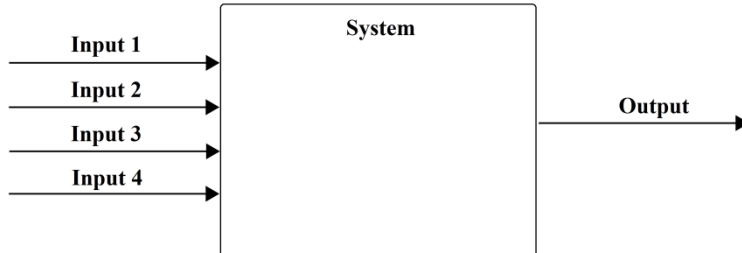


Figure 5.1: NMPC System with 4 inputs, 1 output.

The complete simulation scenario is shown in Figure 5.2, where the real biogas plant is replaced by a fully calibrated biogas plant model (i.e. Sunderhook plant model). The motivation for this is to assess the NMPC algorithm's performance, reliability and effectiveness in a secure environment prior to its implementation in the real system. Additionally, a detailed description of the proposed NMPC algorithm principle and its implementation is provided in section 3.4.

Furthermore, the simulation scenario in Figure 5.2 comprehends two nonlinear systems (i.e. biogas plant model), a dynamic optimizer (i.e. optimization method) and cost functions and constraints (i.e. fitness function  $F$  and cost benefit ratio  $CB$ ).

The biogas plant model is a multi-input system that comprises four manipulated variables, which consists of three different substrate feed and one volume flow recirculation at model's plant.

The three substrate feeds are: maize, manure and manure solids; while the recirculation consists of a constant volume flow between fermenters (i.e. sludge recirculation).

Consequently, these manipulated variables are utilized by the optimization method in accordance to the fitness function  $F$  and the cost benefit ratio  $CB$  to obtain the optimal substrate mixture inlet  $u$  that forces the system to an optimal operating point (e.g. see Figure 5.2). As a result, this optimal state is mainly achieved through the fitness function and the cost benefit ratio analysis that indicates how the system behaves to the given input.

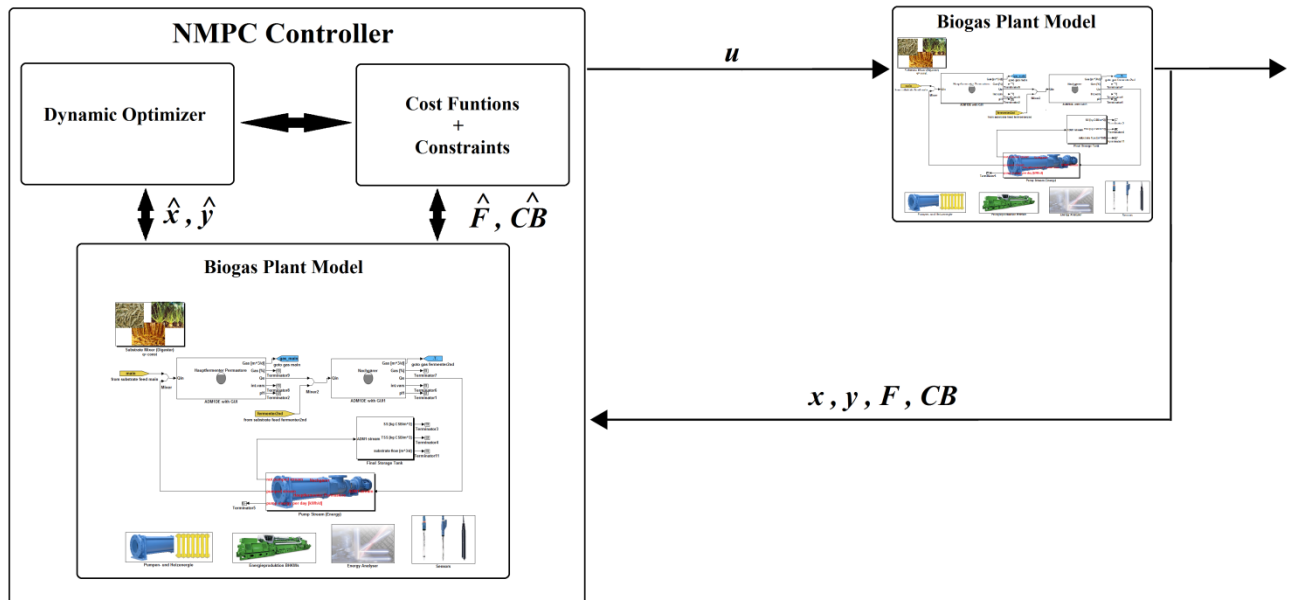


Figure 5.2: NMPC algorithm simulation scenario.

Therefore, the NMPC algorithm tries to optimize the substrate mixture inlet according to user defined optimization methods, fitness function, cost benefit ratio and a stepwise control that maximize biogas production and minimize operational costs.

Moreover, the cost benefit function compares all variable costs (e.g. substrate costs) and the gained profit (e.g. benefit of selling electrical and thermal energy) from the biogas production. And the fitness function is the weighted sum out of the cost benefit ratio and a couple of constraints. These constraints concern the biological processes within the plant's reactors, e.g., the pH value inside the digesters, a maximal dry matter content of the substrate mixture, and a minimal methane fraction of 50% inside the produced biogas.

Finally, the tests described in the next sections intend to evaluate how effectively NMPC algorithm is to find control strategies for biogas plants in accordance to the proposed simulation scenario of Figure 5.2. Also, these tests compare different tunings of the NMPC algorithm's parameters in order to obtain the best possible results with certain reliability and speed. Additionally, all tests are performed on a Windows XP PC with an Intel® Core™ 2 Quad CPU (2.4 GHz) and 3.25 GB RAM.

## 5.2 First Experiment

The first experiment purpose is to assess the NMPC efficiency according to different prediction horizon and control horizon simulation time setups. And additionally, evaluate how the step size influences the overall response of the controlled system.

To accomplish such objective, the overall number of simulations during the control horizon was fixed by a hundred day constant; i.e., "Number of iterations"×"Control horizon [d]" = 100 days. Therefore, enabling a fixed time range in which the NMPC control strategies could be evaluated and compared in all simulation tests.

Table 5.1 illustrates the NMPC optimization setting used in the first set of tests; the "prediction horizon time"  $T_P$ , "control horizon time"  $T_C$  and "change value" (i.e. step size) are the manipulated variables in these tests. Appendix A presents further information about these simulation tests results and the NMPC optimization setup.

**Table 5.1: NMPC optimization tool settings.**

NMPC parameter name	NMPC parameter value	Manipulated variable
Plant model	Sunderhook	
Optimization method	CMAES	
Population size	8	
Number of generations	4	
Prediction horizon time [d]	50, 100 or 150	✓
Control horizon time [d]	3, 7, 14 or 21	✓
Change type	Percentual [%]	
Change value	1, 2.5 or 5	✓
Number of iterations	$N = \text{round}\left(\frac{100}{\text{Control horizon [d]}}\right)$	
Fitness trigger	OFF	

Additionally, as mentioned in section 4, the step size can either be a percentage value [%] or an absolute value [ $\text{m}^3/\text{d}$ ] of the substrate mixture inputs (e.g. see Table 5.1). On the other hand the percentage step size has a flaw, if the substrate feed become zero throughout the simulation then the resulting percentage increment is also zero during the stepwise control. Therefore, is advisable to use the absolute value [ $\text{m}^3/\text{d}$ ] increment option if the initial states of the system are unknown.

Nevertheless, all substrate feeds utilized in the simulation results are known (e.g. see Table 5.2); thus the percentage step size does not represent a problem in the data analysis.

As stated in section 3.4, the initial states are delimited by a maximal and a minimal volume flow inlet that defines the search space for the optimization algorithm. This search space is moved throughout the NMPC optimization in accordance to the step size defined by the “change value” parameter. Thus, the step size increment is not over the optimized substrate inlet given by optimization method, but over the permissible search space.

Moreover, this upper and lower boundaries are implemented to avoid the over feeding of the reactor during the NMPC; this is essential since too much substrate feed can lead the reactor to instability. Additionally, for modeling purposes (i.e. caused by the “Biogas Plant Modeling Toolbox”) the recirculation between fermenters is considered to be constant and with a volume flow of 40 m<sup>3</sup>/d as shown in Table 5.2.

**Table 5.2: NMPC optimization - Substrate mixture initial state.**

Substrate name	Initial state n°1	Maximum substrate	Minimum substrate
	[m <sup>3</sup> /d]	inlet [m <sup>3</sup> /d]	inlet [m <sup>3</sup> /d]
Maize	30	40	20
Silo seepage	1.5	3	1
Manure	15	30	10
Manure solids	3	5	0
Recirculation b/t fermenters	40	40	40

In addition, the proposed initial state places the biogas plant model at an intermediary state of operation given the high inlet of maize substrate at the beginning of the optimization. This is predictable since the maize substrate possesses the highest potential of methane production in comparison to the remaining substrates (e.g. manure and manure solids). Thus, the proposed initial state aims a more realist optimization scenario, where the biogas production is at a regular state but not at its optimum.

Figure 5.3 illustrates the first set of test results, in this plot the overall fitness (goodness) is evaluated against the different setups scenarios proposed for the NMPC optimization tool; see Appendix A. These test scenarios concern the manipulation of the NMPC function parameters as described in the table above, where the manipulated variables were changed in order to assess the NMPC optimization performance.

Therefore, three curves can be seen representing the three different step sizes used in these tests, i.e., the substrate feed boundaries were increased by ratios of 1%, 2.5% and 5% during the stepwise control. From now on, these curves will be referenced as: test curve n°1 (step size of 1%), test curve n°2 (step size of 2.5%) and test curve n°3 (step size of 5%). Furthermore, in each test curve the NMPC setup had its prediction horizon and control horizon times altered and ranging from 50 to 150 days and 3 to 21 day, respectively.

Moreover, the color gradient shown in the curves of Figure 5.3 represents the overall fitness progress for each test result. Thus, the smaller the value, the cooler is the color and the better is the result.

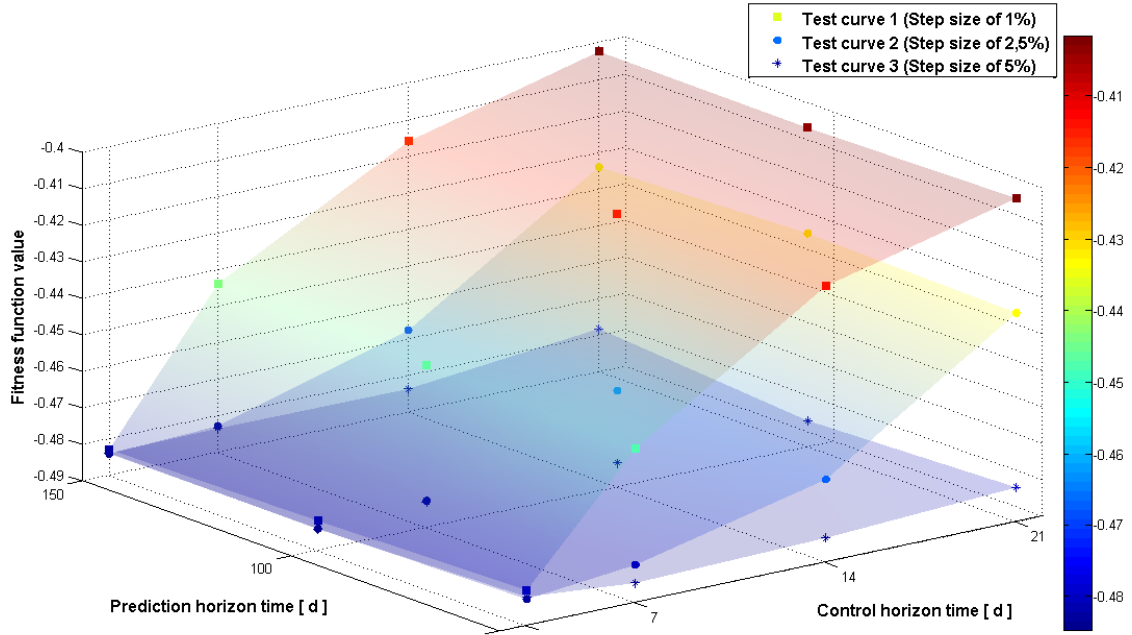


**Figure 5.3: Stepwise control evaluation versus fitness function values (The smaller the value (the colder the color), the better the result).**

Accordingly, results shown in Figure 5.3 reveal that the overall response of the system improves significantly with higher prediction horizon and lower control horizon values and, nevertheless, suffers substantial influence over the step size during the optimization.

The test curve n°3 in Figure 5.3 clearly presents the best fitness values within the one hundred day stepwise control; such result is caused by the higher step size used in these tests (i.e. five percent increment), which allowed the NMPC optimization tool to finely search the whole search space spectrum (i.e. substrate feed mixtures and rates). While the test curve n°1, see Figure 5.3, is quite the opposite of the test curve number there. This curve shows a gradual improvement on the fitness values according to its “control horizon time” and “prediction horizon time” configuration; lower “control horizon times” in combination with higher “prediction horizon times” result in substantially good fitness values independently of the step size. Such observation is also applied for the test curve n°2 in Figure 5.3.

Another key aspect to be considered in these simulations is the relationship between the “number of iterations”  $N$  and the “control horizon time”:  $N = \text{round}(100/\text{Control horizon [d]})$ . This relationship affects directly the number of optimization tries to be run in the NMPC optimization. Thus, if a big “control horizon time” is used (e.g. 20 days) the amount of iterations

will drop considerably (e.g.  $N = 100 / 20 = 5$ ), and in combination with small step sizes will result in bad responses of the system.

Hence, the differences observed in these test curves in Figure 5.3 leads to the assumption that in the cases the chosen step size is small the NMPC optimization will require lower “control horizon” and higher “prediction horizon” times (e.g., see test curve number one in Figure 5.3); and for the cases in which the step size is high, the NMPC optimization will require higher “control horizon” and lower “prediction horizon” times. Additionally, this last statement goes only if the computational time factor is taken into account (e.g. see Figure 5.4), since higher step sizes also have shown reasonable system responses with lower “control horizon” and higher “prediction horizon” times.

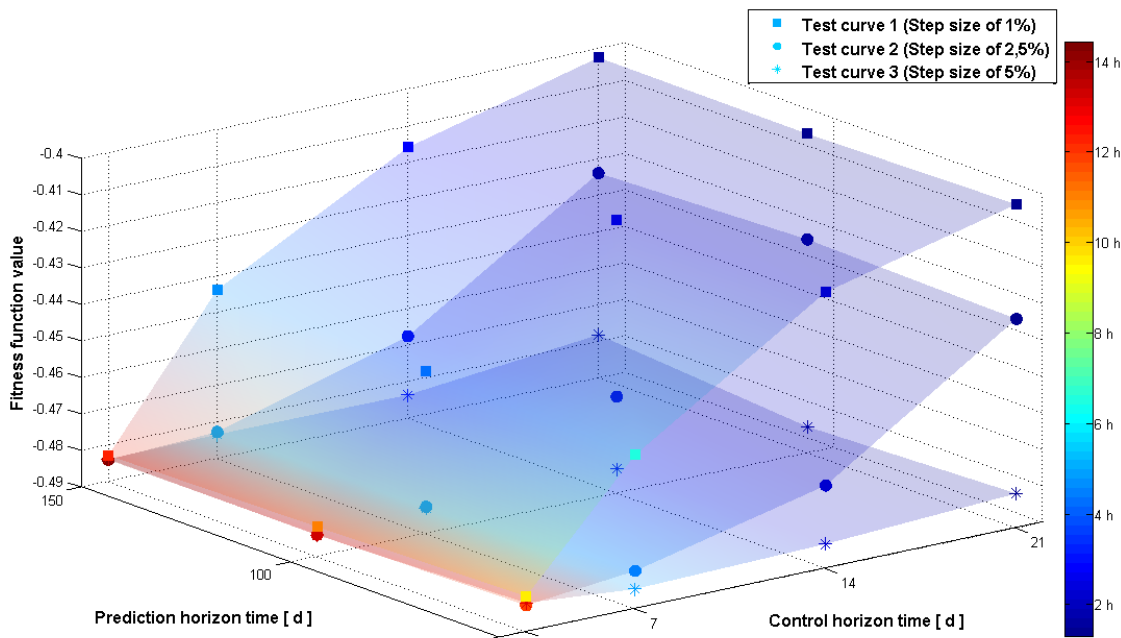


**Figure 5.4:** Stepwise control evaluation versus simulated control duration. The color gradient represents the simulated control duration in hours [h].

Furthermore, it is important to point out that the NMPC optimization is bounded by a fixed number of simulations in order to establish a tangible time range for the data analysis. Therefore, the tests in Figure 5.3 has shown that smaller step sizes will only lead to better results if the NMPC optimization is submitted to lower “control horizon” and higher “prediction horizon” times. However, smaller step sizes can also reach satisfactory optimization results if the “number of iterations” (i.e. more steps) is large enough and, consequently, resulting in longer simulation times.

Accordingly, the step size must be carefully chosen. Intermediary step sizes, not too big or too small, should be a possible solution to find reliable control strategies that are stable and computationally fast (e.g. Test curve 2 in Figure 5.4). These relationships will be exposed in detail in the following sections, where the comparison between best and the worse results is presented.

Moreover, Figure 5.4 illustrates the simulation times for all simulation tests; in this case the color gradient represents the time scale, i.e., the cooler the color is the less amount of simulation time was required by NMPC optimization. Thus, the “prediction horizon time” has greater influence over the NMPC computational times; as can be seen in Figure 5.4. In addition, the “number of iterations”  $N$  also has its influence over the “simulated control times” given the formulation  $N = \text{round}(100/\text{Control horizon [d]})$ ; as mentioned previously. Thus, the increment in the “prediction horizon time” in combination with the decrement in the “control horizon time” (i.e. sampling time) yields higher “simulated control times”:

$$\uparrow T_p \& \downarrow \delta \xrightarrow{\text{yields}} \uparrow \text{"Simulated control times"}. \quad (14)$$

Finally, the test curves in Figure 5.3 and in Figure 5.4 show that the system could reach its optimal operation point regardless of the step size if the relationship between prediction and control horizons is adequate; in other words, higher prediction horizon times with smaller control horizon times. On the other hand, the time required for the NMPC optimization run must be taken into account; Figure 5.4 corroborates the previous assumption, in which intermediary step sizes (e.g. 2.5% in Figure 5.4) could be a possible solution to find reliable control strategies that are stable and computationally fast (e.g. four hours simulation with a “control horizon time” of 7[d] and a “prediction horizon time” of 50[d]).

The next sections present the worse and the best simulation results obtained with the NMPC optimization tool.

### 5.2.1 Worse Results

This section presents the worse results obtained during the first experiment set of tests to evaluate the NMPC algorithm (e.g. Test n° 10 and marked in red on Table A.1). The settings utilized in this NMPC optimization test is provided in Table 5.3, followed by the plant’s initial states specification in Table 5.2 (e.g. the volume flows of manure, maize, etc.).

**Table 5.3: Test n°10 (Worse) - NMPC optimization tool settings.**

NMPC parameter name	NMPC parameter value	Manipulated variable
Plant model	Sunderhook	
Optimization method	CMAES	
Population size	8	
Number of generations	4	
Prediction horizon time [d]	50	✓
Control horizon time [d]	21	✓
Change type	Percentual [%]	
Change value	1	✓
Number of iterations	5	

As stated previously, the NMPC optimization tests for the first experiment aims to evaluate the NMPC algorithm efficiency according to different prediction horizon and control horizon simulation time setups. Therefore, the test exposed in this section was performed in accordance to the pre-established formulation for NMPC optimization tests:  $N \times T_C [d] = 100 \text{ days}$ . Such formulation locks the total “simulation control time” for all simulation runs.

Moreover, this test is evaluated in the following pictures according to its final state (biogas production), optimal substrate mix sequence of inputs (i.e. control strategy), overall fitness value and the gained cost benefit ratio.

Figure 5.5 presents the substrate mixture evolution throughout the NMPC optimization with respect to the overall fitness (goodness). In this figure is possible to observe the entire number of simulation runs executed by the CMAES optimization method, where each square represent a simulation run and the arrow its evolution direction. In addition, the color gradient represents the fitness function values progression in this NMPC optimization run, i.e., the smaller the value, the cooler is the color and the better is the result.

Furthermore, Figure 5.5 shows that the NMPC algorithm configuration resulted in a small amount of simulation tries, which is a result of the small number of iterations  $N$ . Thus, the small  $N$  resulted in a poor improvement in the fitness values as can be seen from the arrow’s linear trajectory in Figure 5.5 and the lower fitness values (e.g. just an  $-0.03$  difference).

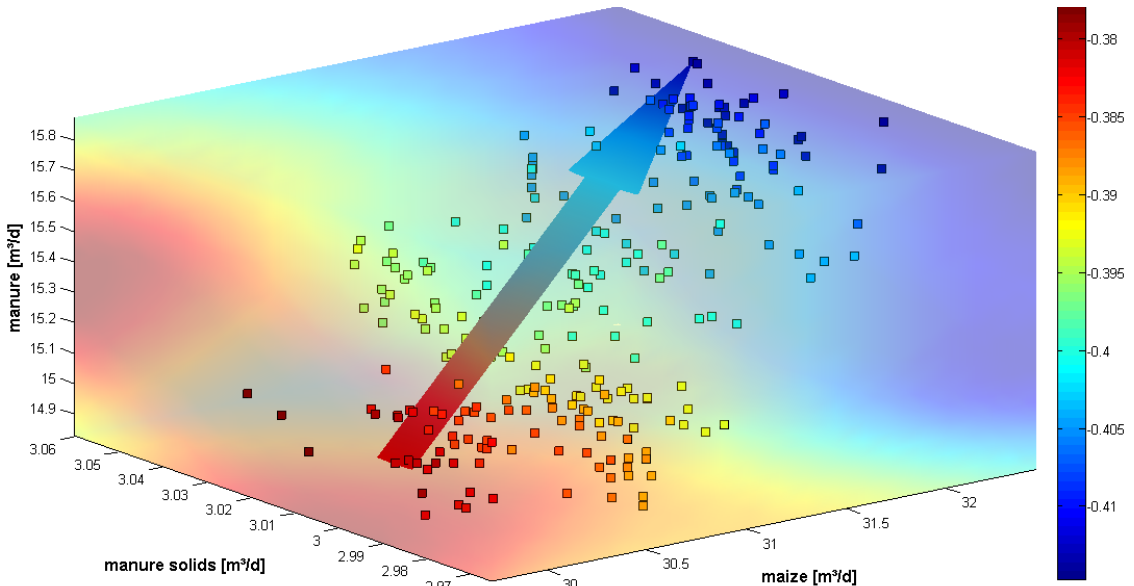


**Figure 5.5: Test n°10 (Worse) - Evolution of fitness function values against maize, manure and manure solids substrate feeds (The smaller the value (the colder the color), the better the substrate mix).**

Moreover, this slight improvement in the fitness value is also a result of the small “change value” parameter (i.e. the step size), which strongly influences the overall NMPC optimization. This can be seen in the Appendix A, where the same configuration achieved considerably better results when submitted to higher step sizes.

Figure 5.6 shows the substrate mixture evolution in the NMPC optimization with respect to a cost vs. benefit analysis (i.e. cost benefit ratio). Differently from the previous plot, this figure presents an overall improvement in the profit if the NMPC control strategy is implemented. Thus, the gained profit at the end of the NMPC optimization is a total of 121 euro per day, which is a slight improvement as expected from the color gradient shown in the Figure 5.6 and the small amount of simulation tries.

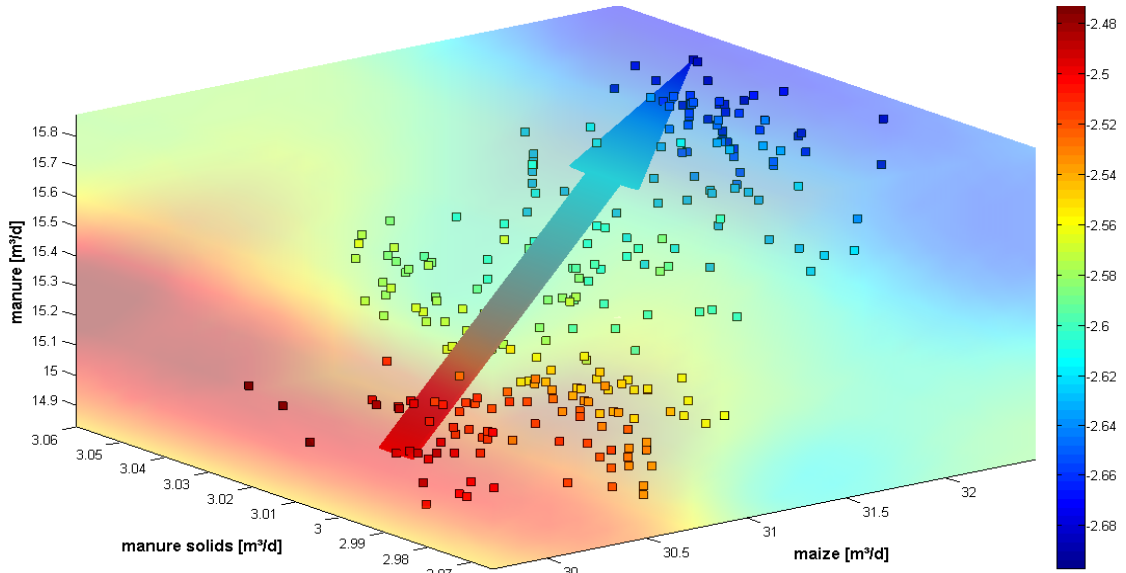
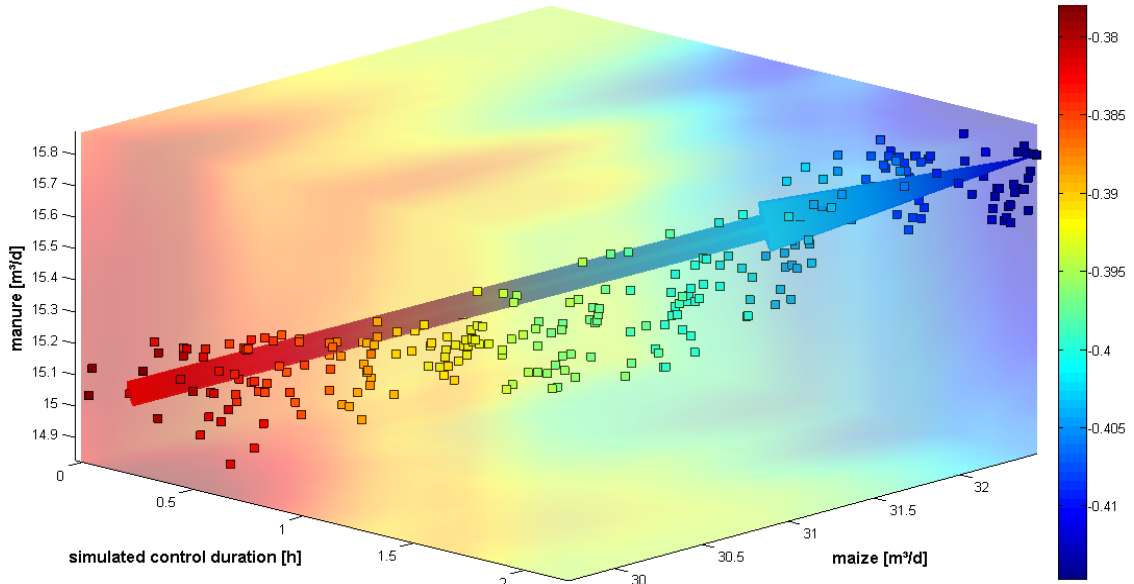


**Figure 5.6: Test n°10 (Worse) - Evolution of cost benefit ratio against maize, manure and manure solids substrate feeds (The smaller the value (the colder the color), the better the substrate mix).**

Therefore, a closer analysis of the obtained substrate mixtures in figures 5.5 and 5.6 show that during the NMPC optimization the substrate sequence of inputs were changed at very small step sizes during optimization run, what greatly affected the overall system response; fitness and cost benefit ratio were less than satisfactory when compared to other simulation runs. Such outcome was expected since this NMPC optimization run was performed with a very small step size ratio, (i.e. one percent increment of the substrate feed inlet) and a small number of iterations  $N$ .

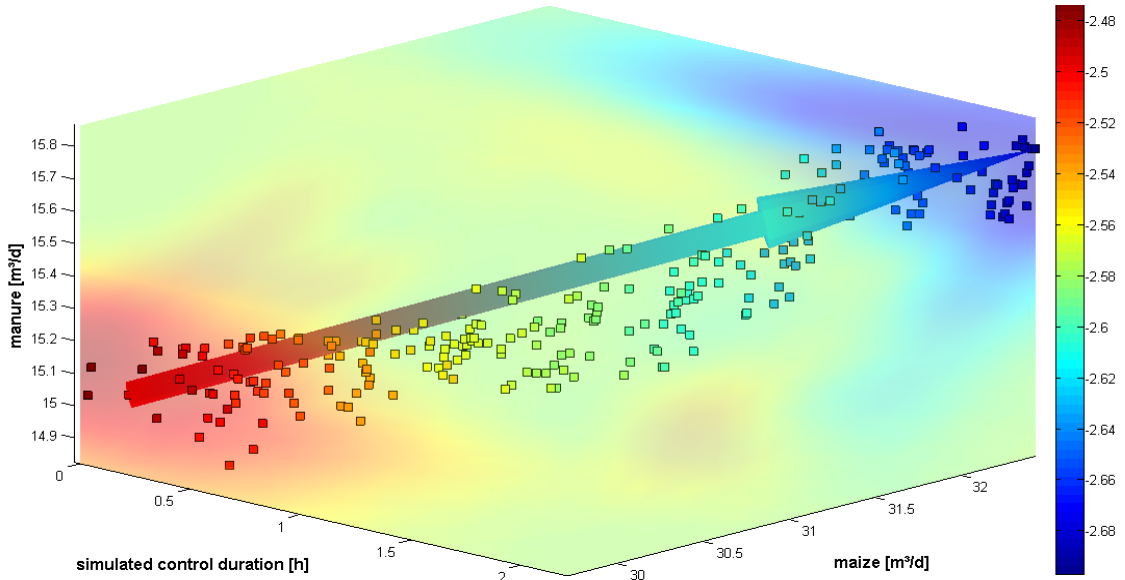
The following figures intend to assess the overall system response throughout the “simulation control time” in accordance to the substrate mixture inlet. Therefore, given the limitation in the available number of axes only the two most important substrates are shown in these plots. In addition, the “simulated control duration axis” represent the actual NMPC optimization time duration in hours and the arrow its growth direction tendency.

Figure 5.7 provide a clear view of how the fitness and the substrate mixtures evolved during the “simulated control duration”, where the arrow indicates a linear trajectory tendency. In this case the substrates feed are to be increased in order to obtain an enhanced biogas production according to the NMPC optimization. Furthermore, the whole NMPC optimization took about two hours in this simulation run, which is quite expected given the small number of iteration  $N$ .



**Figure 5.7:** Test n°10 (Worse) - Evolution of fitness function values against time and substrate feeds of maize and manure (The smaller the value (the colder the color), the better the substrate mix).

Moreover, Figure 5.8 shows how the “cost benefit ratio” and the substrate mixtures evolved during the “simulated control duration”, where the arrow indicates a similar linear trajectory tendency as shown in Figure 5.7.



**Figure 5.8:** Test n°10 (Worse) - Evolution of cost benefit ratio against time and substrate feeds of maize and bull manure (The smaller the value (the colder the color), the better the substrate mix).

Consequently, the linear trajectory shown in the previous figures evidences the actual problem in this simulation test (e.g. test n°10); the NMPC algorithm cannot further improve the system if there is not enough simulation time. This is corroborated by the small substrate mixtures increments throughout the NMPC optimization, e.g. the maize substrate inlet is ranging from 30m<sup>3</sup>/d to 32m<sup>3</sup>/d.

Finally, the NMPC algorithm provides a control strategy that leads the biogas plant to an optimal state. This control strategy or substrate mixture input sequence is shown in figures 5.9, 5.10 and 5.11.

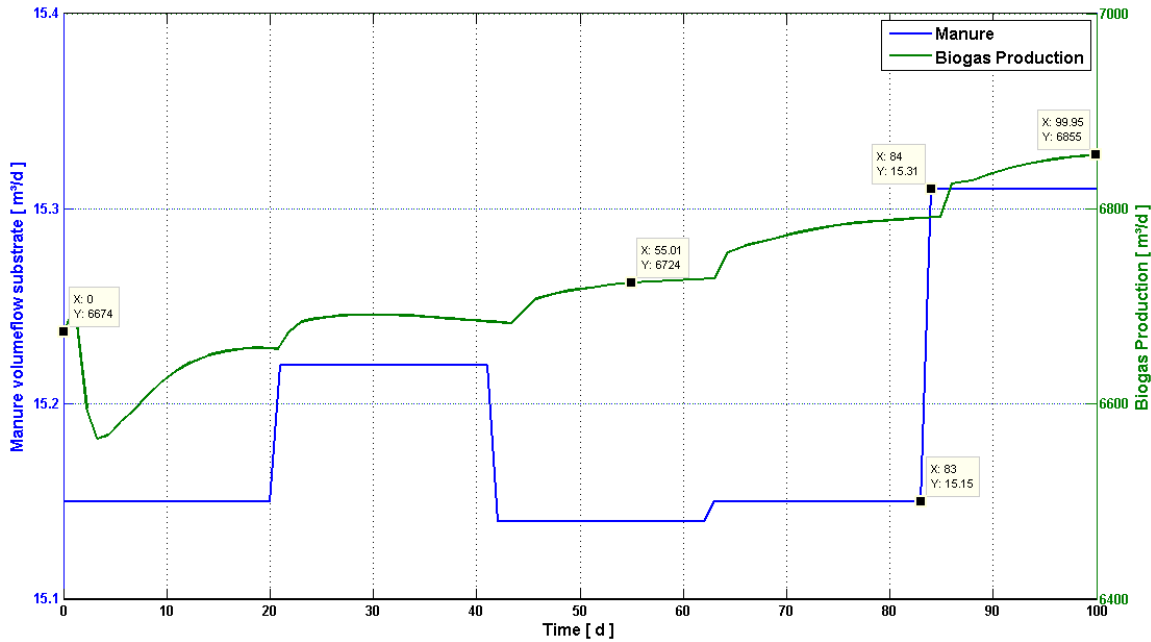


Figure 5.9: Test n°10 (Worse) - Manure stepwise control and biogas production.

These plots illustrate, as well, how the control input sequence affects the biogas production within the fixed time range of one hundred days of control simulation. The small amount steps in combination with a step size increment of one percent induced the system to a poor improvement in the biogas production; the biogas production increased by merely 192 m<sup>3</sup>/d, without reaching its steady state.

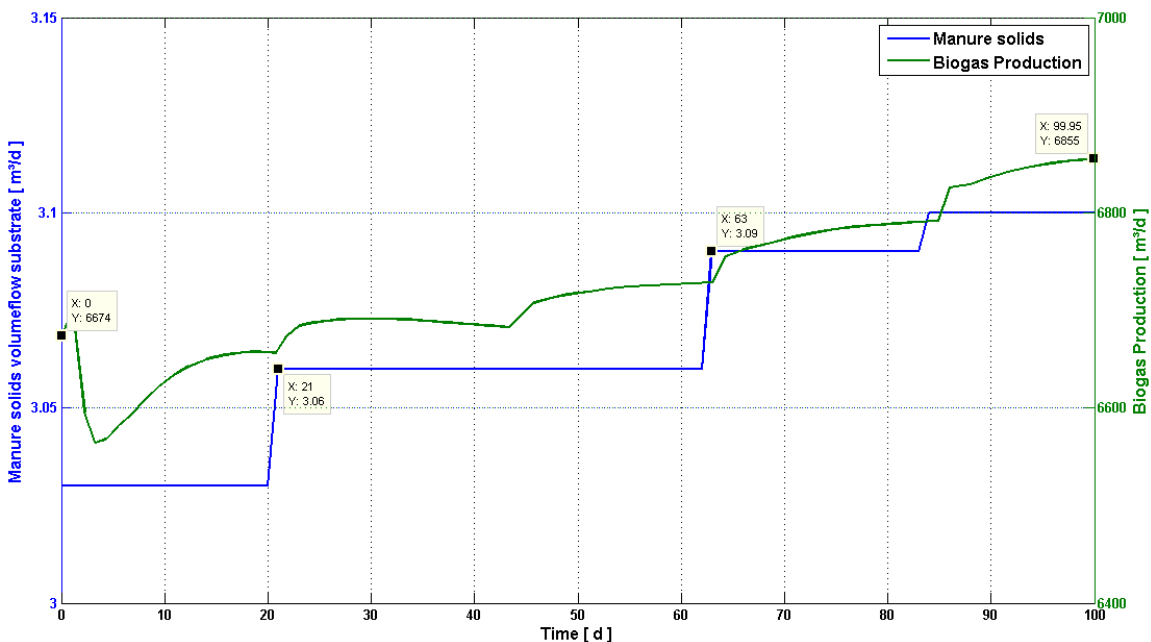


Figure 5.10: Test n°10 (Worse) - Manure solids stepwise control and biogas production.

Additionally, the biogas production curves tend to be irregular and non-smooth since the steps are too small and numerically fewer for a long period of time throughout the NMPC optimization. Moreover, the maize substrate in Figure 5.11 shows a stronger influence in the biogas production as anticipated from Table 1.3 in section 1.3

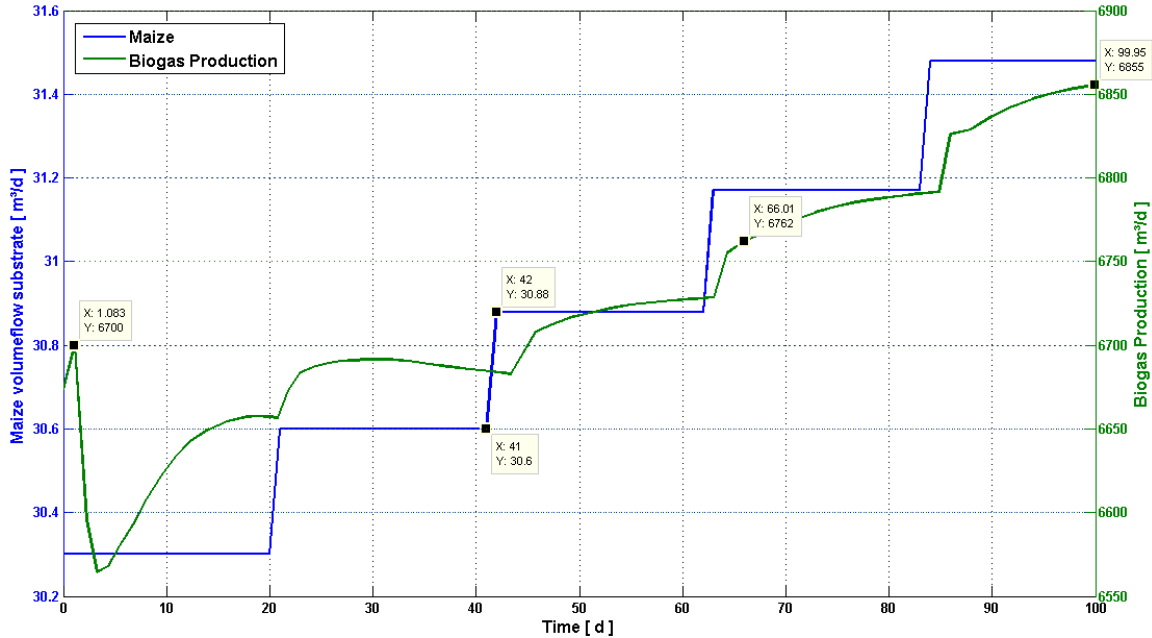


Figure 5.11: Test n°10 (Worse) - Maize stepwise control and biogas production.

### 5.2.2 Best Results

This section presents the best results obtained during the NMPC optimization tests (e.g. Test n° 16 and marked in red on Table A.3); these tests aim is to find an optimal substrate mix sequence of inputs (i.e. control strategy) that will force the system to an optimal state of operation.

Table 5.4: Test n°16 (Best) - NMPC optimization tool settings.

NMPC parameter name	NMPC parameter value	Manipulated variable
Plant model	Sunderhook	
Optimization method	CMAES	
Population size	8	
Number of generations	4	
Prediction horizon time [d]	50	✓
Control horizon time [d]	7	✓
Change type	Percentual [%]	
Change value	5	✓
Number of iterations	15	
Fitness trigger	OFF	

As stated previously, this test was performed in accordance to the pre-established formulation proposed for NMPC optimization tests (i.e.  $N \times T_C$  [d] = 100 days). The settings

utilized in this NMPC optimization test is provided in Table 5.4, followed by the plant's initial states specification in Table 5.2. The initial states represent the plant's substrate mixture inlet at the beginning of the optimization (e.g. the volume flows of manure, maize, etc.).

The following pictures evaluate the best test results according to its final state (biogas production), optimal substrate mix sequence of inputs (i.e. control strategy), overall fitness value and the gained cost benefit ratio.

Figure 5.12 presents the substrate mixture evolution throughout the NMPC optimization with respect to the overall fitness (goodness). In this figure is possible to observe the entire number of simulation runs executed by the CMAES optimization method, where each square represent a simulation run and the arrow its evolution direction. In addition, the color gradient represents the fitness function values progression in this NMPC optimization run, i.e., the smaller the value, the cooler is the color and the better is the result.

Clearly, the arrow trajectory in Figure 5.12 shows a more realistic optimization, in which the substrate mixture tend to increase at the beginning of the optimization to further enhance the biogas production and once the steady state is accomplished it is gradually reduced.

In addition the color gradient is mostly cooler (i.e. blue color) throughout the Figure 5.12, what reflects over the overall fitness improvement of  $-0.1$ . This value might seem small but it actually results in a substantial system's enhancement as can be confirmed by the cost benefit ratio.

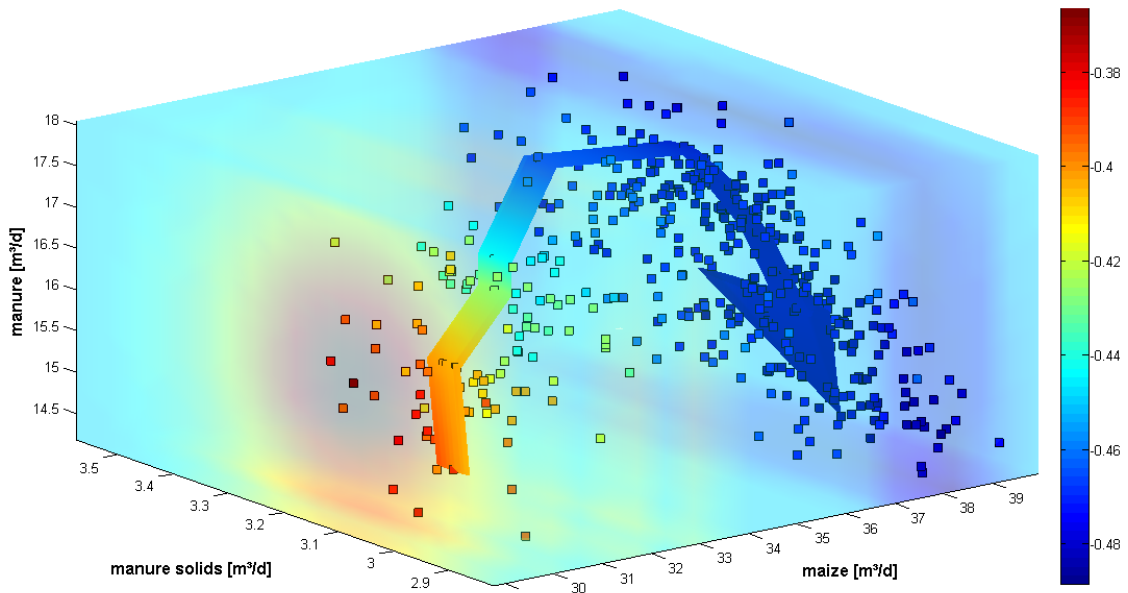


**Figure 5.12: Test n°16 (Best) - Evolution of fitness function values against maize, manure and manure solids substrate feeds (The smaller the value (the colder the color), the better the substrate mix).**

Figure 5.13 shows the substrate mixture evolution in the NMPC optimization with respect to a cost vs. benefit analysis (i.e. cost benefit ratio). This figure presents the overall gained profit at the end of the NMPC optimization, which results in an additional 628 euro per day.

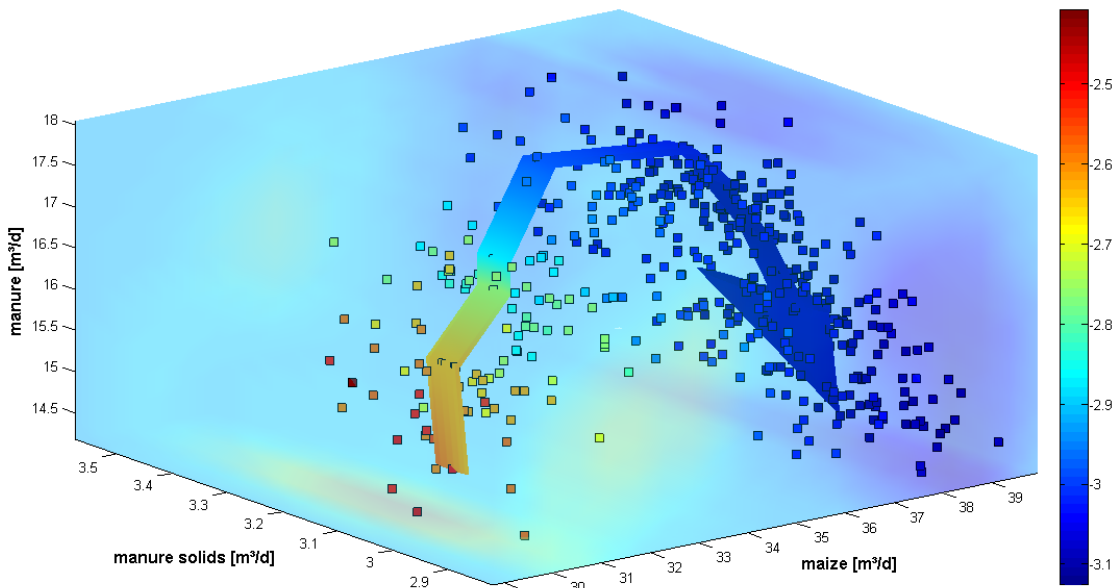


**Figure 5.13:** Test n°16 (Best) - Evolution of cost benefit ratio against maize, manure and manure solids substrate feeds (The smaller the value (the colder the color), the better the substrate mix).

Differently from the previous result (i.e. section 5.2.1), the obtained substrate mixtures in figures 5.12 and 5.13 are much more realistic and show a considerable improvement in the overall fitness (goodness) and the cost benefit ratio. Additionally, this NMPC optimization run was performed with a higher step size ratio, i.e., five percent increment of the substrate feed inlet. Such increment had a strong influence in the optimization outcome and its direction of change, as can be seen in the figures 5.12 and 5.13.

Furthermore, figures 5.14 and 5.15 provide a clear view of how fitness and cost benefit ratio evolved during the simulation run. The “simulated control duration axis” represent the actual NMPC optimization time duration in hours and the arrow its growth direction tendency.

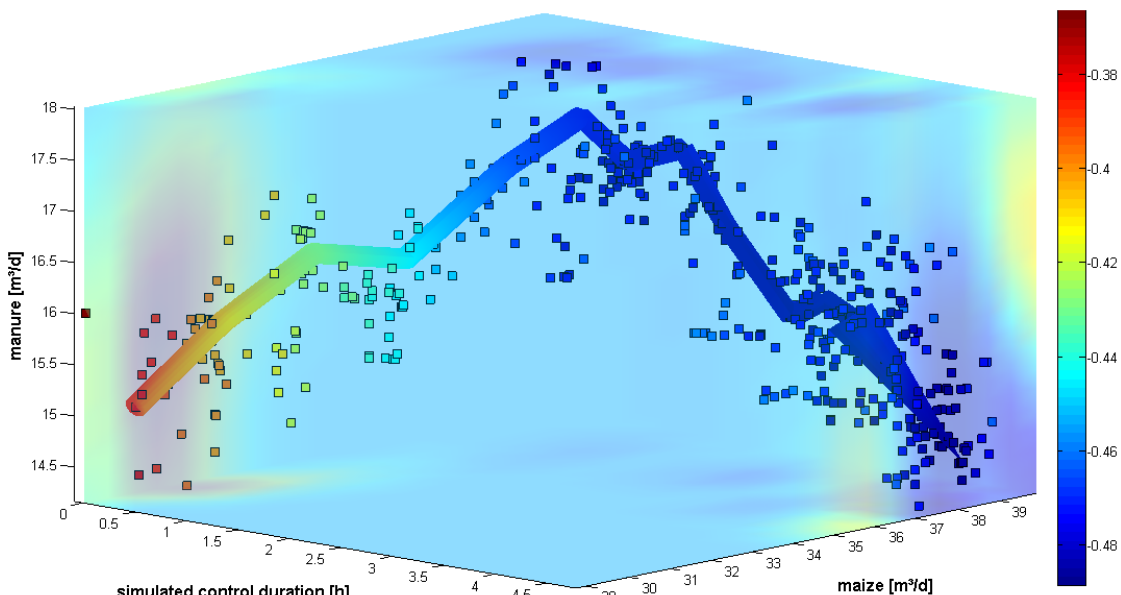


**Figure 5.14:** Test n°16 (Best) - Evolution of fitness function values against time and substrate feeds of maize and manure (The smaller the value (the colder the color), the better the substrate mix).

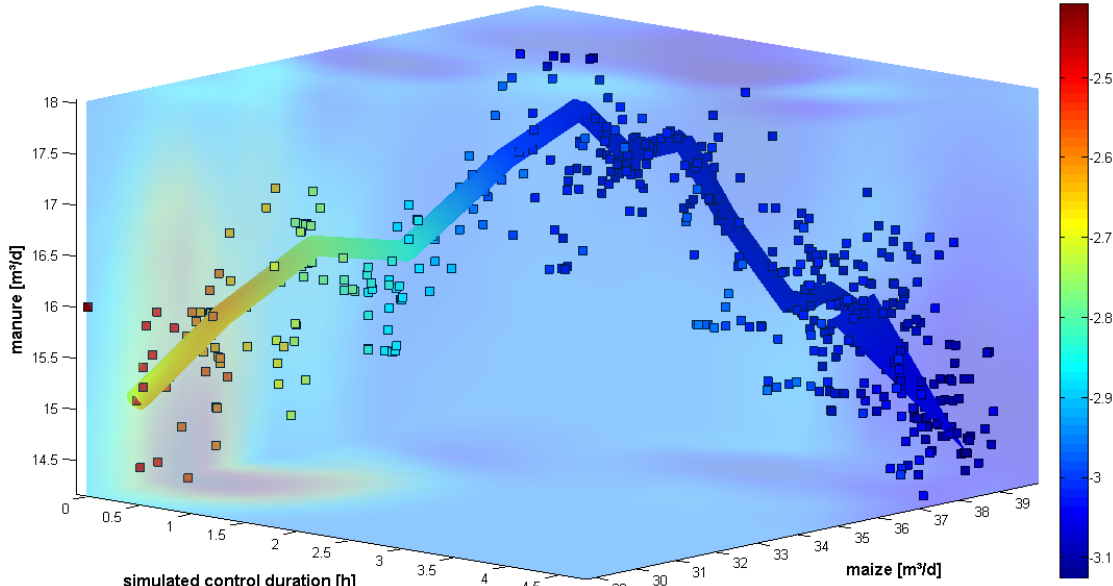


Figure 5.15: Test n°16 (Best) - Evolution of cost benefit ratio against time and substrate feeds of maize and manure (The smaller the value (the colder the color), the better the substrate mix).

Finally, this growth direction tendency given by the arrow dictates how the input sequence of substrates should be executed in order to obtain a better biogas production over the one hundred day control simulation, starting at the biogas plant's original state of operation and concluding at the optimal state calculated by the NMPC optimization algorithm. In addition, the NMPC optimization required approximately five hours to complete the optimization run, which is quite expected given the larger number of iteration  $N$ .

The defined NMPC control strategy is shown in figures 5.16, 5.17 and 5.18, where the combined substrate inlet sequences (e.g. maize, manure and manure solids) accomplished the biogas production steady state at the 45<sup>th</sup> day of simulation control (e.g. see figure 5.16).

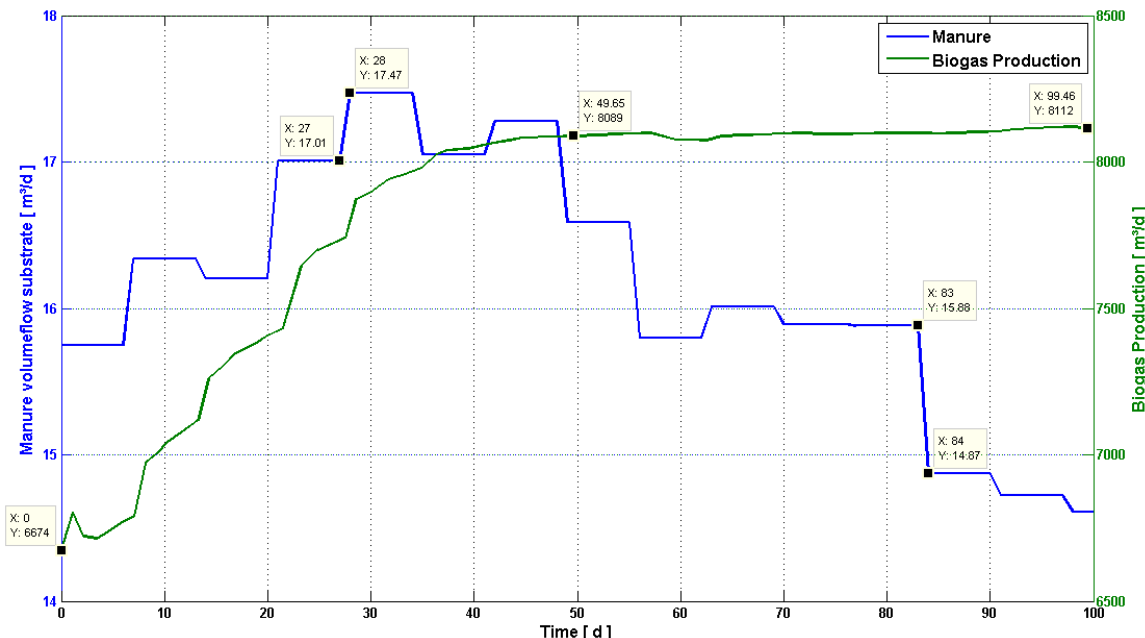


Figure 5.16: Test n°16 (Best) - Manure stepwise control and biogas production.

Figures 5.16, 5.17 and 5.18 illustrate, as well, how the control input sequence affects the biogas production within the fixed time range of one hundred days control simulation. The biogas production improved considerably from its starting point at around  $6673\text{m}^3/\text{d}$  to the optimal biogas production of  $8115\text{m}^3/\text{d}$  (i.e. the steady state). Consequently, a higher number of steps in combination with a bigger step size increment ratio permitted such improvement in the biogas production.

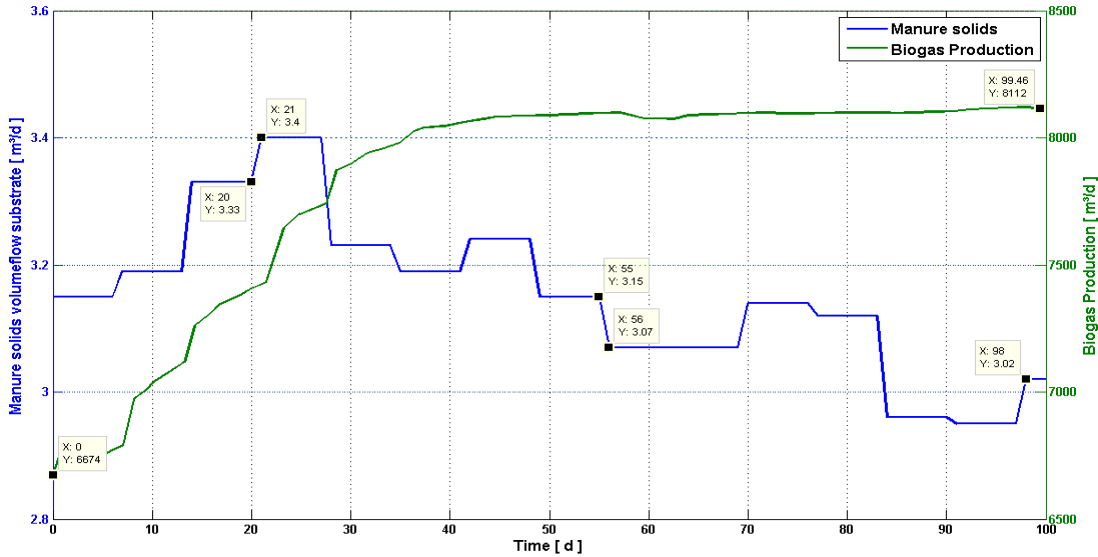


Figure 5.17: Test n°16 (Best) - Manure solids stepwise control and biogas production.

Moreover, figure 5.18 show that the biogas production is strongly influenced by the maize substrate feeds; where, the biogas production (e.g. green curve) almost follows the sequence of maize volume flow inputs (e.g. blue curve). This is expected given the maize substrate higher potential of methane production. Additionally, the manure and manure solids tend to decrease once the steady state is achieved; might be caused by the necessity in reducing the solids concentration to avoid the compromise of the overall substrate mixture and maintain the level o production.

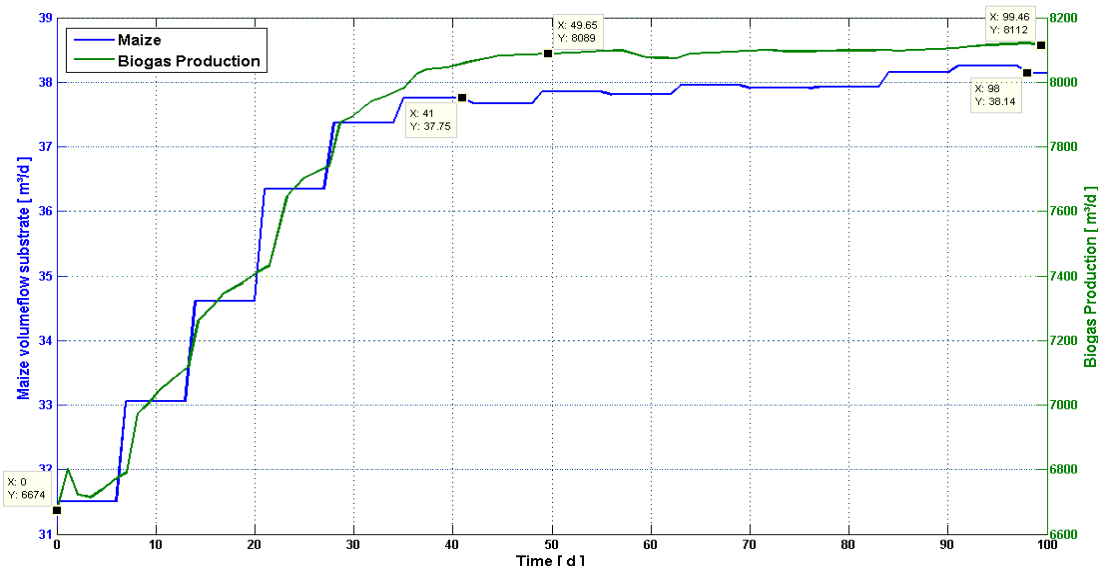
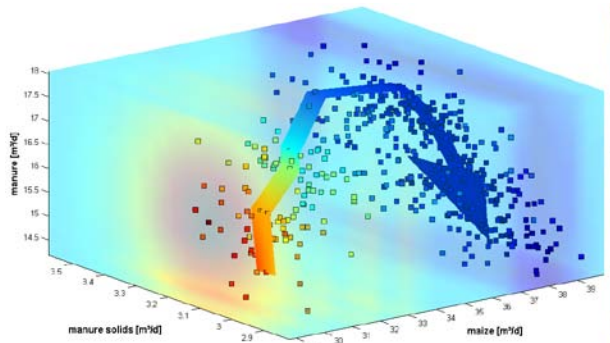


Figure 5.18: Test n°16 (Best) - Maize stepwise control and biogas production.

### 5.2.3 Comparison between Best and Worse results

This section presents the comparison between the best and worse results obtained during the NMPC optimization tests; these tests aim is to find an optimal substrate mix sequence of inputs (i.e. control strategy) that will force the system to an optimal state of operation.

In figures 5.19 and 5.20, the overall fitness improvement with respect to the substrate mixture input sequence is shown. The best result (i.e. figure 5.19) clearly shows that the NMPC optimization performed more tries if compared to the figure 5.20; and also, given the higher step size ratio executed a methodical search in the search space; changing the arrow direction a few times during the optimization. Differently, the worse result shown in figure 5.20 presents only a linear tendency in the improvement direction, which is probably caused by the fewer number of iterations and its small step size ratio used in this test setup. Thus, the overall fitness in both cases was quite different as can be verified by the color gradient of these pictures. The picture on the left (i.e. figure 5.19) is clearly cooler then the figure on the right (i.e. figure 5.20); which translates fitness values progress, with peaks of 0,48 for the best result and 0,41 for the worse result.



**Figure 5.19:** Test n°16 (Best) - Evolution of fitness values against maize, manure and manure solids substrate feeds.

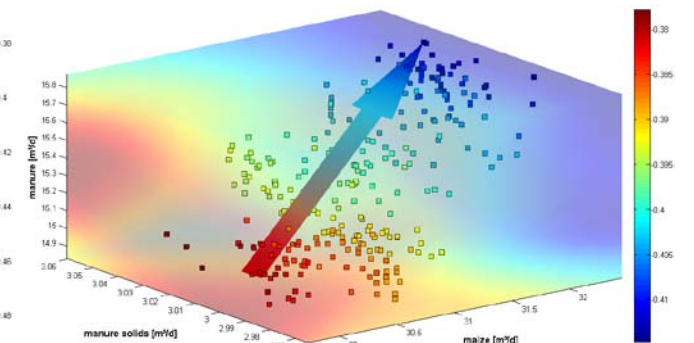


**Figure 5.20:** Test n°10 (Worse) - Evolution of fitness values against maize, manure and manure solids substrate feeds.

Similarly, the same analysis goes for the results shown in the figures 5.21 and 5.22 in which the cost benefit ratio is considered. The result on the left (i.e. 628 €/d in figure 5.21) is economically the best alternative as a control strategy for the biogas plant when compared to the results on the right (i.e. 121 €/d in figure 5.22). Thus, figure 5.21 results in a gained profit five times higher.

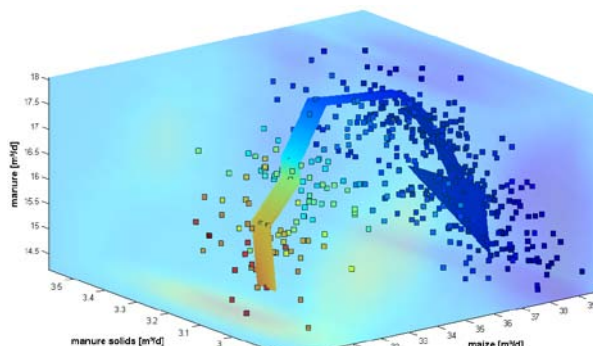


**Figure 5.21:** Test n°16 (Best) - Evolution of cost benefit ratio against maize, manure and manure solids substrate feeds.

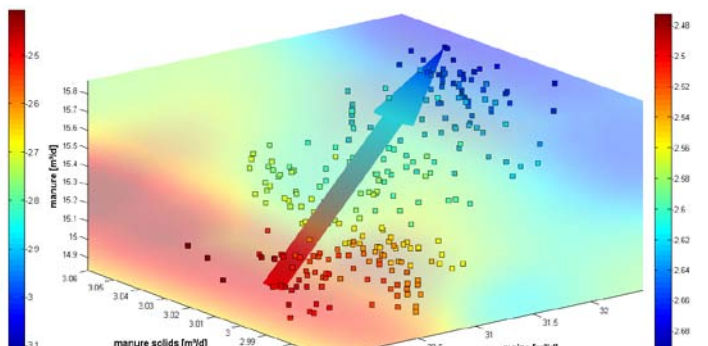


**Figure 5.22:** Test n°10 (Worse) - Evolution of cost benefit ratio against maize, manure and manure solids substrate feeds.

Furthermore, figures 5.23 and 5.24 provide the comparison between the “fitness growth direction tendencies” (i.e. the arrows) against the “simulated control duration” of the best and worse results. This growth direction tendency given by the arrows in these figures indicates merely how the substrate mixture evolves throughout the NMPC optimization and also its overall fitness (goodness) evolution. In addition, figures 5.25 and 5.26 provide the similar analysis for the cost benefit ratio.

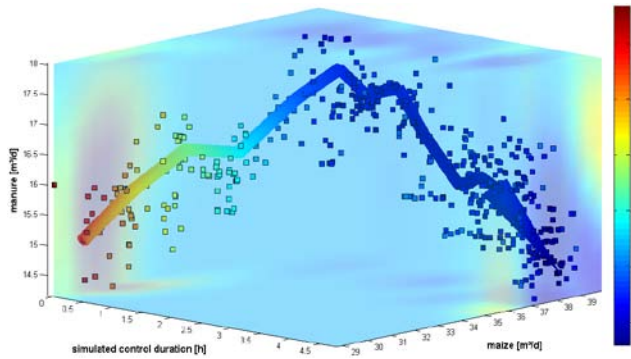


**Figure 5.23:** Test n°16 (Best) - Evolution of fitness function values against time and substrate feeds of maize and manure.

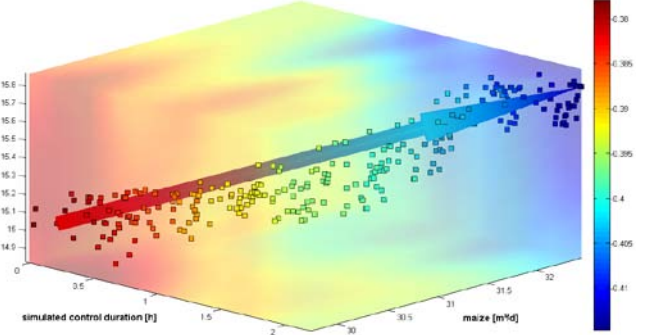


**Figure 5.24:** Test n°10 (Worse) - Evolution of fitness function values against time and substrate feeds of maize and manure.

Moreover, figures 5.23 and 5.25 shows that the optimization will take more computational time to be executed if submitted to higher numbers of iteration and higher step sizes; in the figure 5.23 the optimization took approximately four hours and a half, while in the figure 5.24 it took only two hours. However, “higher computational times” leads to significantly better optimization results as can be seen in the comparison of these pictures, e.g., the cooler color gradient shown by the figures 5.23 and 5.25.

Furthermore, the trajectory pattern in the figures 5.23 and 5.25 shows a more realistic optimization, as previously stated, where the substrate mixture tend to increase at the beginning of the optimization to further enhance the biogas production and once the steady state is accomplished it is gradually reduced.

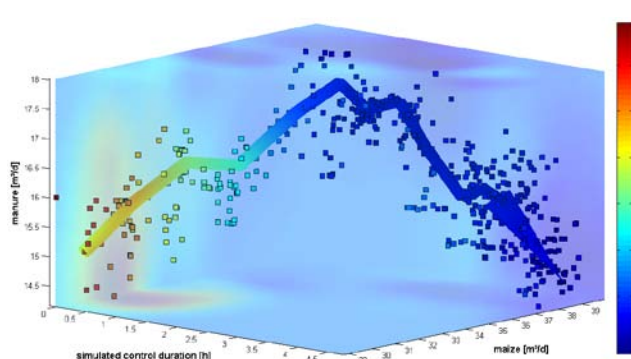


**Figure 5.25:** Test n°16 (Best) - Evolution of cost benefit ratio against time and substrate feeds of maize and manure.

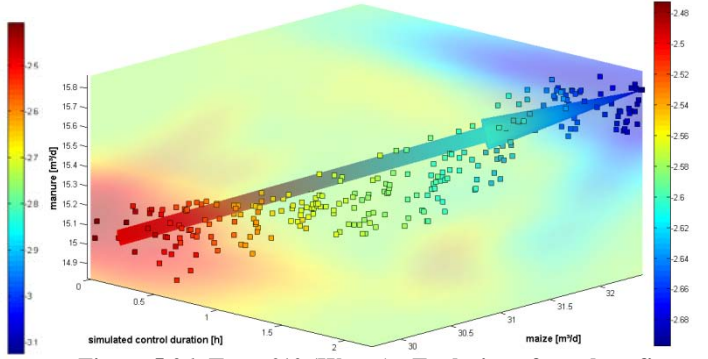
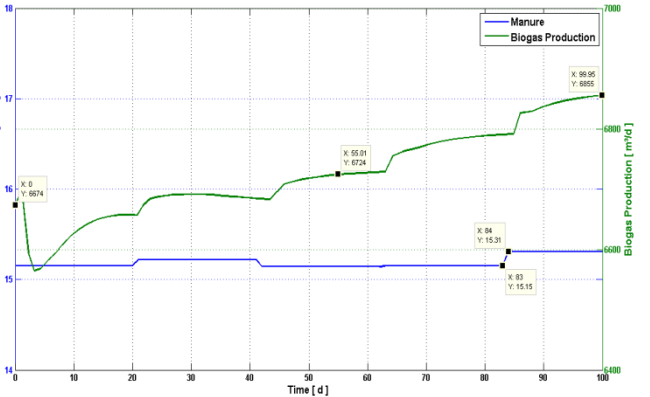
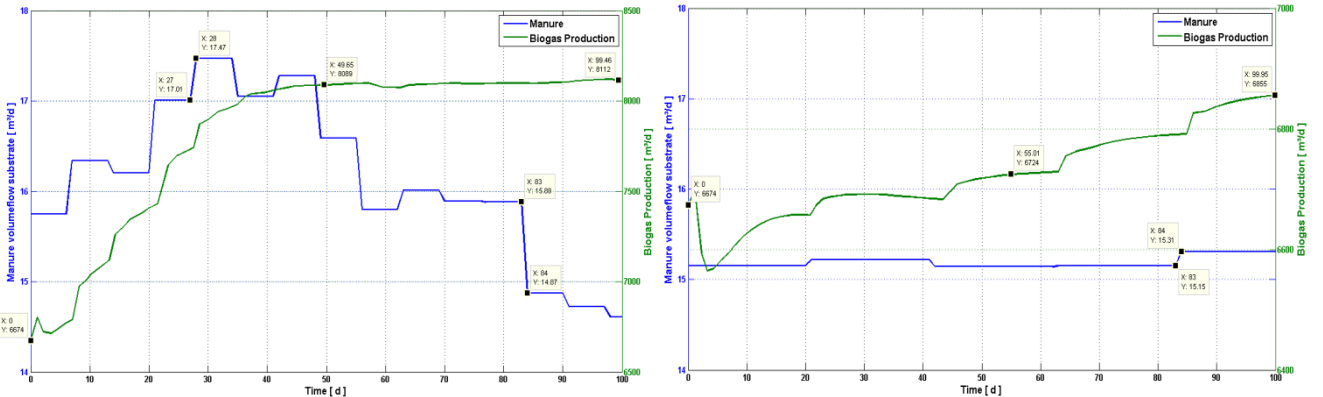


**Figure 5.26:** Test n°10 (Worse) - Evolution of cost benefit ratio against time and substrate feeds of maize and bull manure.

Therefore, it can be concluded that, the number of iterations in the NMPC optimization setup is a key aspect for finding a control strategy which is, economically, the best alternative to increase biogas production. Nevertheless, the time is also another key factor to be considered in the implementation of NMPC online optimization.

Such observation corroborates the fact that the stepwise control shown in the figures 5.27, 5.30 and 5.32 results in a superior biogas production if compared to the stepwise control of the figures 5.28, 5.31 and 5.33; and caused by the higher numbers of iterations.



Higher step sizes will also have an influence in the biogas production and mostly in how fast will the system react. The poor optimization improvement shown in the figures 5.28, 5.30 and 4.32 is a result of small step sizes and fewer “number of iterations”. However, if the system were simulated for longer times (e.g. three hundred days) the biogas production would, eventually, accomplish better results. Figure 5.29 confirms this affirmation, where the NMPC test n°10 (Worse) was submitted to a longer simulation control time. In addition, the NMPC test n°10 accomplished the steady state at around the 180<sup>th</sup> day.

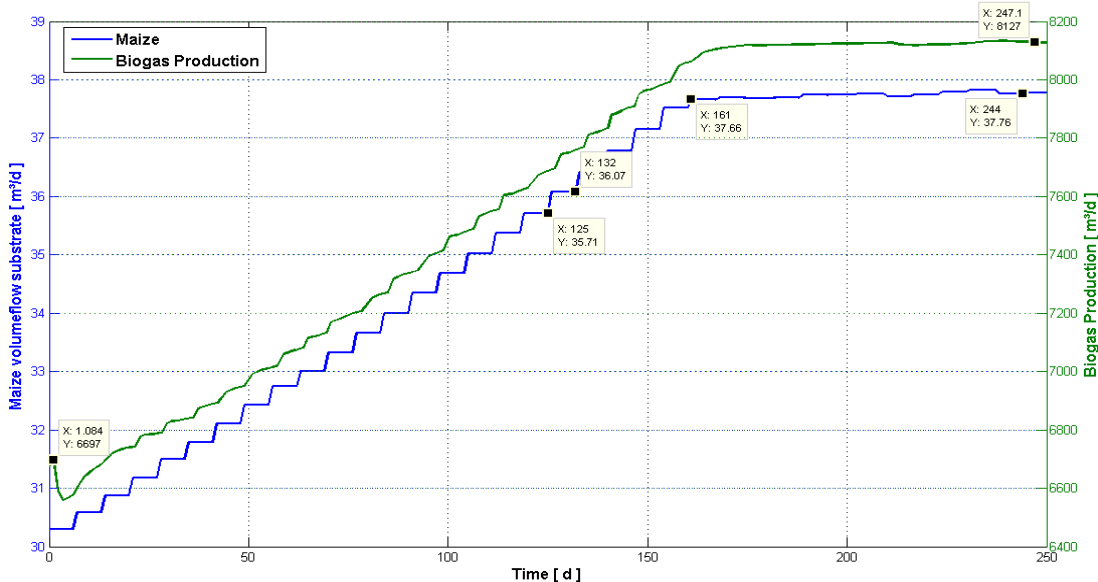


Figure 5.29: Test n°10 (Worse) with NMPC optimization of 250 days- Maize stepwise control and biogas production.

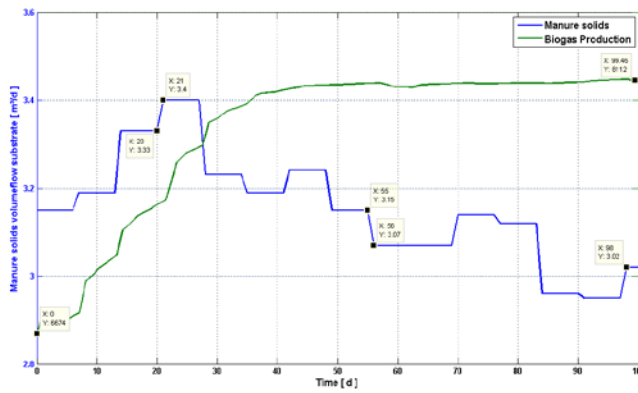


Figure 5.30: Test n°16 (Best) - Manure solids stepwise control and biogas production.

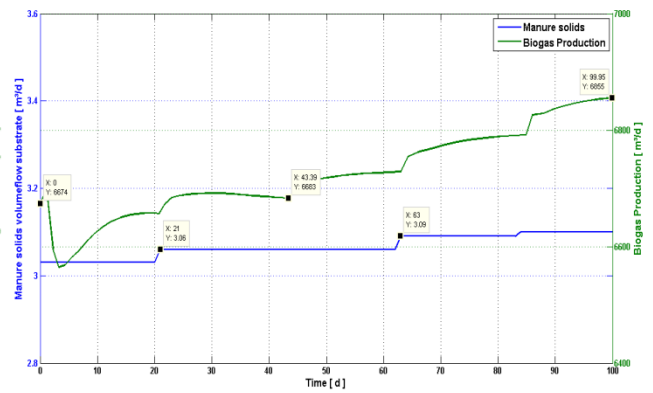


Figure 5.31: Test n°10 (Worse) - Manure solids stepwise control and biogas production.

Moreover, figures 5.31 and 5.32 shows that the biogas production is strongly influenced by the maize substrate in detriment to other substrates, i.e., bigger amounts of maize substrate feed into the biogas plant will lead the system to an higher biogas production; as expected and stated in Table 1.3 in section 1.3.

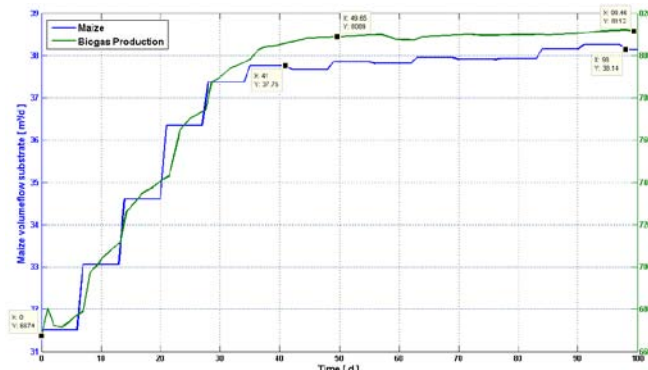


Figure 5.32: Test n°16 (Best) - Maize stepwise control and biogas production.

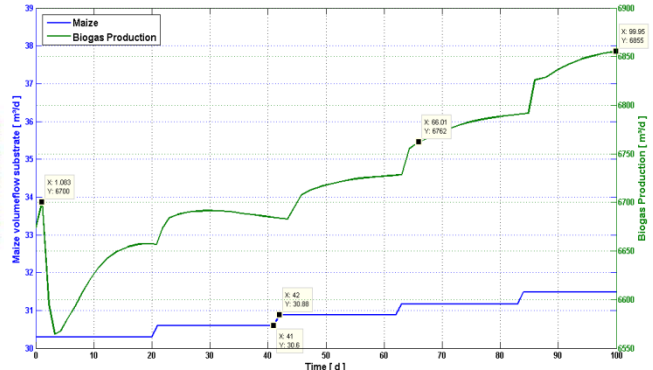


Figure 5.33: Test n°10 (Worse) - Maize stepwise control and biogas production.

To conclude, the stepwise control given in the figures 5.27, 5.30 and 5.32 provides a faster, smoother and economically viable control strategy for the biogas production.

### 5.3 Second Experiment

The purpose of the second experiment is to assess the NMPC efficiency according to different optimization methods, e.g., Particle Swarm Optimization Toolbox (PSO), Covariance Matrix Adaptation Evolution Strategy (CMAES) and Differential Evolution (DE). And additionally, evaluate how the employment of different optimization methods influences the overall response of the controlled system (i.e. Biogas plant).

Table 5.5 illustrates the NMPC optimization setting used in the second set of tests; the “optimization method”, “population size” and “number of generations” (i.e. step size) are the

manipulated variables in these tests. Thus, each test had its manipulated variables modified to check its influence in the NMPC optimization. Appendix B presents further information about these simulation tests results and the NMPC optimization setup.

**Table 5.5: NMPC optimization tool settings in dependence of optimization methods.**

NMPC parameter name	NMPC parameter value	Manipulated variable
Plant model	Sunderhook	✓
Optimization method	CMAES, DE or PSO	
Population size	4, 6, 8 or 10	
Number of generations	2, 4 or 6	
Prediction horizon time [d]	100	
Control horizon time [d]	7	
Change type	Percentual [%]	
Change value	1	
Number of iterations	15	
Fitness trigger	OFF	

As previously mentioned, the initial states are delimited by a maximal and a minimal volume flow inlet to avoid the over feeding of the reactor during the NMPC; this is essential since too much substrate feed can lead the reactor to instability. Table 5.6 shows the initial state configuration for each substrate feed and their limits.

**Table 5.6: NMPC optimization - Substrate mixture initial state.**

Substrate name	Initial state n°1	Maximum substrate	Minimum substrate
	[m <sup>3</sup> /d]	inlet [m <sup>3</sup> /d]	inlet [m <sup>3</sup> /d]
Maize	30	40	20
Silo seepage	1.5	3	1
Manure	15	30	10
Manure solids	3	5	0
Recirculation b/t fermenters	40	40	40

The “optimization method” is great importance in the NMPC algorithm since it takes part in the “prediction horizon” during the NMPC optimization; being responsible to search the whole spectrum of a bounded search space for the best substrate feed ratios that lead to an optimal operating point. The correct tuning of these powerful optimization methods is of crucial to obtain feasible results from the NMPC optimization.

Figure 5.34 presents the NMPC optimization performance according to three different “optimization algorithms” (e.g., CMAES, DE and PSO) and their diverse configurations; which are exposed in Table 5.5. In addition, each method is represented by a different curve as shown in

Figure 5.34; where its “population size” and “number of generations” values were altered in order to evaluate the specific “optimization algorithm” behavior and which method yields the best optimization result. Lastly, the NMPC algorithm performance is described by the overall fitness values that correspond to the color gradient in each curve (e.g. see CMAES curve in Figure 5.34).

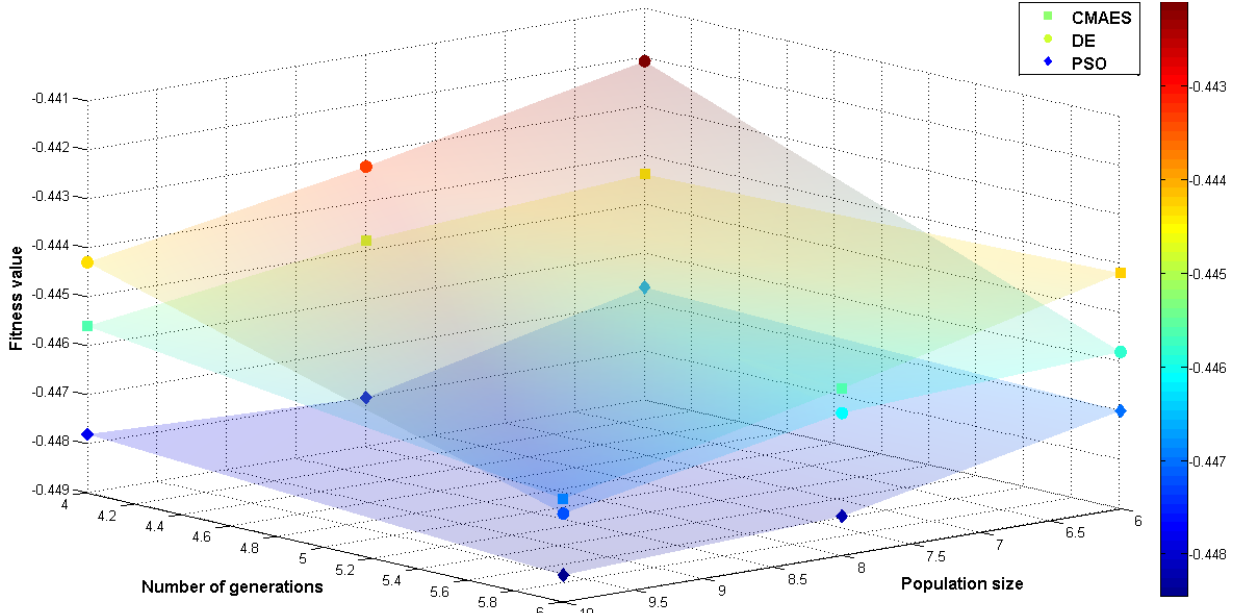


**Figure 5.34: Overall fitness values in dependence of “optimization methods” & method configuration (“population size” and “number of generations”).** The smaller the fitness value (the colder the color), the better is the result.

From Figure 5.34, the DE surface evidences an improvement tendency in the overall fitness response with the increase of “population size” and “number of generations” values. Such observation also applies for the CMAES and PSO surfaces; although the PSO surface presents certain homogeneity of results (i.e. PSO surface is almost linear in some instances).

Furthermore, Figure 5.34 shows that all methods yielded very satisfying results, where PSO was the best. However, the required optimization time is another feature to be observed in these tests. The “optimization methods” influence over the NMPC algorithm’s simulation time is illustrated in Figure 5.35; where the shown color gradient represents the simulated control duration in hours (i.e. smaller simulation times are represented by cooler colors).

PSO is the slowest method (e.g. see Figure 5.35) since it evaluates about 25% more simulations than the other two methods, even though “population size” and “number of generations” was set equally for all three methods. This is due to the fact that PSO does a lot more repetitions of already simulated substrate mixtures to consider possible stochastic influences on the fitness function. Thus, in some occurrences the PSO method required additional time to execute the NMPC optimization, e.g., red shaped diamonds in Figure 5.35 took approximately two hours in comparison to other methods.

Accordingly, the DE and CMAES optimization methods are faster than the PSO method at all instances as shown in Figure 5.35. In addition, DE is the least time consuming method.

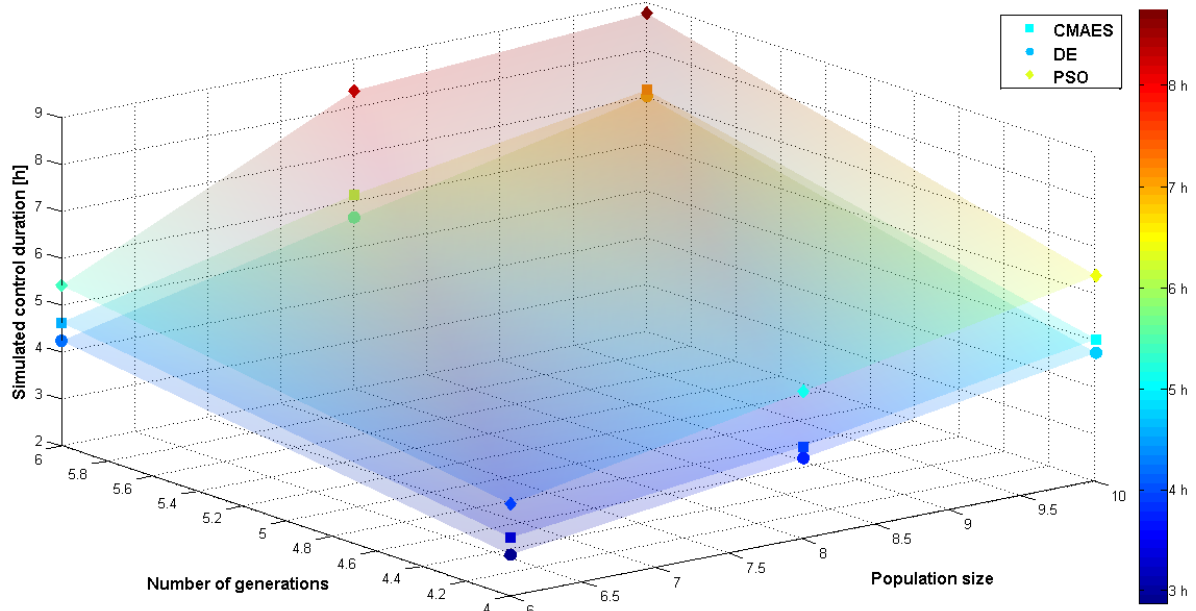


Figure 5.35: Simulated control duration in dependence of “optimization methods” & method configuration (“population size” and “number of generations”). The color gradient represents the simulated control duration in hours [h].

Moreover, Figure 5.36 presents the connection between the overall fitness value and the NMPC simulation times; where the color gradient represents overall fitness value (i.e. better fitness values are symbolized by cooler colors). The surfaces in Figure 5.36 demonstrate that higher computational times produce better system responses (i.e. overall fitness value). Along with this, more simulation time means more optimization runs performed by the NMPC algorithm (e.g. PSO surface in Figure 5.36).

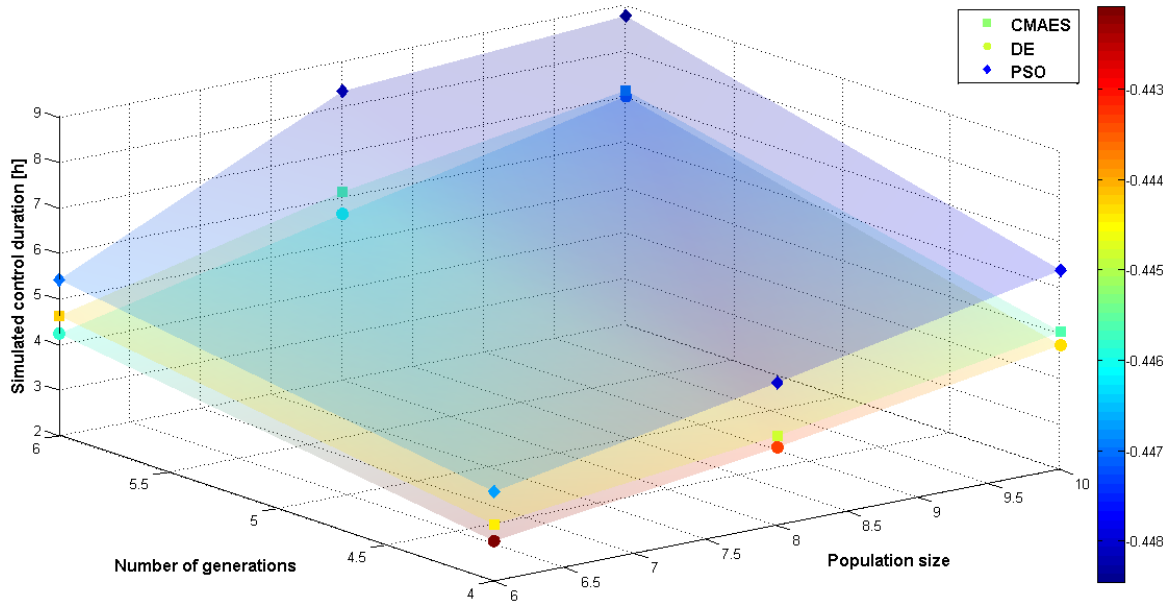


Figure 5.36: Overall fitness values in dependence of “optimization methods”, method configuration (“population size” and “number of generations”) and simulated control duration. The color gradient represents the overall fitness values.

Nevertheless, the number of optimization runs depends on the “population size” and “number of generations” values. Thus, the NMPC optimization time and performance is directly proportional to the chosen “optimization method” in combination to the “population size” and “number of generations” values.

Hence, given the exposed simulation results (i.e. simulated control times are quite closer to each other) it can be concluded that all three methods are about equally suitable for the NMPC optimization, where the NMPC performance increases with the “number of generations” and “population sizes”; and as well, the increase of simulation control times.

## 5.4 Third Experiment

The third experiment has the objective of assess the fitness trigger option in the NMPC algorithm and how this option improves the overall optimization performance. The fitness trigger consists of an extra feature developed for the NMPC optimization tool; its purpose is to evaluate the fitness values throughout the NMPC optimization and take action if the overall system’s response has not improved in the last five NMPC iterations. This action involves increasing (i.e. +Inf), decreasing (i.e. -Inf) or adding by a constant the step size value (i.e. substrate mixture feed) in the NMPC stepwise control.

Thus, the fitness trigger option tries to further improve the optimization for the cases in which the system reached its optimal state or if the selected parameters could not enhance system’s response.

To accomplish the analysis of the fitness trigger option, a new set of tests were performed; where this new test set comprises two kinds of scenarios. The first has the fitness trigger disabled and the second has the fitness trigger enabled; and both having a fixed step size of one percent (e.g. see Table 5.7).

Accordingly, the third experiment has different “prediction horizon time” and “control horizon time” setups (e.g. see Table 5.7) in order to assess the whole optimization spectrum. In addition, these tests have a fixed overall number of simulations for the control horizon (i.e. “Number of iterations” $\times$ “Control horizon [d]” = 100 days).

Table 5.7 illustrates the NMPC optimization setting used in the third set of tests; the “prediction horizon time”  $T_P$ , “control horizon time”  $T_C$  and “fitness trigger option” are the manipulated variables in these tests.

**Table 5.7: NMPC optimization tool settings for fitness trigger option evaluation.**

NMPC parameter name	NMPC parameter value	Manipulated variable
Plant model	Sunderhook	
Optimization method	CMAES	
Population size	8	
Number of generations	4	
Prediction horizon time [d]	50, 100 or 150	✓
Control horizon time [d]	3, 7, 14 or 21	✓
Change type	Percentual [%]	
Change value	1	
Number of iterations	$N = \text{round}\left(\frac{100}{\text{Control horizon [d]}}\right)$	
Fitness trigger	ON, OFF	✓
Fitness trigger value	+Inf	

The initial states utilized for the third experiment tests are exposed in Table 5.8. 0 presents further information about these simulation tests results and the NMPC optimization setup.

**Table 5.8: NMPC optimization & Fitness trigger evaluation - Substrate mixture initial state.**

Substrate name	Initial state n°1	Maximum substrate	Minimum substrate
	[m <sup>3</sup> /d]	inlet [m <sup>3</sup> /d]	inlet [m <sup>3</sup> /d]
Maize	30	40	20
Silo seepage	1.5	3	1
Manure	15	30	10
Manure solids	3	5	0
Recirculation b/t fermenters	40	40	40

Correspondingly, Figure 5.37 presents the overall fitness (goodness) evolution according to the different scenarios designed for the NMPC algorithm assessment, as exposed in Table 5.7.

Test curve one (e.g. see Figure 5.37) represents the overall fitness evolution with the fitness trigger disabled, while test curve two shows the same tests configuration but with the fitness trigger enabled. From now on, these curves will be referenced as: test curve n°1 (fitness trigger OFF) and test curve n°2 (fitness trigger ON).

Test curve n°1 is used here as a reference to determine the NMPC algorithm performance when utilizing its fitness trigger parameter. Thus, test curve n°2 (e.g. Figure 5.37) evidences a clear improvement of the system response in comparison to the test curve one, as shown by cooler gradient and reduced fitness values throughout test curve n°2. Such improvement is caused by the fitness trigger that induces step size increments throughout the NMPC stepwise control.

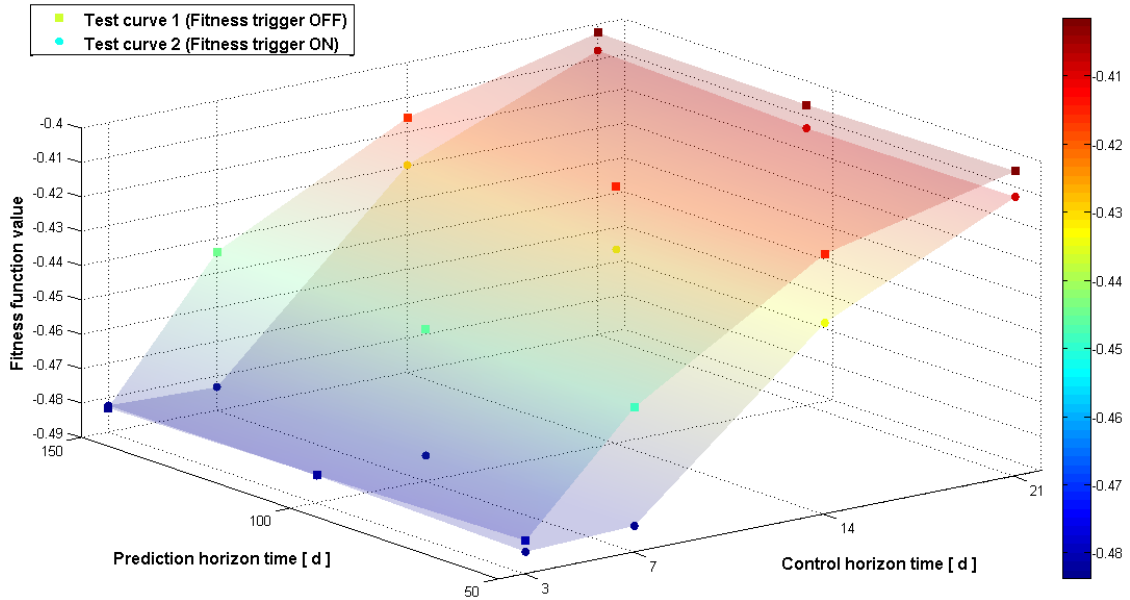


**Figure 5.37:** Stepwise control evaluation versus fitness function values and fitness trigger active (The smaller the value (the colder the color), the better the result).

Furthermore, the Figure 5.38 illustrates the required simulation time by NMPC optimization in relation to the fitness trigger scenarios (i.e. enabled or disabled); where the color gradient is the simulated control time.

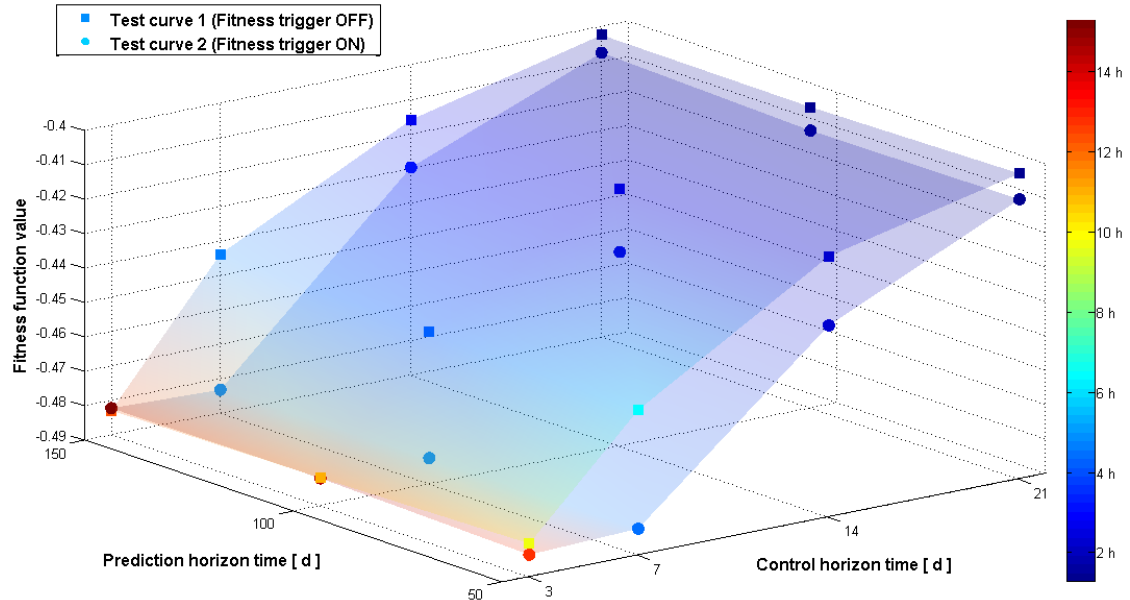


**Figure 5.38:** Stepwise control evaluation versus simulated control duration and fitness trigger active. The color gradient represents the simulated control duration in hours [h].

Figure 5.38 show that the NMPC optimization of biogas plants reaches the global optimum much faster when the fitness trigger is enabled. The rapidly improvement in the fitness values is also illustrated by the cooler color gradient in test curve two.

In order to numerically measure the improvement provided by the fitness trigger option, a fitness error percentage is provided in Table 5.9. This error percentage represents the overall

enhancement difference among the fitness values of all data sets, i.e., test results between test curve n°1 and n°2. In addition, fitness error percentage is a negative value since it corresponds to the overall fitness reduction [%] once the fitness trigger is employed.

**Table 5.9: Fitness error percentage [%] of NMPC optimization with fitness trigger.**

Prediction Horizon \ Control Horizon	Number of iterations	50	100	150
3	34	-0.66 %	-0.02 %	0.14 %
	15	-8.04 %	-7.62 %	-8.12 %
	7	-4.6 %	-4.24 %	-3.21 %
	5	-1.82 %	-1.67 %	-1.26 %

Hence, from Table 5.9 it can be seen that the NMPC optimization in combination with the fitness trigger enabled could, in some instances, improve the biogas production considerably (e.g. with a maximum of 8.12%).

Evidently, the tests executed with intermediary number of iterations (e.g. seven and fifteen) could be further improved. However, higher number of iterations (e.g. 34) resulted in no actual improvement in the biogas production since the reference (i.e. test curve one) was already at the global optimum for these test sets.

Therefore, the enhancement in the fitness values tends to increase with the number of NMPC iterations  $N$  (e.g. see  $N$  formulation in Table 5.7). This is expected, since the raise in the number of iterations  $N$  also increases the probability in which the fitness trigger will interfere in the NMPC optimization. On the other hand, the fitness trigger cannot further improve biogas production if the global optimum has already been reached.

Moreover, the figures 5.39, 5.40 and 5.41 presents the NMPC stepwise control in which the fitness trigger parameter obtained its best improvement in the biogas optimization (e.g. Test n°6 in Table 5.9). This test had a 8.12% reduction in the overall fitness value followed by the decrease on the required simulation control time, as shown previously in Figure 5.38. In addition, these figures also provide the comparison between the NMPC stepwise control with and without the fitness trigger.

As can be seen in the figures 5.39, 5.40 and 5.41, the NMPC stepwise control is quite different when the fitness trigger is either enabled (e.g. blue lines) or disabled (e.g. red lines). A closer survey of these control strategies, leads to the conclusion that the fitness trigger allows the enlargement of the search space within the NMPC optimization. Thus, the blue stepwise control presents higher steps if compared to the red stepwise control.

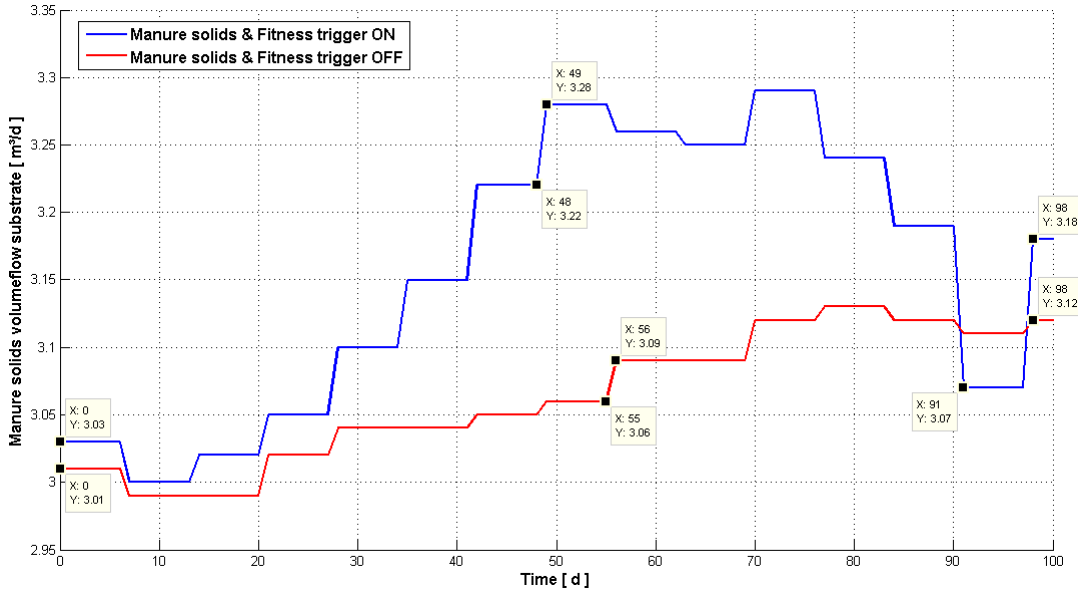


Figure 5.39: Test n°6 (Best) - Manure solids stepwise control with and without fitness trigger option (Test n°6 set n°1 and Test n°6 set n°3).

This search space enlargement is achieved throughout the increase in the step size. Conversely, the fitness trigger can also be configured to decrease the step size (e.g.  $-\text{Inf}$  or  $-100 \text{ m}^3/\text{d}$ ). Such possibility is useful for NMPC optimizations in which the used step size is very large.

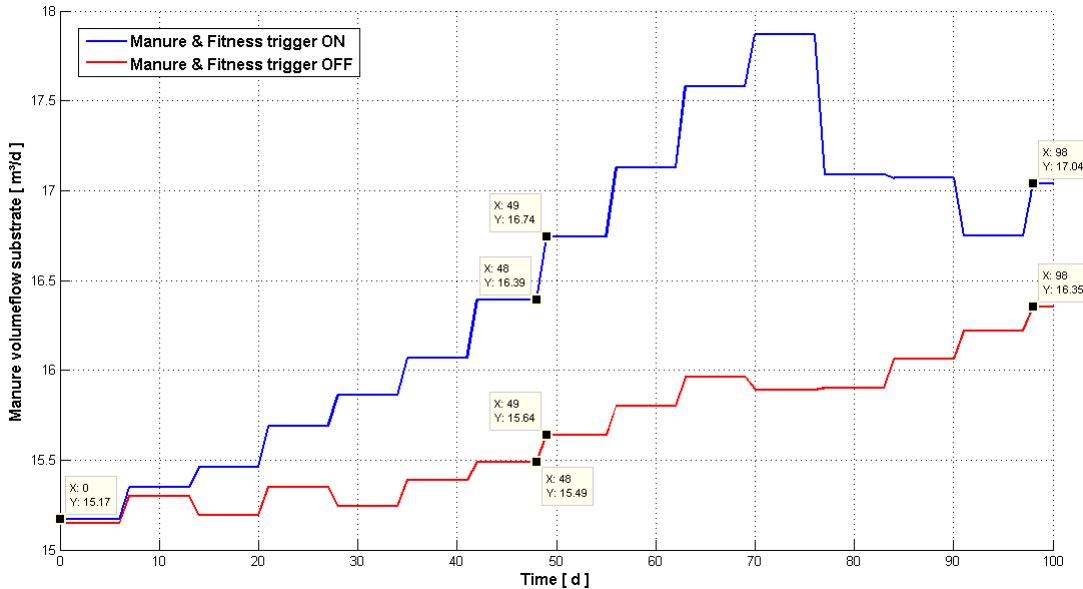


Figure 5.40: Test n°6 (Best) - Manure stepwise control with and without fitness trigger option (Test n°6 set n°1 and Test n°6 set n°3).

On the other hand, the simulation results presented here have small step sizes; and as a consequence, it is preferable to configure the fitness trigger option to increment the step size.

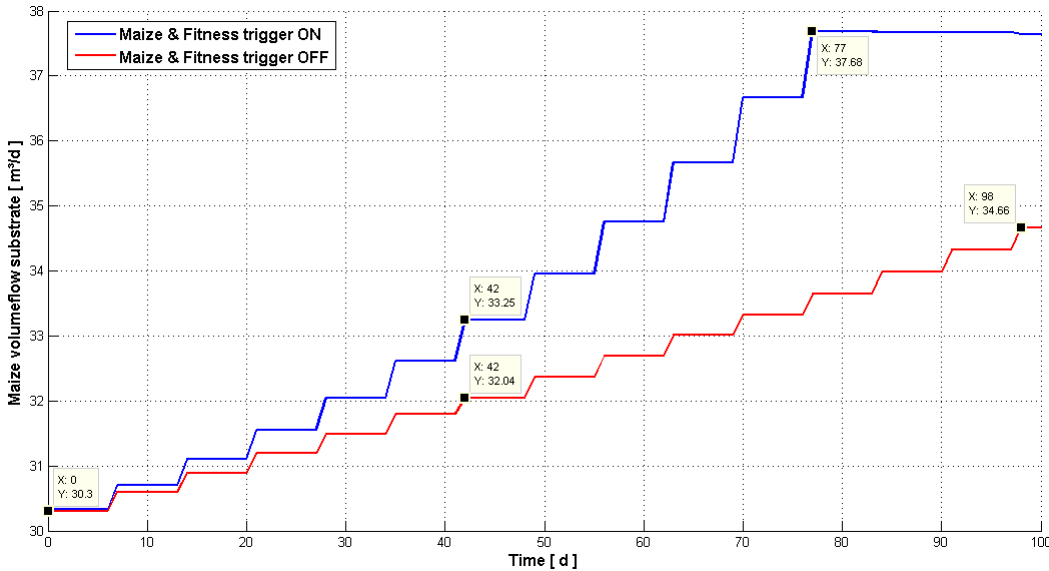


Figure 5.41: Test n°6 (Best) - Maize stepwise control with and without fitness trigger option (Test n°6 set n°1 and Test n°6 set n°3).

Finally, the fitness trigger option has shown to be quite useful to further improve the NMPC optimization; and as well, reduce the simulation times in the NMPC algorithm. Such enhancement can be easily seen through the increase in biogas production as illustrated in figure 4.40; where the blue stepwise control (i.e. fitness trigger enabled) has increased the biogas outlet by approximately  $800 \text{ m}^3/\text{d}$ .

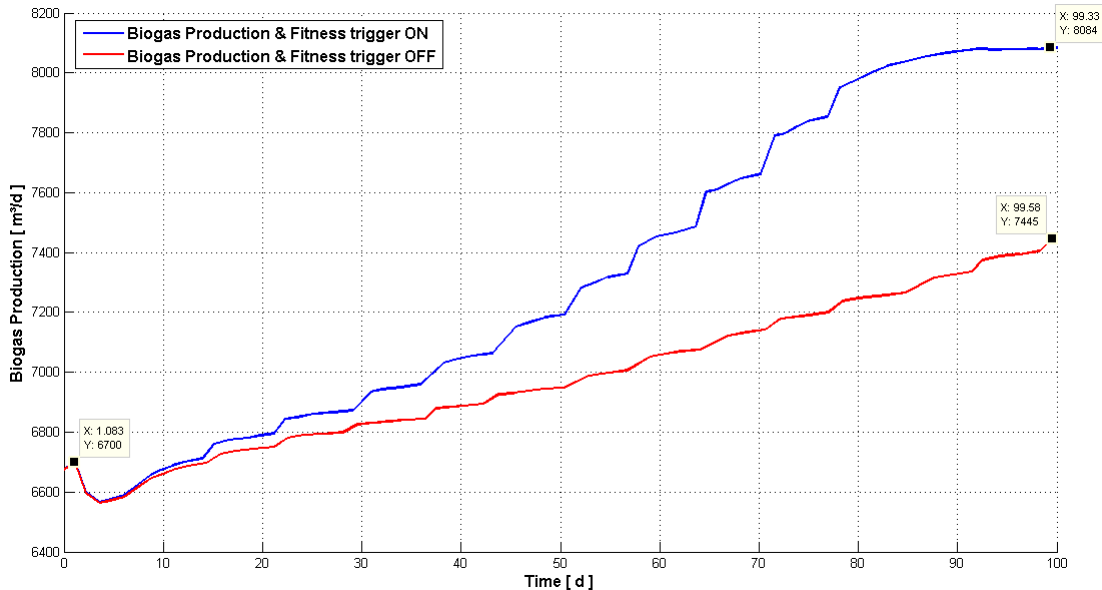


Figure 5.42: Test n°6 (Best) - Biogas production optimization with and without fitness trigger option (Test n°6 set n°1 and Test n°6 set n°3).

Such increment in the biogas production results in an additional profit of  $618\text{€}/\text{d}$  for the fitness trigger enabled optimization, while the original NMPC optimization (i.e. fitness trigger disabled) comprehends only  $379\text{€}/\text{d}$ .

## 5.5 Fourth Experiment

The fourth experiment intention is to assess the NMPC optimization tool reliability. Basically, the NMPC algorithm must be able to achieve similar results if identical parameter configuration is submitted.

Obviously, these NMPC optimization results are evaluated according to acceptable error divergences given the random nature of the employed “optimization methods” in the NMPC algorithm (e.g. CMAES, PSO, GA).

The methodological procedure used in this experiment consists of executing the NMPC optimization for various times and verify the stepwise control discrepancy between different runs and also ascertain the overall response of the controlled system. Table 5.10 illustrates the NMPC optimization setting used in the fourth experiment tests; where every parameter is constant. 0 presents further information about these simulation tests results and the NMPC optimization setup.

**Table 5.10: NMPC optimization tool settings for reliability assessment.**

NMPC parameter name	NMPC parameter value	Manipulated variable
Plant model	Sunderhook	
Optimization method	CMAES	
Population size	8	
Number of generations	4	
Prediction horizon time [d]	50	
Control horizon time [d]	7	
Change type	Percentual [%]	
Change value	5	
Number of iterations	15	
Fitness trigger	OFF	

Accordingly, the fourth experiment set of tests utilizes the same initial states as displayed in Table 5.11, which dictates the operation state of the biogas plant’s reactor.

**Table 5.11: Substrate mixture initial state.**

Substrate name	Initial state n°1	Maximum substrate	Minimum substrate
	[m <sup>3</sup> /d]	inlet [m <sup>3</sup> /d]	inlet [m <sup>3</sup> /d]
Maize	30	40	20
Silo seepage	1.5	3	1
Manure	15	30	10
Manure solids	3	5	0
Recirculation b/t fermenters	40	40	40

In addition, the parameter configuration shown in Table 5.10 comprehends the configuration setting of the best NMPC optimization ever achieved during the NMPC algorithm evaluation (i.e. test n°16 in section 5.2.2). This test is the reference to estimate how reliable the proposed NMPC algorithm is.

Table 5.12 exhibits the two parameters utilized to appraise the NMPC algorithm, they are: the fitness percentage error and the cost benefit absolute error. The cost benefit absolute error concerns the cost benefit difference between the reference test and the actual test (e.g. test n°3 in Table 5.12). In reality, it represents the amount of capital that would be gained or lost if the new NMPC control strategy is employed in detriment to the reference's NMPC control strategy. While the fitness percentage error comprises a value in which the NMPC optimization either improved or deteriorated in relation to the reference fitness test.

Hence, values have shown (e.g. see Table 5.12) an increase in the fitness values with a maximum value 0.52 % of and a minimum of 0.04 %. Thus, in relation to the reference test the NMPC algorithm could not overcome or reproduce the original fitness value. Such occurrence is due to fact that the original test is extremely close to the biogas plant's "global optimum".

Nevertheless, this increase is tolerable since it is reasonably small (i.e. lower than one percent for all simulation tests) and has no substantial repercussions on the capital gains. The Cost benefit absolute error ranges from an eleven euro per day loss to a one euro per day gain, in relation to the reference test.

**Table 5.12: Reliability assessment error of NMPC optimization.**

Substrate name	Fitness percentage error	Cost benefit absolute error
Test n° 1	0.19 %	-3 €d
Test n° 2	0.04 %	-1 €d
Test n° 3	0.52 %	-11 €d
Test n° 4	0.04 %	+1 €d
Test n° 5	0.08 %	-1 €d
Test n° 6	0.25 %	-1 €d
Test n°7	0.49 %	-10 €d

Furthermore, this behavior is anticipated in view of the fact that CMAES method is an evolutionary strategy (ES) class of algorithm, and by definition is a nondeterministic method. Ergo, the calculated control strategies for every new run of the NMPC optimization will not be alike. Consequently, it results in outcome disparities throughout the optimization, although the final optimization result (i.e. at the steady state) is within the range of acceptance (e.g. see Table 5.12).

The following figures present the NMPC stepwise control comparison between best (i.e. test n° 4), worse (i.e. test n° 3) and reference test (i.e. test n°16 in section 5.2.2) as shown in Table 5.12.

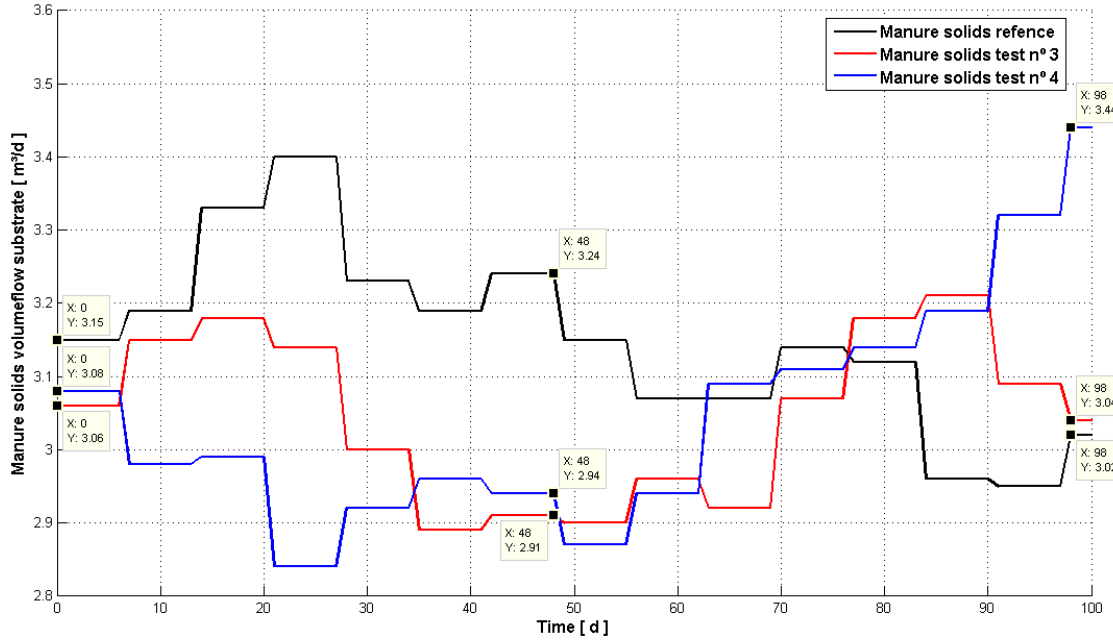


Figure 5.43: Manure solids control strategy & reliability assessment of NMPC optimization.

Figure 5.43 displays the manure solids stepwise control for every optimization run, where their discrepancies are noticeably displayed. The same observation applies for the manure stepwise control shown in Figure 5.44 and also for the maize stepwise control shown in Figure 5.45.

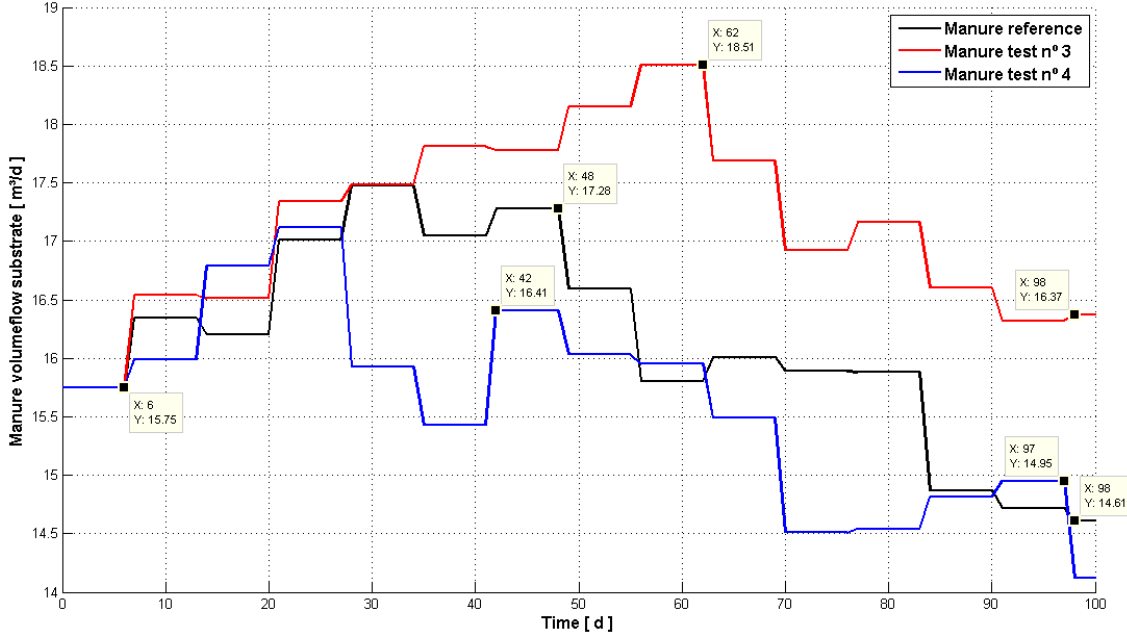


Figure 5.44: Manure control strategy & reliability assessment of NMPC optimization.

Evidently, the NMPC control strategies displayed in figures 5.43, 5.44 and 5.45 are entirely different from one test run to the other. Thus, it exposes the nondeterministic nature of the employed optimization methods.

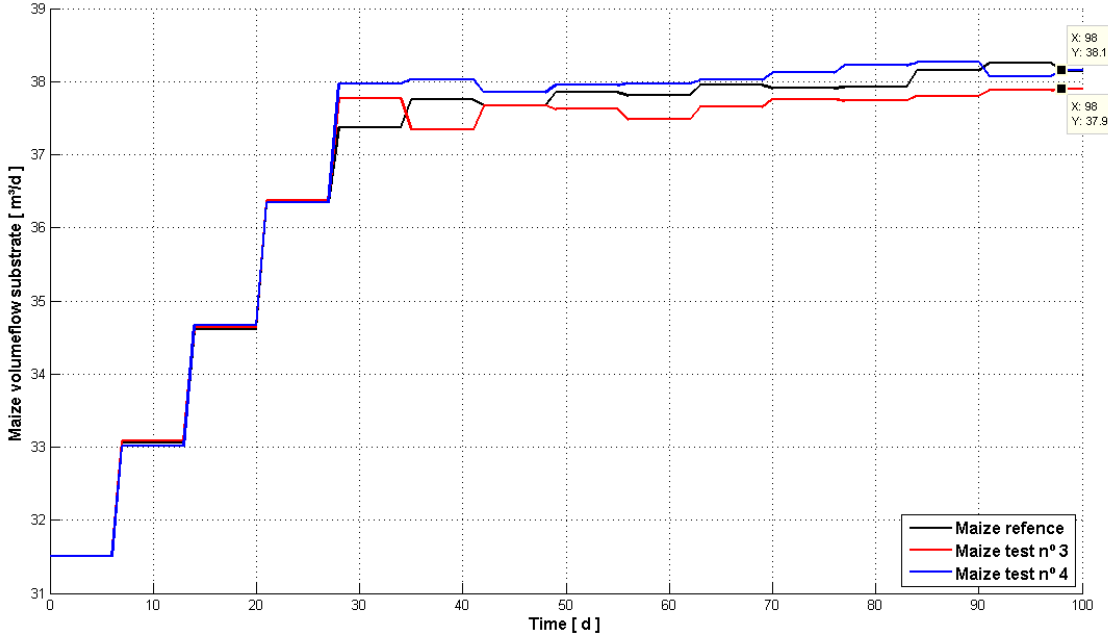


Figure 5.45: Maize control strategy & reliability assessment of NMPC optimization.

Nonetheless, this nondeterministic nature is overcome by the combination of influences of each substrate stepwise control as can be seen in Figure 5.46. Thus, independently of the chosen control strategy the optimal biogas production is accomplished. This can be only achieved through the fitness function that indicates which combination of inputs (e.g. substrate mixture inlet) is better suited to optimize the biogas production.

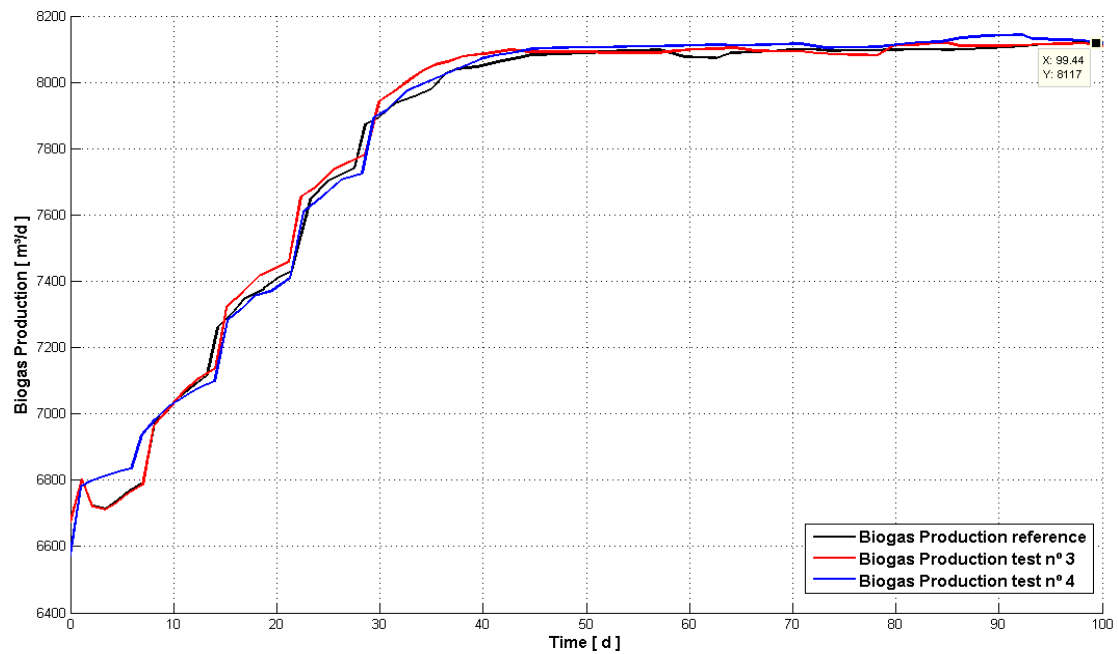


Figure 5.46: Biogas production & reliability assessment of NMPC optimization.

Finally, each control strategy reveals to be equally efficient given the biogas production proximity for different NMPC optimizations (e.g. see Figure 5.46). Therefore, in all instances the NMPC algorithm found adequate control strategies.

## 5.6 Fifth Experiment

The fifth experiment intents to assess the NMPC optimization effectiveness according to three different initial states. The three proposed initial states employed in this experiment are shown in Table 5.13, where each initial state represents the substrate mixture inlet at the biogas plant's reactor prior to the optimization.

**Table 5.13: Substrate mixture initial state.**

Substrate name	Initial state n°1	Initial state n°2	Initial state n°3	Manipulated variable
	[m <sup>3</sup> /d]	[m <sup>3</sup> /d]	[m <sup>3</sup> /d]	
Maize	10	20	40	✓
Silo seepage	2	3	2	✓
Manure	20	30	20	✓
Manure solids	1	2	Zero	✓
Recirculation b/t fermenters	40	40	40	Constant

In view of the fact that the initial state dictates the reactor's condition of operation, the NMPC algorithm will be influenced at the beginning and throughout the optimization. Therefore, in order to utterly evaluate the NMPC algorithm it is crucial to verify if it can achieve reliable results when submitted to different initial states of operation.

Consequently, the methodological procedure used in this experiment consists of executing the NMPC optimization with the same configuration as shown in Table 5.14 for all tests and differing solely by the initial states of the plant (e.g. see Table 5.13).

**Table 5.14: NMPC optimization tool settings for initial states assessment.**

NMPC parameter name	NMPC parameter value	Manipulated variable
Plant model	Sunderhook	
Optimization method	CMAES	
Population size	8	
Number of generations	4	
Prediction horizon time [d]	50	
Control horizon time [d]	7	
Change type	Percentual [%]	
Change value	2.5	
Number of iterations	15	
Fitness trigger	OFF	
Plant initial states	Four different substrate mixtures	✓

The subsequent sections presents the obtained NMPC optimization results in dependency of their substrate mixture inlet (i.e. initial states), followed by the comparison between these optimizations.

### 5.6.1 First initial state

This section presents the NMPC optimization results according to the NMPC algorithm settings provided in Table 5.14 and the initial state n°1 (e.g. see Table 5.15), where the initial state n°1 correspond to the plant's substrate mixture inlet at the beginning of the optimization (e.g., the volume flows of manure, maize, etc). Table 5.15 shows the initial state n°1 configuration for each substrate feed and their upper and lower boundaries.

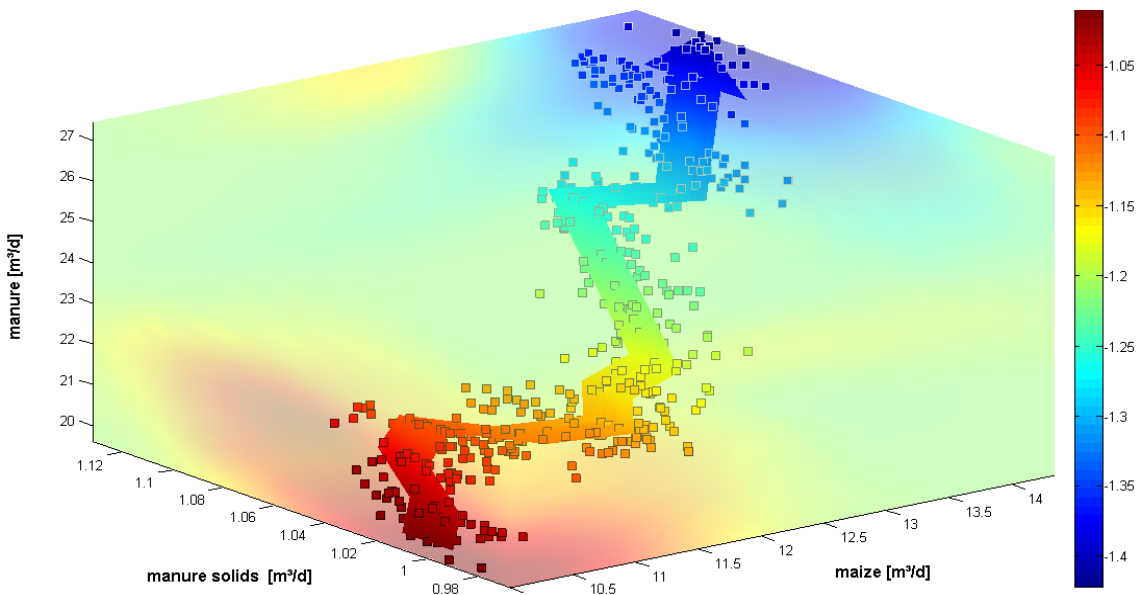
**Table 5.15: NMPC optimization with initial state n°1.**

Substrate name	Initial state n°1	Maximum substrate	Minimum substrate
	[m³/d]	inlet [m³/d]	inlet [m³/d]
Maize	10	40	20
Silo seepage	2	3	1
Manure	20	30	10
Manure solids	1	5	0
Recirculation b/t fermenters	40	40	40

The proposed initial state places the biogas plant model at a lower state of operation given the poor maize substrate feed at the beginning of the optimization (e.g. ten meter cubic per day). This is anticipated since the maize substrate possesses the highest potential of methane production in comparison to the remaining substrates (e.g. manure and manure solids). Approximately 150 meter cubic of methane per ton of raw material as shown in Table 1.3 in section 1.3.

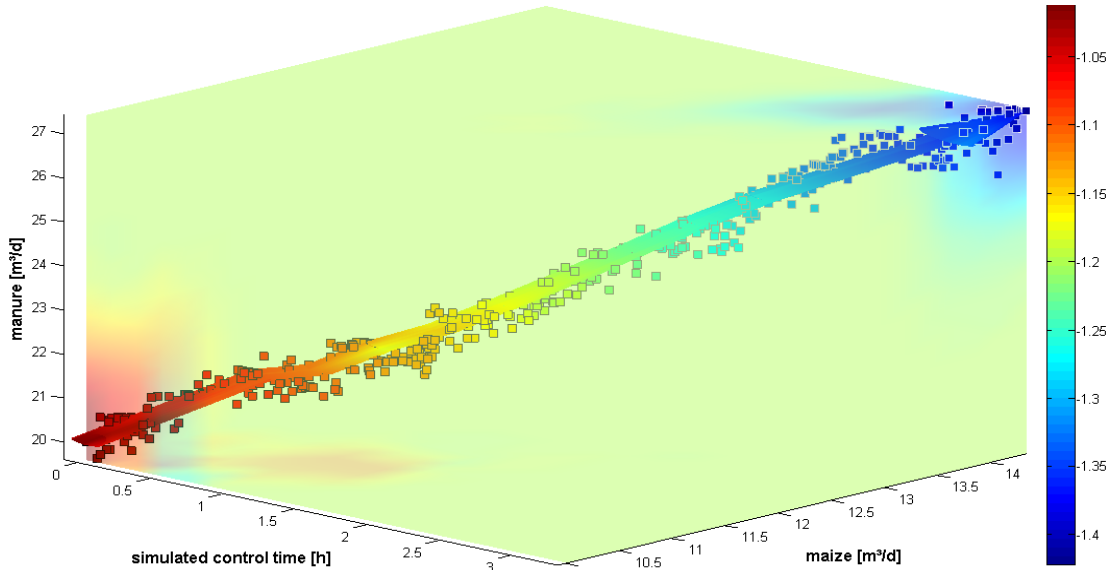
The analysis of how the initial state n°1 affects the NMPC optimization is shown in figures 5.47 and 5.48, where the color gradient portray the evolution of the cost vs. benefit analysis in the direction of the arrow. Thus, the smaller is the cost benefit value, the cooler is the color and the better is the result. Additionally, each square comprehends a further simulation run in the NMPC optimization and the arrow its evolution direction.

Figure 5.47 shows the substrate mixture evolution throughout the NMPC optimization in relation to the cost vs. benefit analysis. Where the arrow's trajectory demonstrates in which way substrate mixture should be employed in order to obtain optimal biogas production with the best cost benefit ratio.



**Figure 5.47: Initial state n°1 - Evolution of cost benefit ratio against maize, manure and manure solids substrate feeds (The smaller the value (the colder the color), the better the substrate mix).**

Noticeably, the arrow's trajectory in Figure 5.47 shows that all substrates are to be increased so that the system is compelled to its optimum. Such observation is also confirmed by the roughly linear trajectory of the arrow in Figure 5.48, where the substrates are increased during the whole simulated control time.



**Figure 5.48: Initial state n°1 - Evolution of cost benefit ratio against time and substrate feeds of maize and bull manure (The smaller the value (the colder the color), the better the substrate mix).**

Furthermore, the color gradient in Figure 5.47 and in Figure 5.48 shows a slight improvement in the system response, what can also be observed in the following figures where the output response is compared to the NMPC stepwise control.

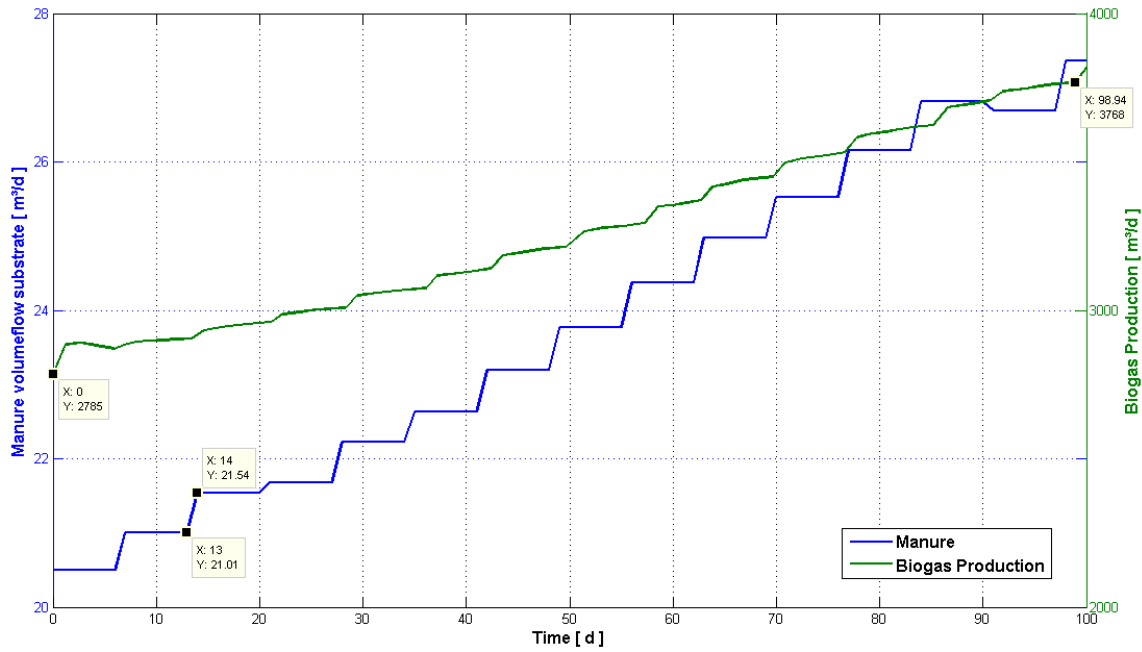


Figure 5.49: Initial state n°1 - Manure stepwise control and biogas production.

The small biogas production preceding the NMPC optimization (i.e.  $2785\text{m}^3/d$  in Figure 5.49) confirms that the initial state n°1 places the plant's model at lower condition of operation. This reflects over stepwise control where the manure substrate feed is consistently increasing throughout the optimization to push further the biogas production, methane content and the manure bonus. In addition, the step size increases by a rate of 2.5% as shown in the Figure 5.49.

Moreover, the same remark applies for the maize stepwise control shown in Figure 5.51. However, the manure solids stepwise control shown in Figure 5.50 displays a different behavior if compared to the maize and manure sequence of inputs.

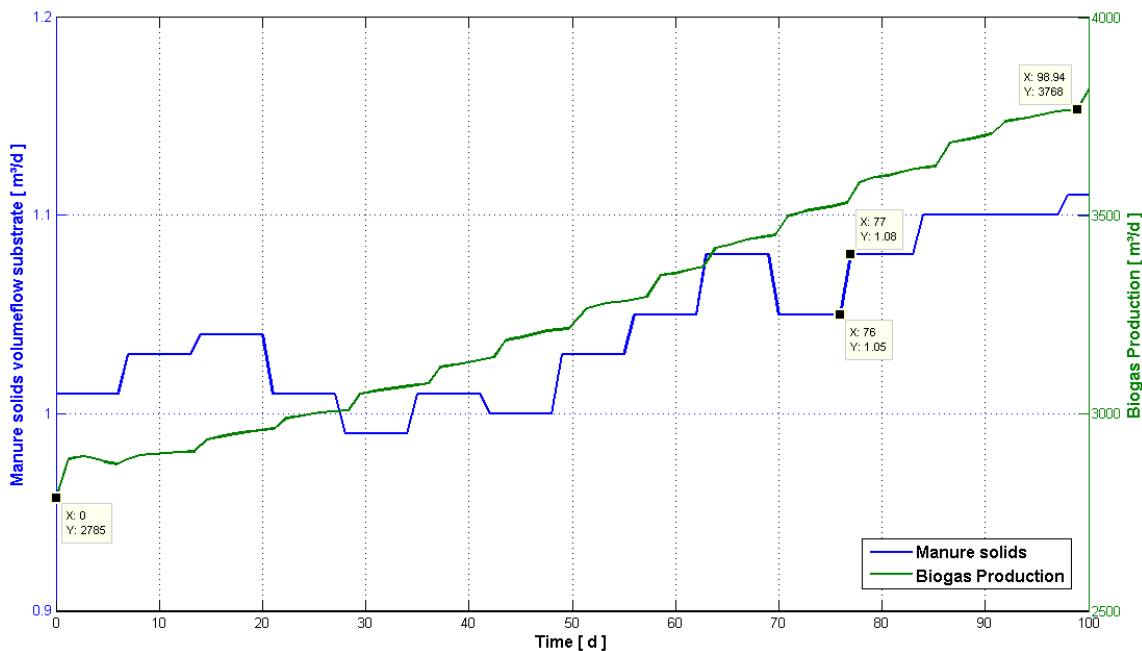


Figure 5.50: Initial state n°1 - Manure solids stepwise control and biogas production.

The reason for the manure solids different behavior comes from the process's biological and physical background, where the reactor tends to produce more biogas if the substrates are very well mixed. Hence, lower amounts of solids within reactor will lead to a substrate mixture with higher quantities of moisture and, consequently, better mixed. Accordingly, the manure solids substrate has not increased significantly during the NMPC optimization as can be seen in Figure 5.50.

Furthermore, the biogas production shown in Figure 5.51 evidences a stronger dependency in relation to the maize sequence of inputs as previously anticipated.

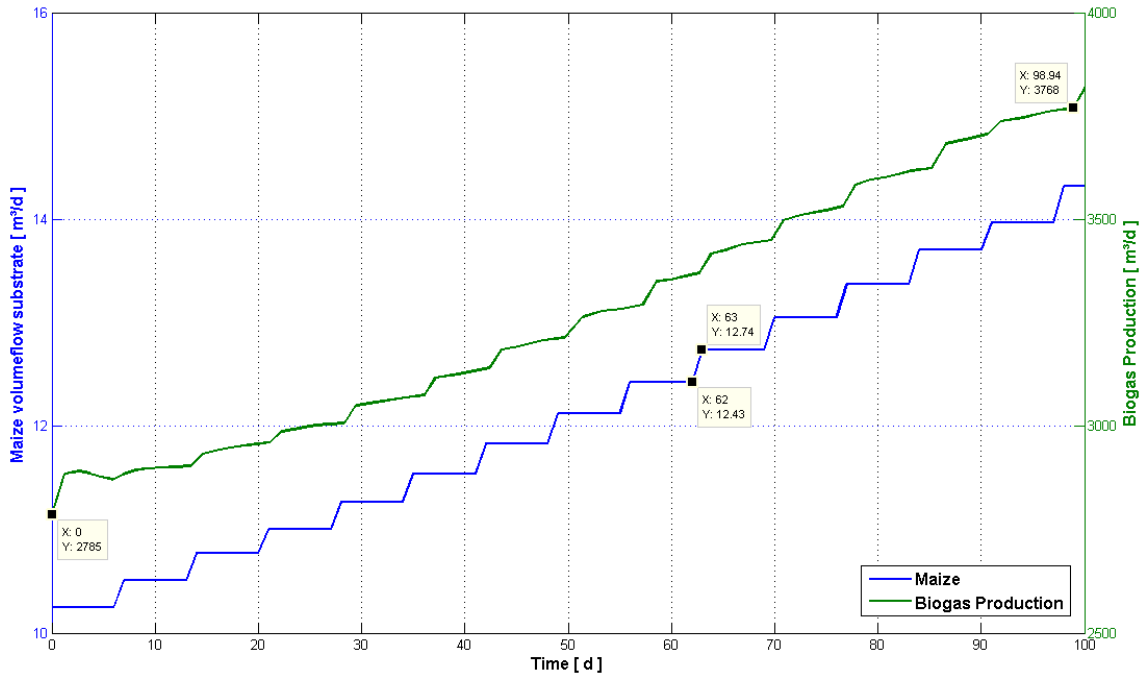


Figure 5.51: Initial state n°1 - Maize stepwise control and biogas production.

Finally, Figure 5.51 displays an additional improvement of  $1083\text{m}^3/\text{d}$  in the biogas production at the end of the NMPC optimization, which is quite interesting but far from the desired optimal values found in previous tests (e.g. test n°16 in section 5.2.2 with approximately  $8100\text{m}^3/\text{d}$  of biogas production).

Ergo, NMPC algorithm was not able to achieve the steady state during the one hundred day stepwise control, even though it improved system's response by additionally  $410\text{€}/\text{d}$  (i.e. profit difference before and after the optimization without fixed costs). Thus, it might require extra simulation times (e.g. two hundred day stepwise control) and/or higher step sizes (e.g. five percent change value) to further enhance the overall system's response and reach the steady state of operation.

Hence, better overall responses can be accomplished through the NMPC algorithm fine-tuning. Figure 5.52 concerns a NMPC setup with higher step size ratio (e.g. five percent increment

ratio), which incites a faster response of the biogas plant. While Figure 5.53 utilizes higher step size ratio in combination longer simulation times in order to finally achieve the plant's steady state.

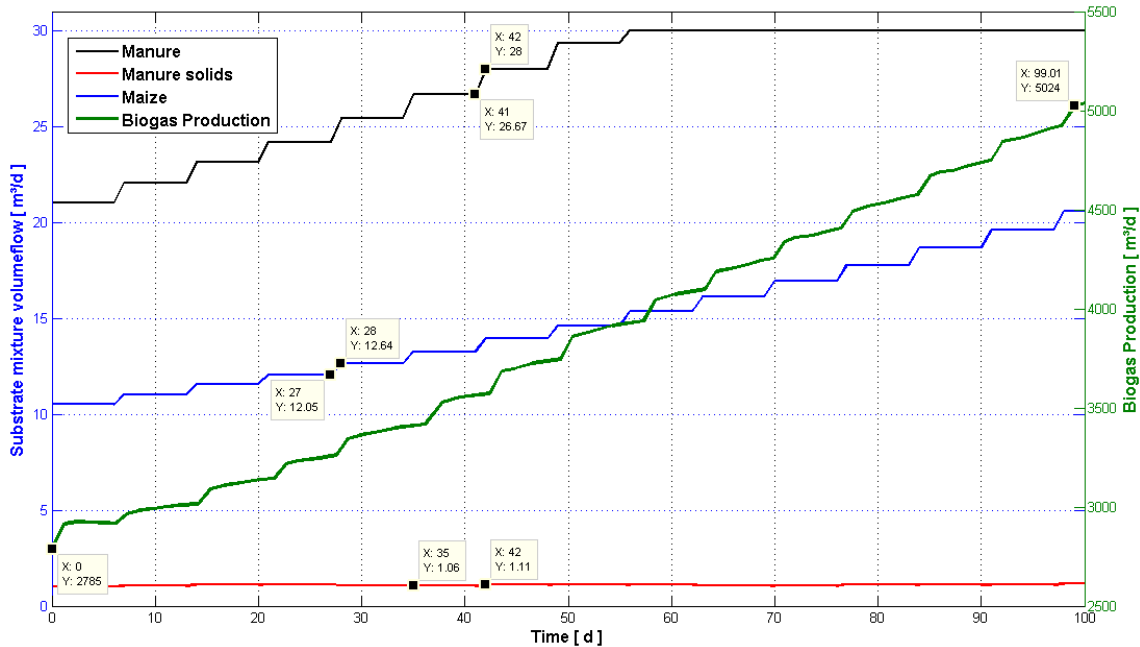


Figure 5.52: Initial state n°1 - NMPC stepwise control with high step size and biogas production.

Figure 5.52 show that the new NMPC control strategy enhances the biogas production much faster than the previous one. Thus, the final result produces an increment of  $2239\text{m}^3/\text{d}$  in the biogas outlet (e.g. twice as much) and an additional increment of  $896\text{€}/\text{d}$  in the profit (i.e. profit difference before and after the optimization without fixed costs).

However, the new NMPC optimization settings could not accomplish the plant's steady state when starting at the initial state n°1. Therefore, the optimum could be achieved if the NMPC optimization is performed with extra control simulation times as can be seen in Figure 5.53.

Needless to pointing out that the extra time of two hundred days is utilized here for explanation purposes since the defined control strategy is impracticable for such a long time of operation; many variables can change during this time (e.g. reactor's temperature with the seasons change). In a real implementation the advisable approach might be to use and NMPC stepwise control with particularly higher step sizes (e.g. ten percent increment ratio or more) just for a small amount of days to push the system out of the lower state of operation and, consequently, gradually reduce it with the approximation to the optimum state of operation.

Naturally, this approach concerns only the off-line NMPC implementation. In an on-line NMPC implementation the algorithm itself would be able to optimize the system as quickly as possible and maintain it at the optimum state of operation.

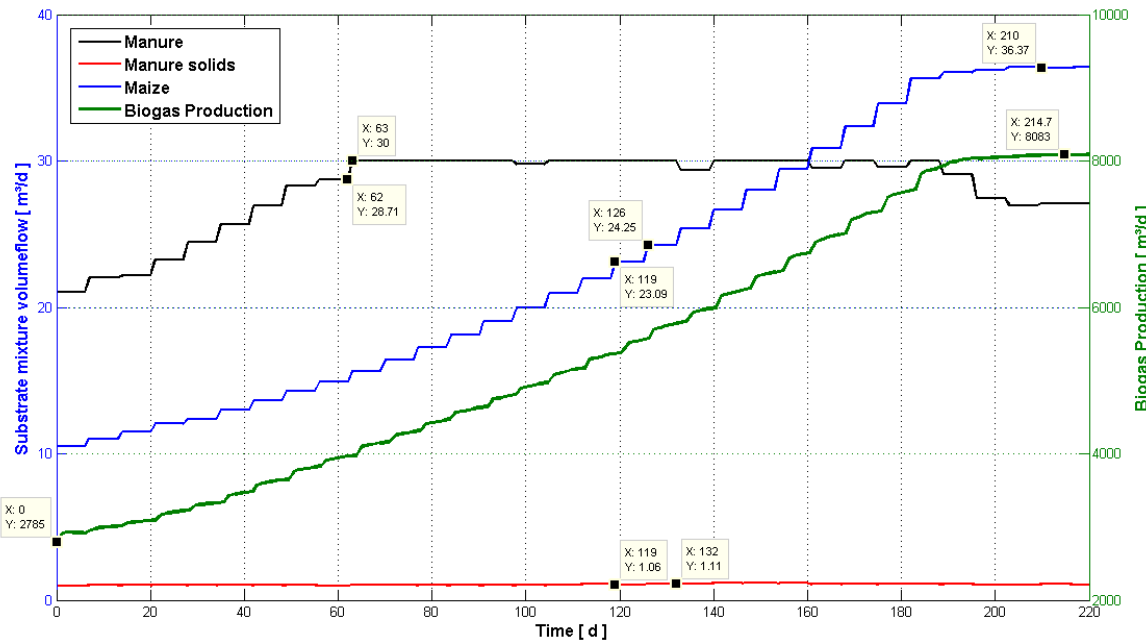


Figure 5.53: Initial state n°1 - NMPC stepwise control with high step size and biogas production.

Moreover, the latest operational state calculated by the NMPC optimization will add to the profit an additional increment of 2089€/d (i.e. without the fixed costs) and also an increment of 5298 m<sup>3</sup>/d in the biogas outlet; at the end of the optimization.

Consequently, it can be concluded that higher step sizes are better suited for biogas plants at lower states of operation, where quicker responses can be obtained. Additionally, the NMPC optimization could enhance biogas production in all circumstances independently of the chosen setting; however, a fine-tuning might be necessary to accomplish the optimum state of biogas production.

### 5.6.2 Second initial state

This section presents the NMPC optimization results according to the NMPC algorithm settings provided in Table 5.14 and the initial state n°2 (e.g. see Table 5.16), where the initial state n°2 correspond to the plant's substrate mixture inlet at the beginning of the optimization (e.g., the volume flows of manure, maize, etc).

Table 5.16: NMPC optimization with initial state n°2.

Substrate name	Initial state n°2	Maximum substrate	Minimum substrate
	[m <sup>3</sup> /d]	inlet [m <sup>3</sup> /d]	inlet [m <sup>3</sup> /d]
Maize	20	40	20
Silo seepage	3	3	1
Manure	30	30	20
Manure solids	2	5	0
Recirculation b/t fermenters	40	40	40

The proposed initial state places the biogas plant model at an intermediary state of operation, which is much closer to the initial state utilized in the first set of tests shown in section 5.2. Thus, all substrate feeds at the beginning of the optimization were slightly increased in comparison to the initial state n°1 (e.g. see Table 5.13); and as a result, the initial state n°2 tends to be more realistic since the biogas production is at a regular level of biogas production but not at its optimum.

The analysis of how the initial state n°2 affects the NMPC optimization is shown in figures 5.54 and 5.55, where the color gradient portray the evolution of the cost vs. benefit analysis in the direction of the arrow. Additionally, each square comprehends a further simulation run in the NMPC optimization and the arrow its evolution direction.

Figure 5.54 shows the substrate mixture evolution throughout the NMPC optimization in relation to the cost vs. benefit analysis.

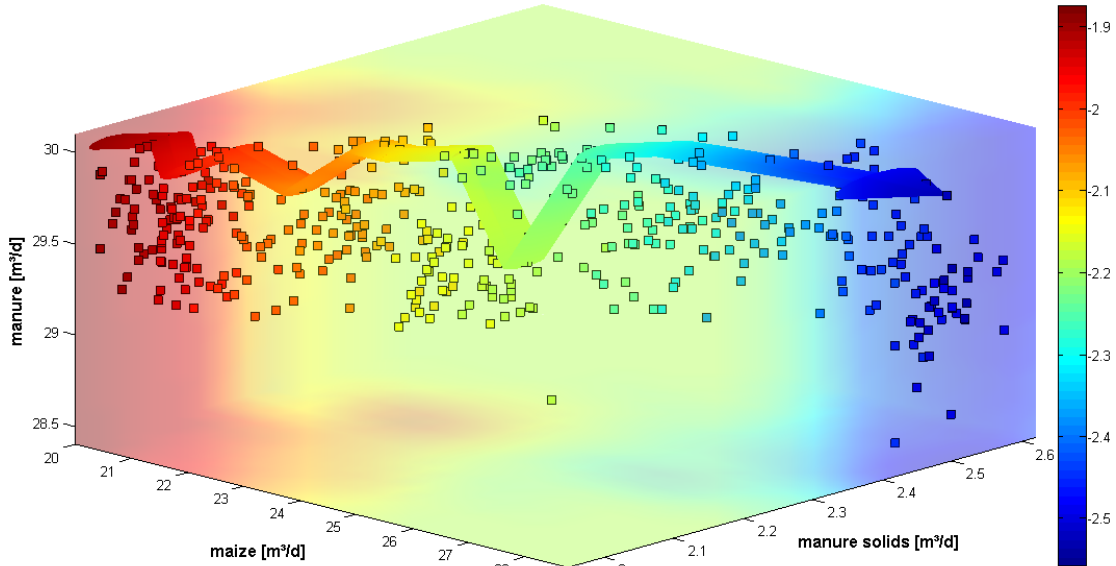


**Figure 5.54: Initial state n°2 – Evolution of cost benefit ratio against maize, manure and manure solids substrate feeds (The smaller the value (the colder the color), the better the substrate mix).**

The arrow's trajectory in Figure 5.54 presents a flat shape in the direction of the manure substrate inlet, which demonstrates that the manure substrate had a stronger influence throughout the optimization. This flat shape is a result of the high manure volume flow values (i.e. between  $29\text{ m}^3/\text{d}$  and  $30\text{ m}^3/\text{d}$ ) that were frequently limited by the “maximum substrate inlet” (i.e. the upper bound).

Furthermore, the arrow's trajectory also shows that the substrate mixture inlet ratios (i.e. maize, manure and manure solids) are to be increased to obtain optimal biogas production with the best cost benefit ratio.

Moreover, Figure 5.55 shows the time required by NMPC algorithm (i.e. approximately four hours) to enhance the cost benefit ratio from roughly  $1900\text{€}/\text{d}$  to  $2558\text{€}/\text{d}$ ; without fixed costs.

Consequently, the NMPC optimization could improve the biogas production and the resulting income by additionally 676€/d at the end of the optimization, if the new control strategy is employed.

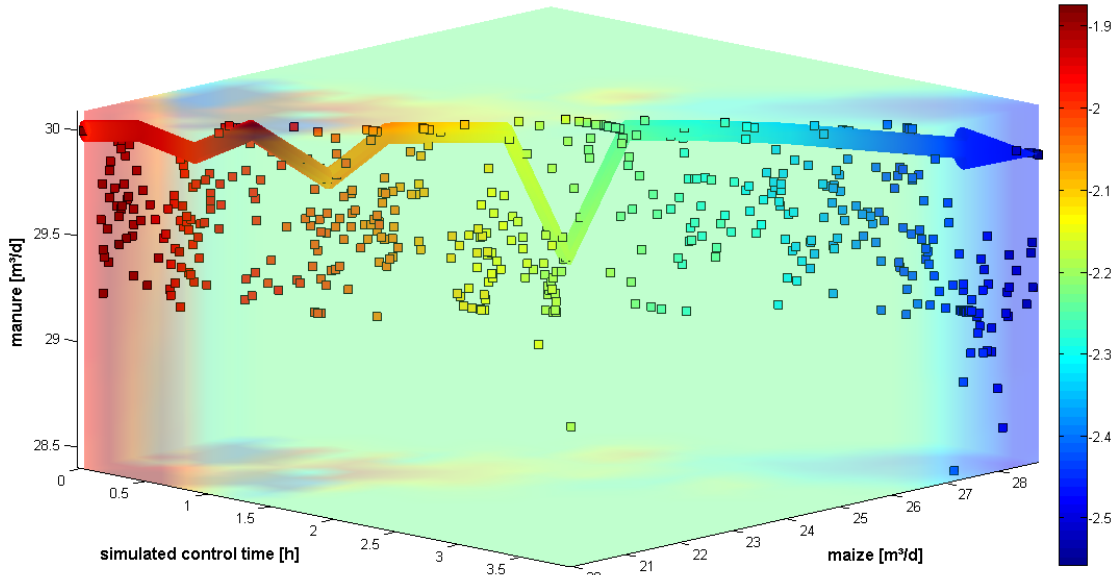


**Figure 5.55: Initial state n°2 - Evolution of cost benefit ratio against time and substrate feeds of maize and bull manure (The smaller the value (the colder the color), the better the substrate mix).**

The following figures present the defined NMPC control strategy in dependency to the initial state n°2. Figure 5.56 concerns the manure sequence of inputs and its influence over the biogas production.

As can be seen in Figure 5.56 the manure inputs sequences is limited, in some instances, at 30 meter cubic per day. This restraint is caused by the “maximum substrate inlet” bound that does not allow the NMPC algorithm to further increase the manure input. Consequently, the manure control strategy could only be reduced; this is also reflected in the arrow’s shape shown in figures 5.54 and 5.55.

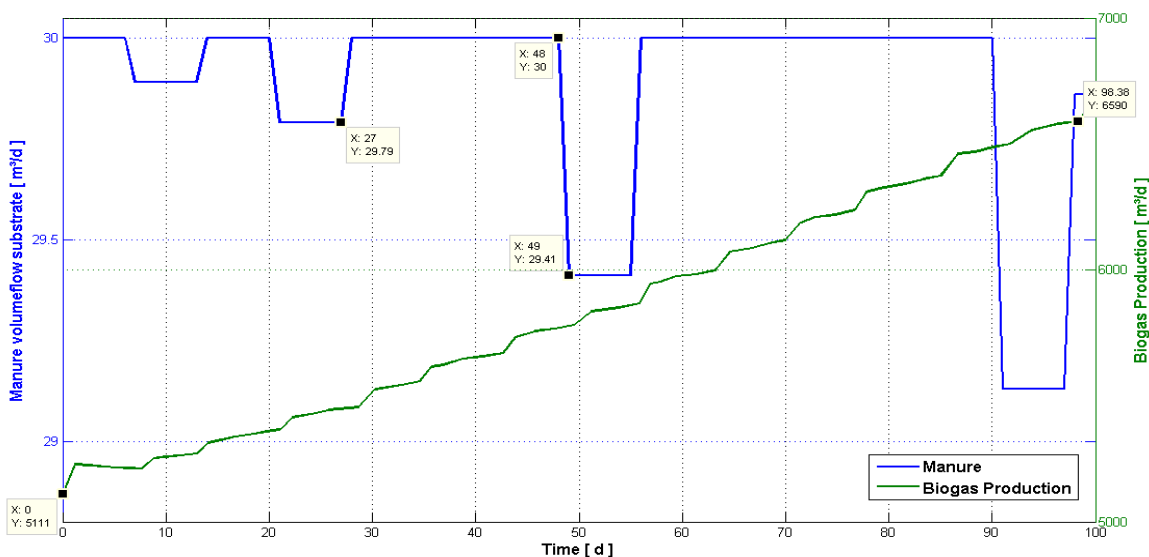


**Figure 5.56: Initial state n°2 - Manure stepwise control and biogas production.**

Furthermore, the manure solids stepwise control shown in Figure 5.57 displays a gradual increase in the substrate inlet to compel the biogas plant to its optimal state of production. This behavior is not observed in the manure stepwise control since it cannot be increased given the upper bound of the optimization and the starting volume flow defined by the initial state n°2.

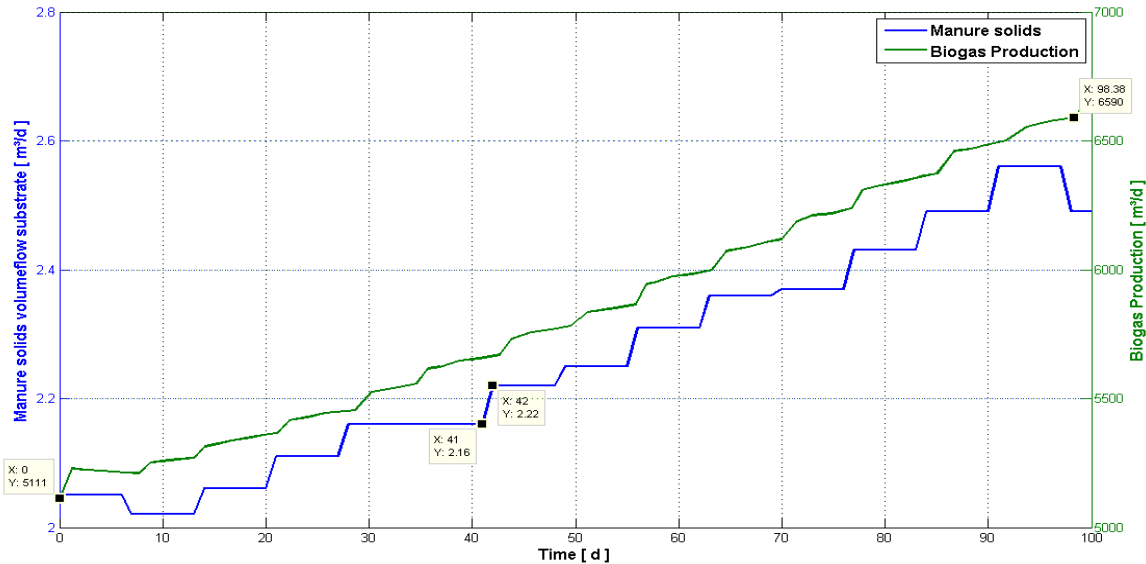


Figure 5.57: Initial state n°2 - Manure solids stepwise control and biogas production.

Moreover, the maize stepwise control shown in Figure 5.58 also displays a gradual increase in the substrate inlet; where the biogas production curve almost follows the maize input sequences. This evidences a stronger dependency in relation to the maize sequence of inputs, which is predicted given the higher potential of methane production in comparison to the remaining substrates (e.g. manure and manure solids). Approximately 150 meter cubic of methane per ton of raw material as shown in Table 1.3 in section 1.3.

Therefore, the maize stepwise control tends to have more volume flow inlet quantities than the other substrates, even though their boundary ranges are different.

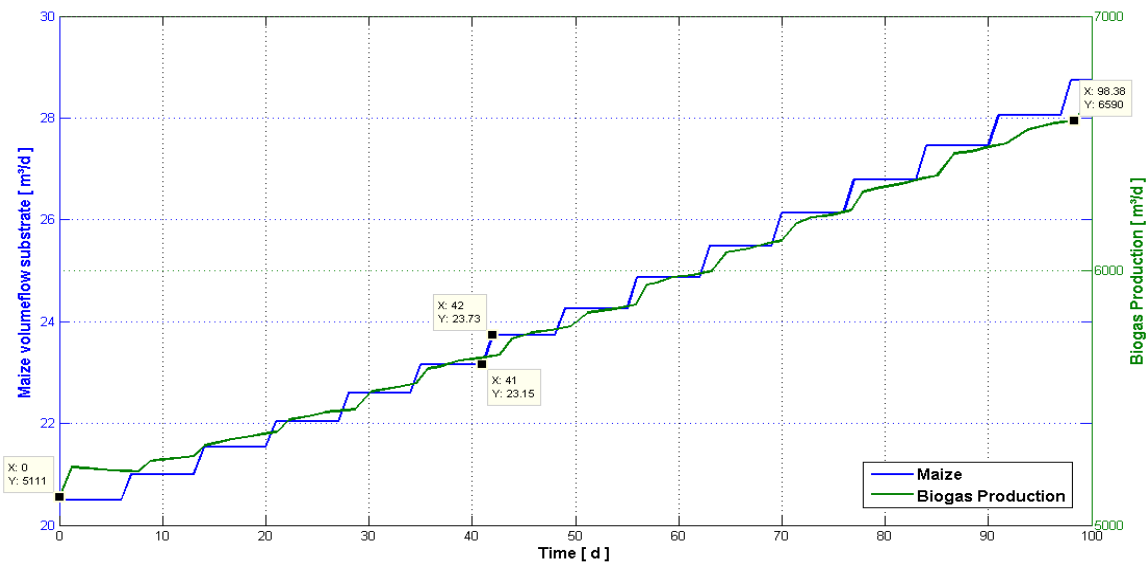


Figure 5.58: Initial state n°2 - Maize stepwise control and biogas production.

Figure 5.58 confirms that the initial state n°2 places the system's model at an intermediary operational state, where the biogas production prior to the optimization has an outlet of  $5111m^3/d$ .

In addition, the NMPC control strategy calculated by the NMPC algorithm provides additional improvement of  $1479m^3/d$  in the biogas production, which is satisfactory given the overall outflow of approximately  $7000m^3/d$  and the resulting income raise (e.g.  $2558\text{€}/d$ ). However, this result can be further improved in order to accomplish the plant's steady state and the optimal biogas production found in previous tests (e.g. test n°16 in section 5.2.2 with approximately  $8100 m^3/d$  of biogas production).

Ergo, NMPC algorithm was configured in order to obtain the best outcome possible, i.e., the steady state. The new configuration concerns extra simulation times (e.g. two hundred day stepwise control) and higher step sizes (e.g. five percent change value).

Figure 5.59 shows the new NMPC control strategy in dependency to the initial state n°2. This new configuration clearly forces the systems to a faster response, where the biogas outlet at the end of the previous optimization (e.g. see. Figure 5.58) was achieved in the 50<sup>th</sup> day of control simulation (i.e. same biogas production in half of the original time as shown in Figure 5.59). Thus, the NMPC algorithm fine-tuning could further enhance the overall system's response, reach the steady state of operation and accomplish it all in less time.

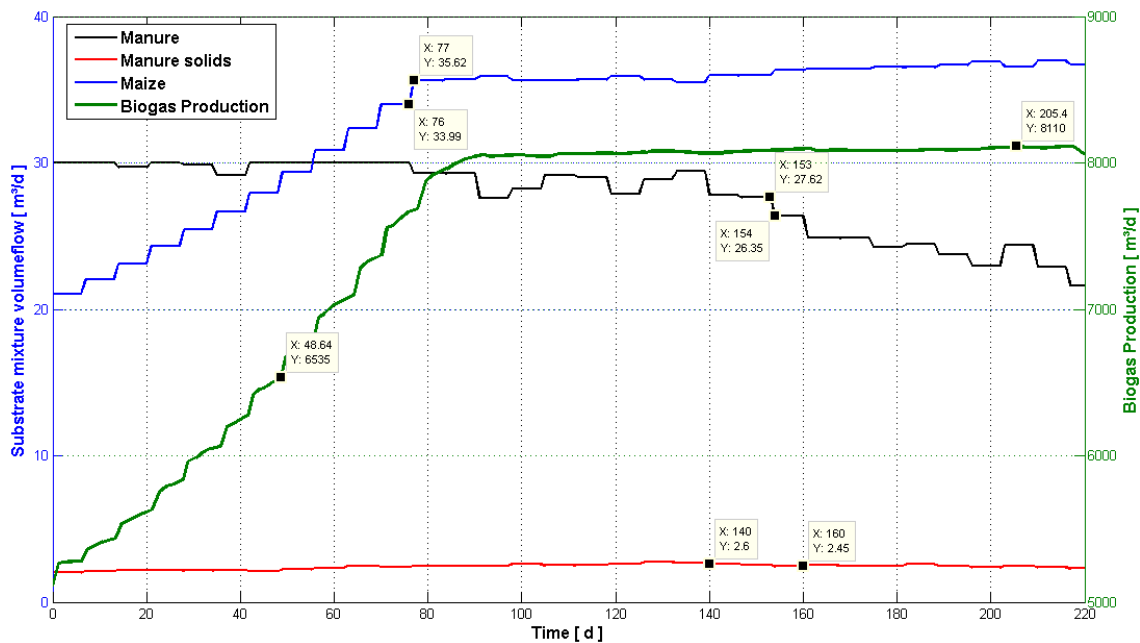


Figure 5.59: Initial state n°2 - NMPC stepwise control with high step size and biogas production.

Moreover, the NMPC algorithm tends to reduce the substrate input sequences for manure and manure solids once the optimal state of operation is accomplished at around the 90<sup>th</sup> day of simulation control. While maize stepwise control is increased at constant rates.

Finally, it can be concluded that the NMPC optimization could enhance biogas production when submitted to the proposed initial state n°2. Although, the obtained results were satisfactory the final biogas outlet (e.g.  $6590 \text{ m}^3/\text{d}$ ) and cost benefit ratio (e.g.  $2558 \text{ €}/\text{d}$ ) could be further improved with a fine-tuning of the NMPC algorithm; resulting in a biogas outlet of  $8110 \text{ m}^3/\text{d}$  (i.e. steady state value) and a cost benefit ratio of  $3102 \text{ €}/\text{d}$  (i.e. additional  $1220 \text{ €}/\text{d}$ ).

### 5.6.3 Third initial state

This section presents the NMPC optimization results according to the NMPC algorithm settings provided in Table 5.14 and the initial state n°3 (e.g. see Table 5.17), where the initial state n°3 correspond to the plant's substrate mixture inlet at the beginning of the optimization (e.g., the volume flows of manure, maize, etc). Table 5.17 shows the initial state n°3 settings for each substrate feed and their limits.

**Table 5.17: NMPC optimization with initial state n°3.**

Substrate name	Initial state n°3 [m <sup>3</sup> /d]	Maximum substrate inlet [m <sup>3</sup> /d]	Minimum substrate inlet [m <sup>3</sup> /d]
Maize	40	40	20
Silo seepage	2	3	1
Manure	20	30	20
Manure solids	1	5	0
Recirculation b/t fermenters	40	40	40

The proposed initial state places the biogas plant model at an advanced state of operation given the greater inlet of maize substrate at the beginning of the optimization (e.g. forty meter cubic per day) and also the lower quantities of manure solids. This is anticipated since the maize substrate possesses the highest potential of methane production in comparison to the remaining substrates (e.g. manure and manure solids); and also, the reduction of solids within the reactor enables a better substrate mixture.

The analysis of how the initial state n°3 affects the NMPC optimization is shown in Figure 5.60, where the color gradient portray the evolution of the cost vs. benefit analysis in the direction of the arrow. Additionally, each square comprehends a further simulation run in the NMPC optimization and the arrow its evolution direction.

Figure 5.60 shows the substrate mixture evolution throughout the NMPC optimization in relation to the cost vs. benefit analysis and required simulation control time.

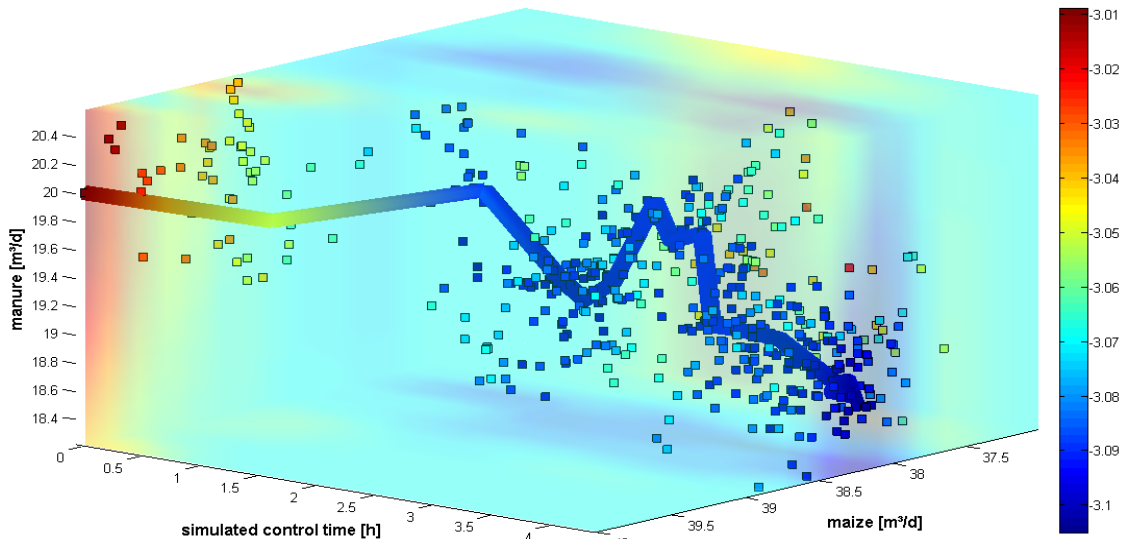


**Figure 5.60: Initial state n°3 - Evolution of cost benefit ratio against time and substrate feeds of maize and bull manure (The smaller the value (the colder the color), the better the substrate mix).**

The initial state n°3 induces the plant's model to an over production of biogas as can be seen in Figure 5.61. Such biogas over production is not interesting from the economical point of view if it cannot be sold or used to produce electrical energy. This is also reflected in the cost benefit ratio, which weights the over production in its formulation, and the color gradient change shown in Figure 4.58.

Consequently, the arrows trajectory in Figure 5.60 tends to descend throughout the NMPC simulation control in order to push down the biogas outlet, i.e., it reduces the substrate mixture feed in the biogas plant. Hence, at the end of the optimization the final profit has improved by an additional 106 euro per day without fixed costs. This value is quite small since the plant was quite close its optimum.

The following figures present the defined NMPC control strategy in dependency to the initial state n°3.

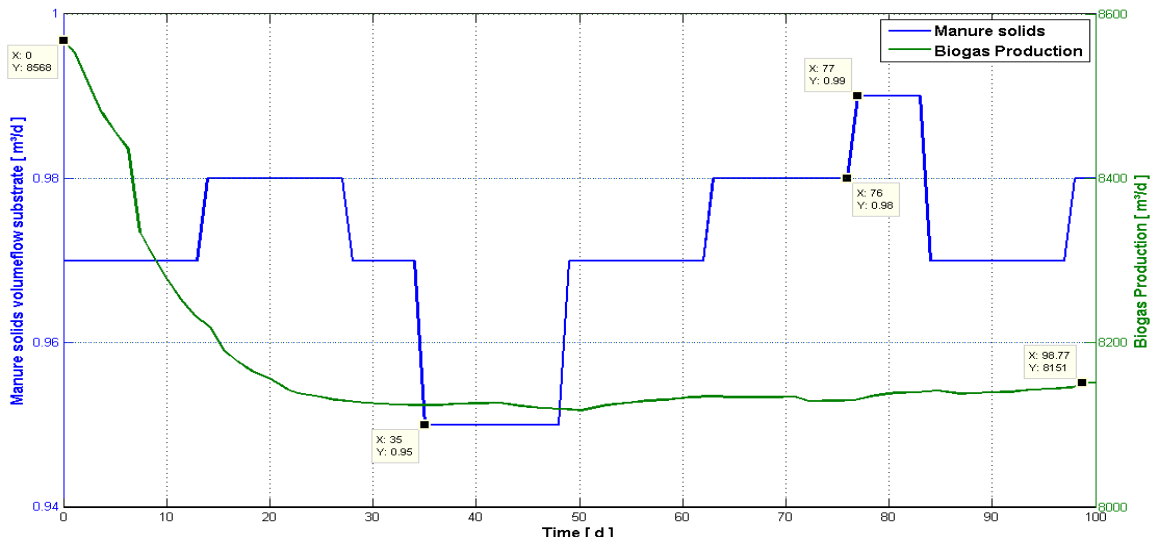


**Figure 5.61: Initial state n°3 - Manure solids stepwise control and biogas production.**

Figure 5.61 concerns the manure solids sequence of inputs and its influence over the biogas production. As can be seen in Figure 5.61, the manure solids substrate is practically unmodified throughout the NMPC optimization, i.e., its small range of variance in the Y-axes from  $0.95 \text{ m}^3/d$  to  $0.99 \text{ m}^3/d$ .

Differently from the manure solids, the manure stepwise control in Figure 5.62 is gradually reduced in order to push down the biogas production excess. However, this gradual reduction only takes place after the 20<sup>th</sup> day of simulation control. This is possibly caused by the combined influences of the other substrates in the reactor's substrate mixture (e.g. reduced maize substrate inlet rates in Figure 5.63).

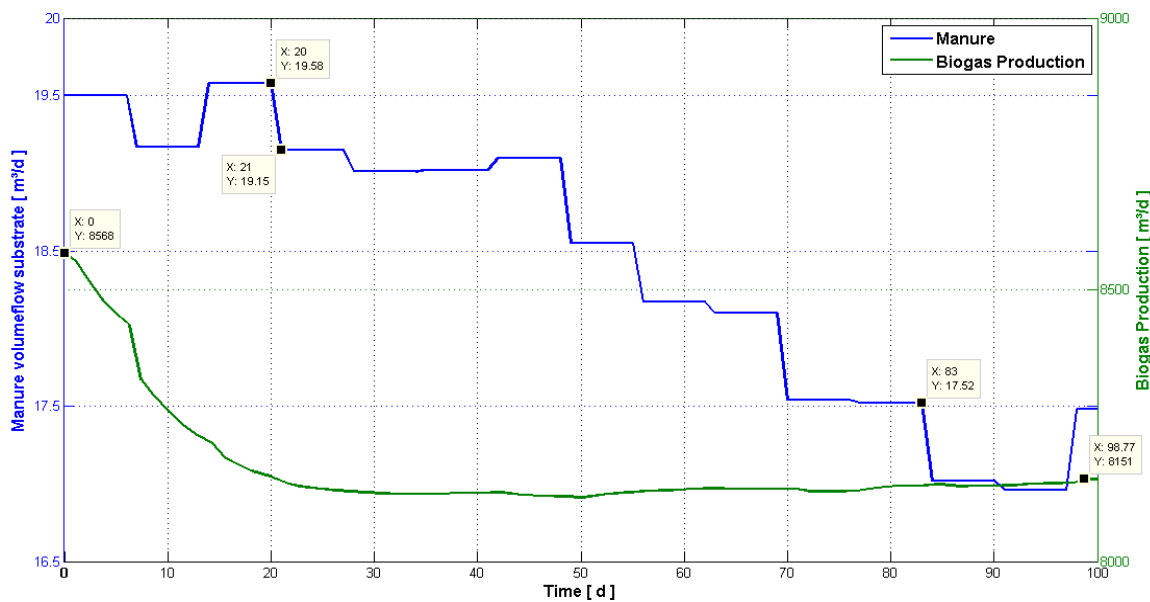


Figure 5.62: Initial state n°3 - Manure stepwise control and biogas production.

Furthermore, the maize stepwise control shown in Figure 5.63 suffers a significant drop at the beginning of the NMPC optimization, e.g., from  $40\text{m}^3/d$  to  $38\text{m}^3/d$ .

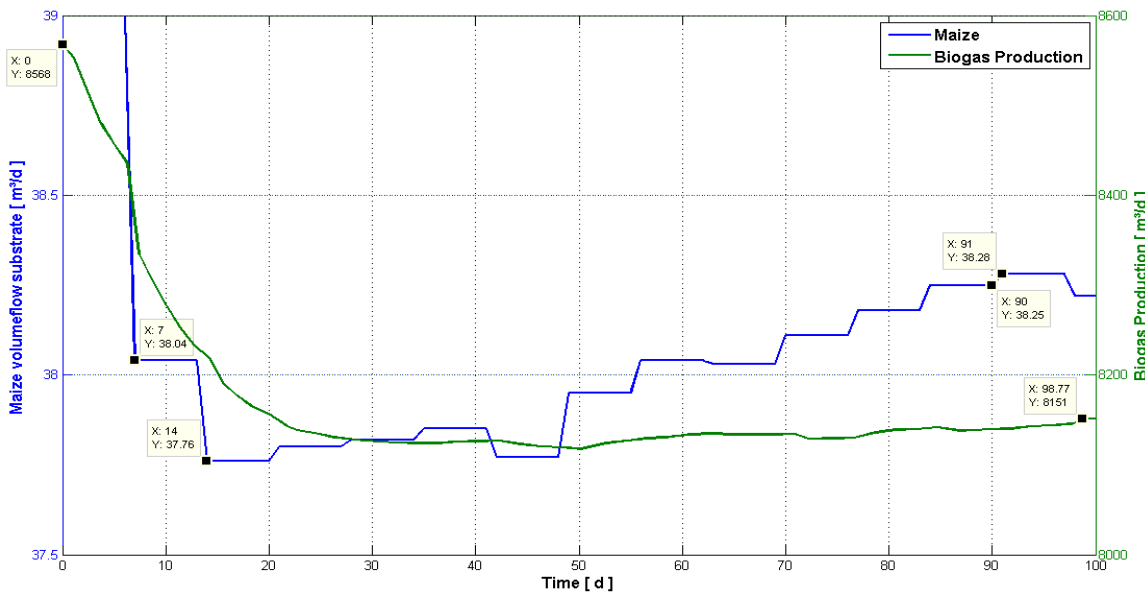


Figure 5.63: Initial state n°3 - Maize stepwise control and biogas production.

Such reduction in the maize stepwise control is a consequence of the maize's stronger methane potential in comparison to the other substrates (e.g. see Table 1.3 in section 1.3), where by reducing the maize inlet rates there is a substantial drop in the biogas production; as can be seen in Figure 5.63. Additionally, the final reduction in the biogas production at the end of the NMPC optimization is  $401\text{m}^3/\text{d}$ .

In conclusion, the NMPC optimization could avoid biogas over production and, consequently, decrease profit losses when submitted to the initial state n°3. Therefore, the NMPC algorithm is able not only to enhance biogas production but also able to diminish it when necessary to improve system's profitability.

#### 5.6.4 Comparison between initial states

Figure 5.64 shows the biogas production comparison for each initial state utilized in the NMPC optimization (e.g. initial state n°2). In addition, the data displayed in Figure 5.64 concerns only the tests settings in which the steady state was accomplished.

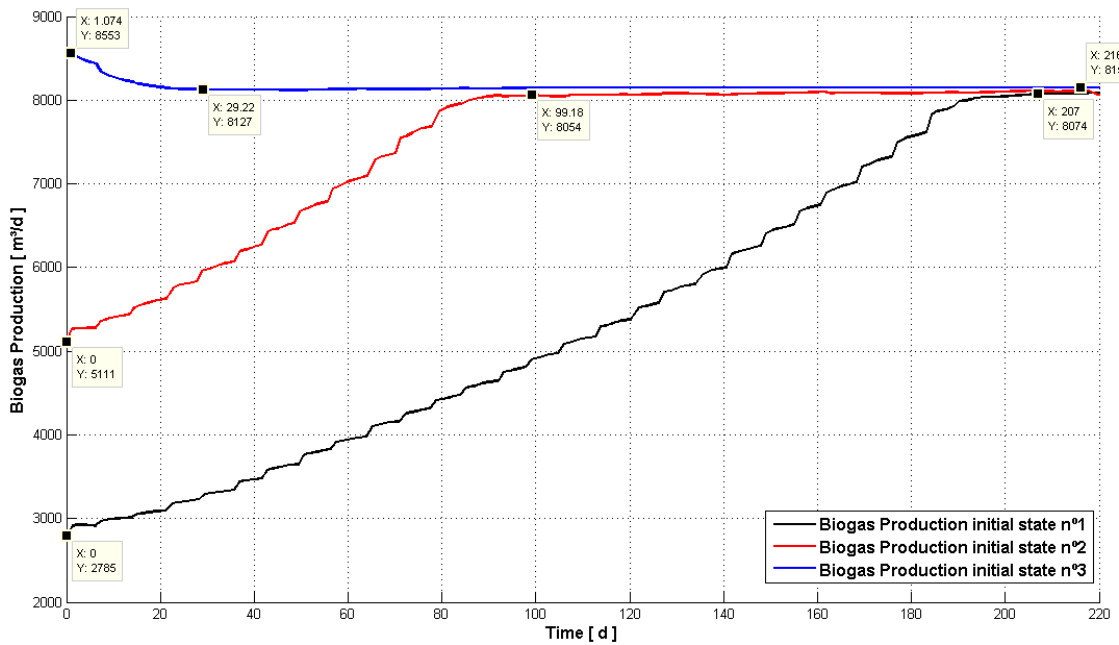


Figure 5.64: Biogas production and initial states comparison.

Evidently, each initial state defines a different operational condition that reflects over the initial biogas production and throughout the optimization. Thus, each curve in Figure 5.64 has a distinct starting point and simulation times.

Moreover, the NMPC algorithm could optimize the biogas plant model for all proposed initial states (i.e. advanced, intermediary and lower conditions of operation) and, eventually, achieve the steady state of plant. In addition, depending on the plant's initial state, the NMPC optimization might require longer simulation control times to accomplish the steady state.

Therefore, these results evidence the flexibility of the proposed NMPC algorithm to work in a wide range of scenarios, which is quite important to optimize different biogas plants and their inner characteristics (i.e. reactor's operational condition).

## 5.7 Sixth Experiment

The sixth experiment purpose is to assess how efficient is the NMPC algorithm in comparison to the previous optimization technique employed in the biogas plant.

In the view of the fact that the “findOptimalEquilibrium” (i.e. previous optimization technique) utilizes totally different concept from the NMPC algorithm, the only way in which these two techniques could be compared is when the overall number of simulation tries are the same.

Therefore, to accomplish such objective, the overall number of simulations for the NMPC algorithm and the “findOptimalEquilibrium” were maintained at the same value of approximately 480 simulation tries. In addition, the chosen NMPC test is the test n°16, i.e., the best NMPC algorithm result.

**Table 5.18: NMPC optimization tool and findOptimalEquilibrium settings.**

NMPC parameter name	NMPC parameter value	findOptimalEquilibrium
Plant model	Sunderhook	Sunderhook
Optimization method	CMAES	CMAES
Population size	8	35
Number of generations	4	14
Prediction horizon time [d]	50	450
Control horizon time [d]	7	×
Change type	Percentual [%]	×
Change value	5	×
Number of iterations	15	×
Fitness trigger	OFF	×

Additionally, both optimizations were performed with identical initial states as shown in Table 5.19.

The “findOptimalEquilibrium” concept is based in an open-loop control problem, which defines an optimal substrate mixture for the biogas plant's reactor in accordance to the given state of operation (i.e. initial state) and implements this optimal substrate mixture without any feedback control (i.e. does not reevaluate the new system's state). In essence, it uses the ADM1 to find optimal and constant substrate mixtures for long-term optimal steady-state operation of full-scale biogas plants. In addition, this optimal substrate mixture is accomplished through the optimization

algorithm (e.g. CMAES), which searches the whole spectrum (i.e. from the maximum to minimum substrate inlet) for the optimal mixture that will optimize the production of biogas. However, this technique limits itself in defining merely a fixed optimal substrate mixture, which results in a large step input that remain constant once is employed (e.g. see Figure 5.65).

**Table 5.19: NMPC optimization and findOptimalEquilibrium - Substrate mixture initial state.**

Substrate name	Initial state n°1 [m <sup>3</sup> /d]	Maximum substrate inlet [m <sup>3</sup> /d]	Minimum substrate inlet [m <sup>3</sup> /d]
Maize	30	40	20
Silo seepage	1.5	3	1
Manure	15	30	10
Manure solids	3	5	0
Recirculation b/t fermenters	40	40	40

The figure 5.65, 5.66 and 5.67 illustrates the optimal substrate mixture defined by the “findOptimalEquilibrium”. In these plots the overall biogas production reached its steady state at around the 50<sup>th</sup> day of simulation. However, it can be seen a slight overshoot in the biogas production (i.e. between the 20<sup>th</sup> and 30<sup>th</sup> day of simulation); what can be problematic given the highly nonlinear characteristic of the system.

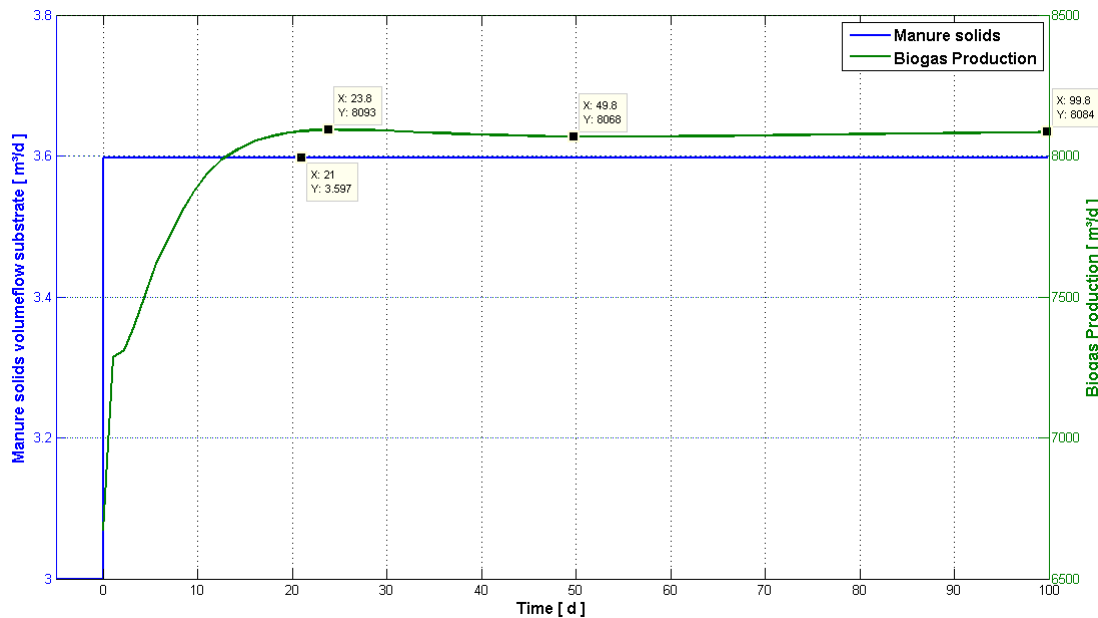


**Figure 5.65: Manure solids substrate feed “findOptimalEquilibrium” optimization and biogas production.**

Furthermore, such high steps might lead not only to system's instability but it can also disrupt the biological processes inside the reactor causing a total digestion failure. If this happens, the whole reactor's content must be disposed and the complete process is restarted from zero.

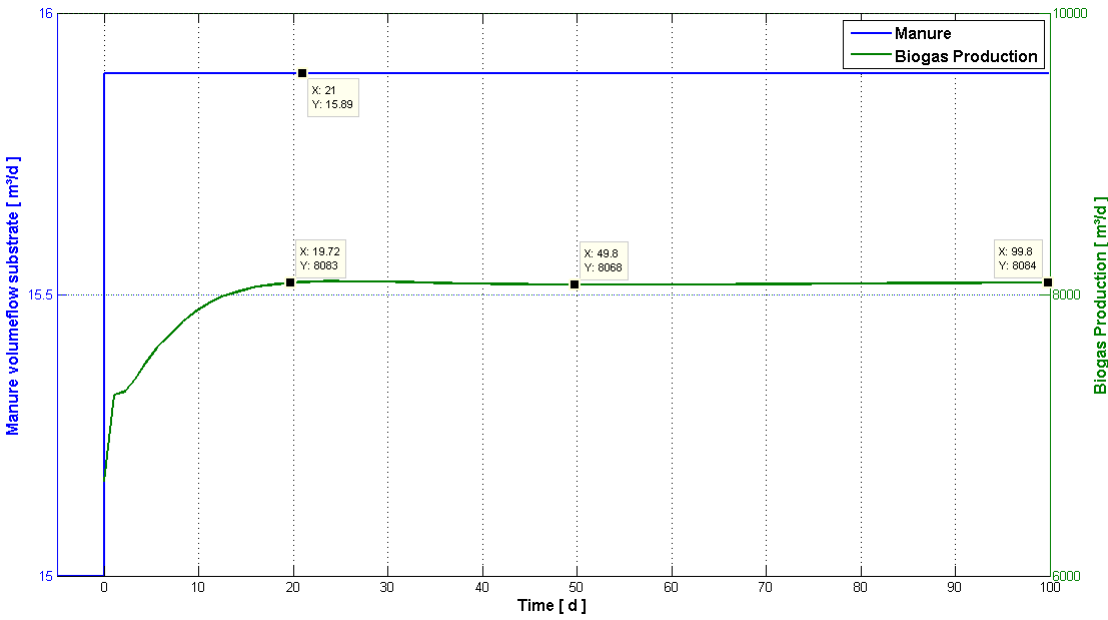


Figure 5.66: Manure substrate feed “findOptimalEquilibrium” optimization and biogas production.

Moreover, the “findOptimalEquilibrium” achieved an optimal biogas production of  $8084\text{m}^3/\text{d}$  with a gained profit of  $493\text{€}/\text{d}$  (i.e. cost benefit ratio).

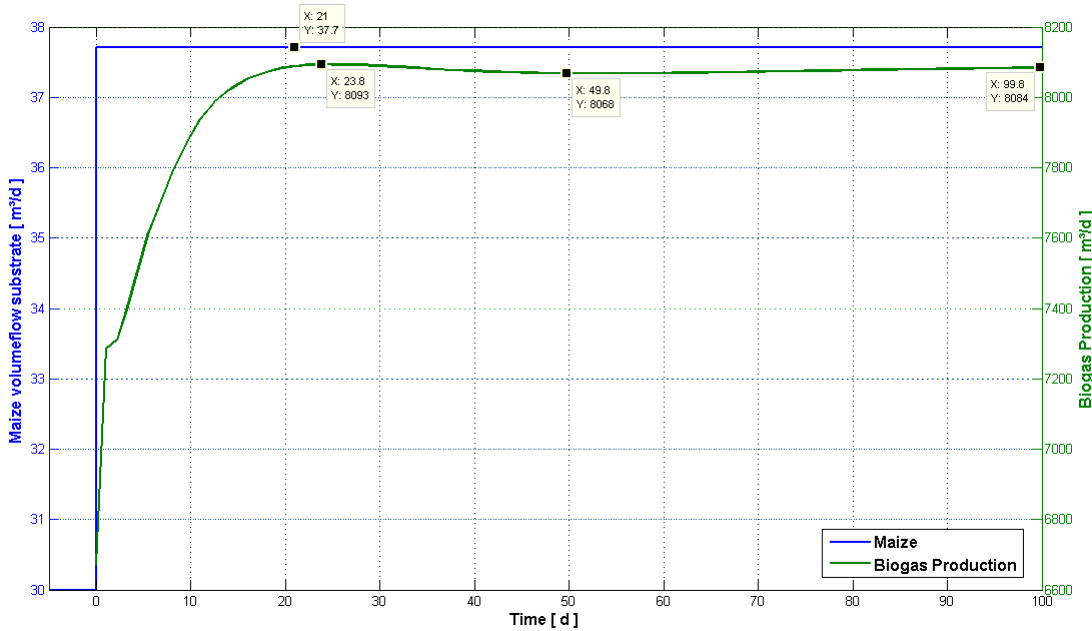


Figure 5.67: Maize substrate feed “findOptimalEquilibrium” optimization and biogas production.

Differently from the “findOptimalEquilibrium” optimization (i.e. open-loop control), the NMPC optimization provides a “self adaptive concept” (i.e. closed-loop control), where the algorithm checks the actual behavior of the system right after the implementation of every new optimal substrate mixture inlet (e.g. see Figure 5.68).

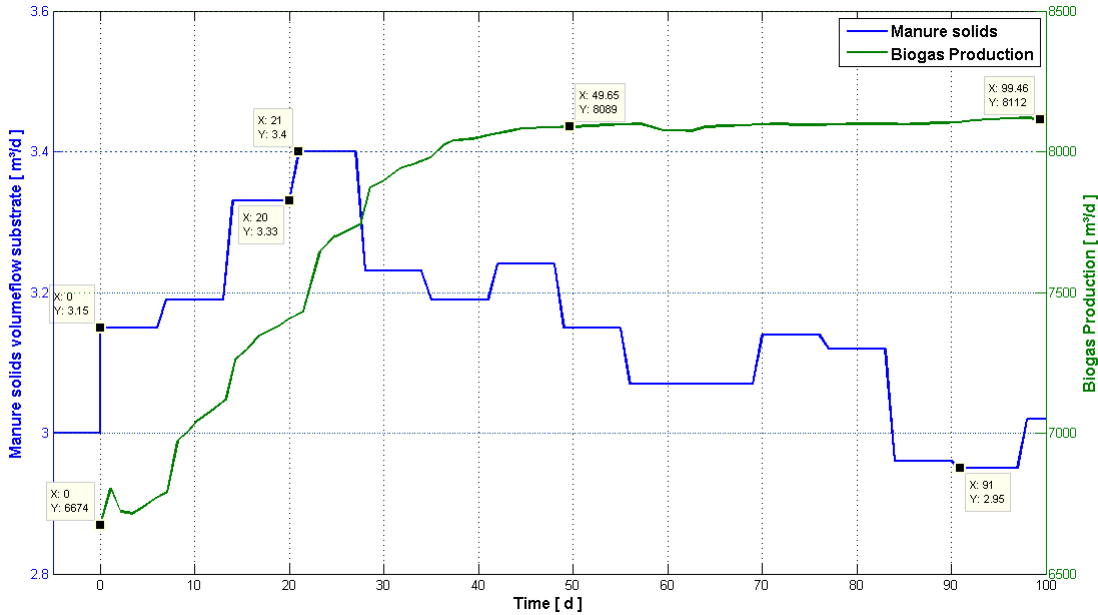


Figure 5.68: Test n°16 (Best) - Manure solids stepwise control and biogas production.

Therefore, in the NMPC optimization the chances that the system is led to instability or a total digestion failure are reduced. Furthermore, the biogas production accomplished the steady state at around the 50<sup>th</sup> day of simulation without overshoot. However, the biogas production in Figure 5.69 is not as smooth as in Figure 5.67, this possibly caused by the different combinations of substrate inlets throughout the optimization.

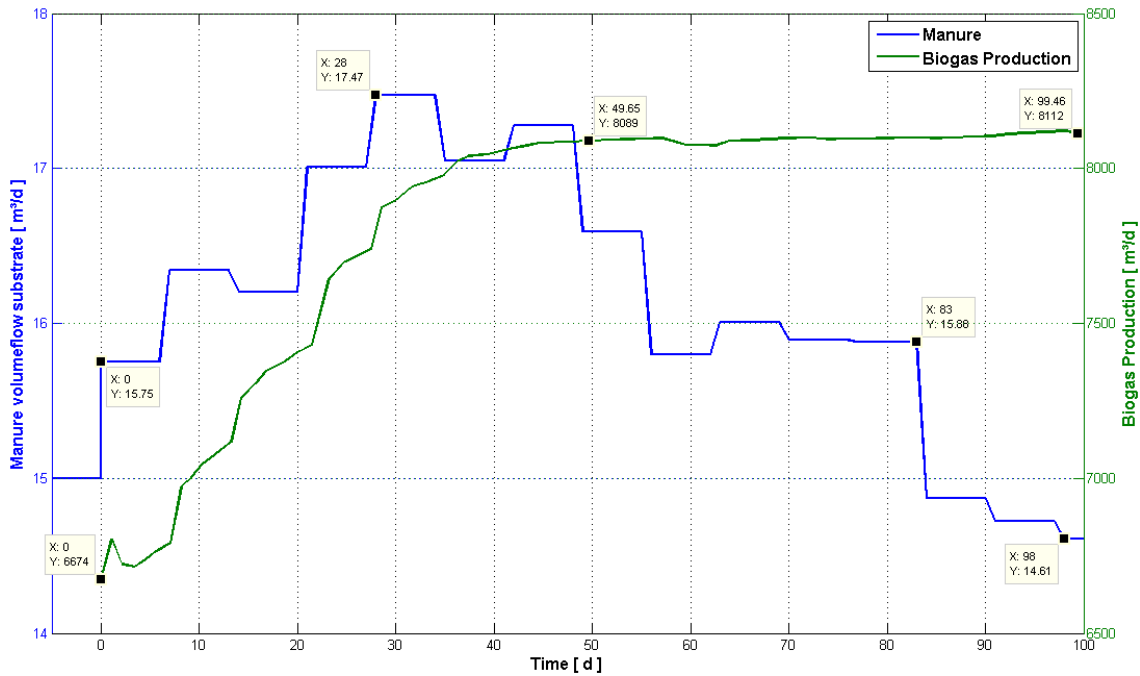


Figure 5.69: Test n°16 (Best) - Manure stepwise control and biogas production.

Moreover, the NMPC optimization achieved an optimal biogas production of  $8115\text{m}^3/\text{d}$  with a gained profit of  $628\text{€}/\text{d}$  (i.e. cost benefit ratio).

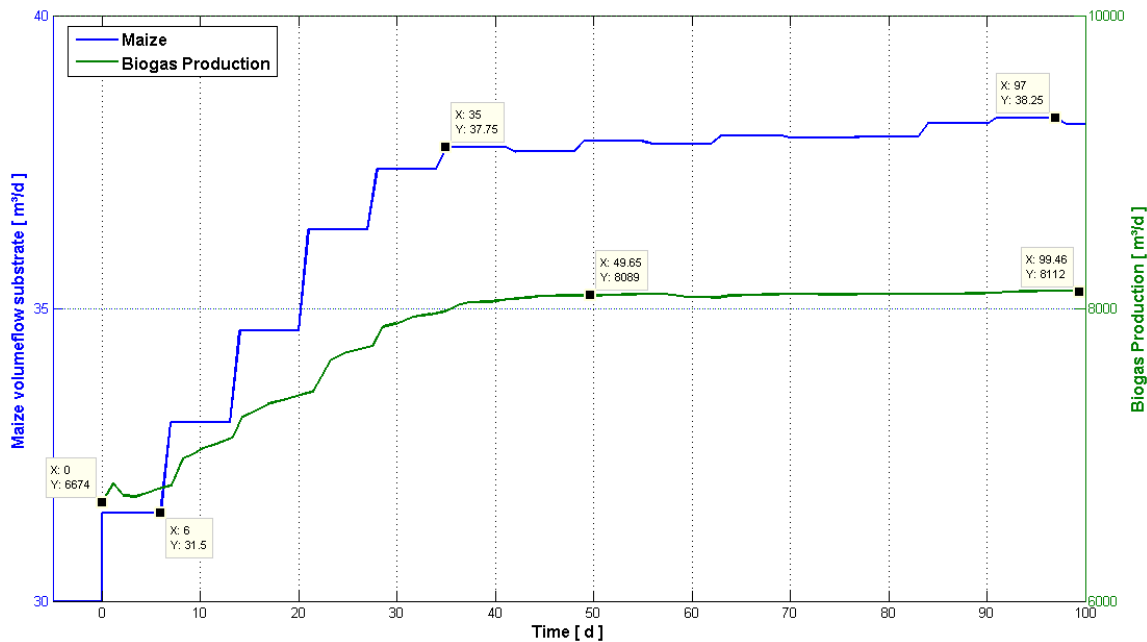


Figure 5.70: Test n°16 (Best) - Maize stepwise control and biogas production.

Finally, by comparing both optimization techniques (i.e. open-loop and closed-loop control) it can be concluded that they are quite similar with regard to the cost benefit ratio and the final state of biogas production. However, the NMPC control strategy (i.e. closed-loop control) reveals to be more reliable and less vulnerable to instabilities given its “self adaptive nature”. In addition, NMPC algorithm also provides a control strategy (i.e. substrate mixture sequence of inputs) to achieve the optimal biogas production.

## 6 Conclusion

The results accomplished in this thesis demonstrate that an advanced control system technique such as Nonlinear Model Predictive Control can be successfully introduced to optimally control full-scale biogas plants. This approach reveals to be a feasible solution for a field area that has an increasing demand for applications capable of delivering superior cost-effective performance.

The proposed NMPC algorithm was systematically and extensively tested to assess its performance and reliability. Tests results have shown that in order to achieve plant's steady state in less simulation time, a fine tuning of the algorithm's parameters is required. However, similar optimization results can be accomplished without a fine tuning if longer simulation times are given.

Furthermore, the obtained results show that the employment of different optimization methods (e.g. PSO, CMAES, etc.) in the NMPC algorithm can accomplish similar optimization results. In most cases, the best outcome is achieved when "prediction horizon" and "change value" parameters have higher values.

In further tests, the NMPC algorithm has proven to be reliable and effective to work in a wide range of biogas plant's scenarios (i.e. reactor's operational condition). In fact, it also proved to be reliable and effective by reproducing similar results when a fixed parameter configuration is submitted.

Additionally, a further parameter was created to avoid unnecessary simulation runs by the NMPC algorithm. This parameter allows the algorithm to evaluate the current state of the optimization and take action if there was no actual improvement in the NMPC optimization; for example, by forcing a large step response. This parameter is denominated "fitness trigger" and has shown to be quite useful for NMPC optimizations that were misconfigured.

Moreover, in order to thoroughly assess the efficiency of the proposed NMPC algorithm, a last experiment was performed. In this experiment, the NMPC optimization results were compared to the previous approach utilized to optimally control the original biogas plant. This approach consists of an open-loop control technique, which tries to find optimal and constant substrate mixtures for long-term optimal steady-state operation of full-scale biogas plants by employing powerful optimization tools (Wolf, 2009).

By comparing these two techniques (i.e. closed-loop control (NMPC) and open-loop control) it is evident that the NMPC closed-loop control is more reliable and less vulnerable to instabilities. Although the open-loop control yields very good results it might provoke an overshoot that could lead the system to instability and, consequently, cause a total anaerobic digestion failure.

In general, the proposed NMPC algorithm achieved the goal of providing a suitable closed-loop control of full-scale biogas plants for eco-friendly energy production. Therefore, the encouraging obtained results in this thesis have indicated that the proposed NMPC algorithm is recommended to be further implemented at the real biogas plant.

It is worth highlighting that a well-defined cost function is a key factor for an effective NMPC optimization. Inherently, this function considers economical and environmental characteristics relative to the system's process.

In this manner, this thesis commences a new trend by applying NMPC into Anaerobic Digestion Model No1 (ADM1), which is an area that is yet to be explored. As a matter of fact, no publications have been found combining these two subjects. However, considering that MPC and NMPC were developed to control complex and multi-variable systems, NMPC reveals to be very promising for ADM1 applications.

As for continuing this thesis research work, it is suggested to start by employing a wider variety of substrate mixtures for the modeled biogas plant as well as different biogas plants configurations. Another aspect to be further addressed in the proposed NMPC algorithm are issues of NMPC stability and required computing times. In addition, the possibility of introducing “initial populations” for the optimization methods utilized by the NMPC algorithm is still an open issue, which could significantly improve computational times and the overall optimization.

Furthermore, a new approach for the NMPC stepwise control might be employed to utilize a sampling time that is independent on the “control horizon time”, i.e.,  $\frac{T_C}{\delta}$ . At the moment, the sampling time is equivalent to the “control horizon time”  $T_C = \delta$ .

Finally, the online NMPC implementation at the real biogas plant would require, in a first moment, the evaluation of the available control and measurement systems (e.g. precision of the monitoring systems). On the other hand, a computational system will be required considering the complexity of an NMPC controller. One probable solution is the employment of a Windows Embedded Controller running the MATLAB’s application in combination with the estimator developed by Gaida (Gaida et al., 2011). Moreover, the hardware of the NMPC controller must ensure fast processing times in accordance to the controlled system’s requirements.

## Bibliography

- [1] Auger, A. & Hansen, N., 2005. A Restart CMA Evolution Strategy With Increasing Population Size. In *Proceedings of the IEEE Congress on Evolutionary Computation.*, 2005. IEEE.
- [2] Bastone, D.J. et al., 2002. *Anaerobic Digestion Model no1 (ADM1)*. London: IWA Publishing.
- [3] Batstone, D.J. et al., 2002. The IWA Anaerobic Digestion Model No 1 (ADM1). *Water Science and Technology*, Vol 45(10), p.65–73.
- [4] BioGeoPerm, 2008. *dancehammer*. [Online] Available at: [http://www.dancehammer.com/bgp/anaerobic\\_digestion.html](http://www.dancehammer.com/bgp/anaerobic_digestion.html) [Accessed 24 January 2011].
- [5] Birge, B., 2006. *Particle Swarm Optimization Toolbox*. [Online] Available at: <http://www.mathworks.com/matlabcentral/fileexchange/7506-particle-swarm-optimization-toolbox> [Accessed 07 February 2011].
- [6] Camacho, Eduardo, Bordons & Carlos, 2004. *Model predictive control*. 2nd ed. London: Springer.
- [7] Chipperfield, A.J. & Fleming, P.J., 1995. Digest No. 1995/014 *The MATLAB Genetic Algorithm Toolbox*. IEE Colloquium on Applied Control Techniques Using MATLAB. Sheffield: University of Sheffield.
- [8] Clisso, M., 2010. *Water/Wastewater Distance Learning Website*. [Online] Available at: <http://water.me.vccs.edu/courses/env108/anaerobic.htm> [Accessed 20 January 2011].
- [9] Findeisen, R. & Allgöwer, F., 2002. *An Introduction to Nonlinear Model Predictive Control*. Technical Report. 70550 Stuttgart, Germany: Institute for Systems Theory in Engineering, University of Stuttgart University of Stuttgart.
- [10] Findeisen, R., Imsland, L., Allgöwer, F. & Foss, B.A., 2003. State and Output Feedback Nonlinear Model Predictive Control: An Overview. *European Journal of Control*, pp.179-95.
- [11] Fischer, S. & Leinen, J., 2010. *Course Corrections for Cancún - The European Union and International Climate Politics*. International Policy Analysis. Berlin: Friedrich-Ebert-Stiftung Friedrich-Ebert-Stiftung.
- [12] Gaida, D. et al., 2011. State Estimation for Anaerobic Digesters using the ADM1 (in review). *International IWA-Symposium on Anaerobic Digestion of Solids Waste and Energy Crops*.

- [13] Hansen, N., 2007. *Covariance Matrix Adaptation Evolution Strategy Toolbox*. [Online] (2.55) Available at: [http://www.lri.fr/~hansen/cmaes\\_inmatlab.html](http://www.lri.fr/~hansen/cmaes_inmatlab.html) [Accessed 7 February 2011].
- [14] Hansen, N.N.S.P., Guzzella, L. & Koumoutsakos, P., 2009. A Method for Handling Uncertainty in Evolutionary Optimization With an Application to Feedback Control of Combustion. *IEEE Transactions on Evolutionary Computation*, 13(I), pp.180-97.
- [15] Hartmann, H. & Ahring, B.K., 2010. *The Environmental Microbiology/Biotechnology Research Group*. Technical. DK - 2800 Lyngby, Denmark: Technical University of Denmark Technical University of Denmark.
- [16] Hoffmann, S., Weiand, S. & Scheuring, R., 2005. *Model Predictive Control mit MATLAB*.
- [17] Jaimuokha, I., 2005. *Imperial College London*. [Online] Available at: <http://www3.imperial.ac.uk/portal/pls/portallive/docs/1/50918.PDF> [Accessed 25 January 2011].
- [18] Jia, L., Li, L., Gong, W. & Huang, L., 2010. Hybrid Differential Evolution for Global Numerical Optimization. In Yu, J. et al., eds. *5th International Conference, RSCT 2010, Beijing, China, October 15-17, 2010*. Beijing, 2010. Springer Berlin / Heidelberg.
- [19] Kangmin, L. & Ho, M.-W., 2006. *Institute of Science in Society*. [Online] Available at: <http://www.i-sis.org.uk/BiogasChina.php> [Accessed 2011 January 20].
- [20] Kenney, C., 2010. *wiseGEEK*. [Online] Available at: <http://www.wisegeek.com/what-is-a-biogas-plant.htm> [Accessed 24 January 2011].
- [21] Kouvaritakis, B. & Cannon, M., 2001. *Nonlinear Predictive Control: theory and practice*. The Institution of Engineering and Technology.
- [22] Maciejowski & Marian, J., 2002. *Predictive control with constraints*. London: Pearson Education.
- [23] Magni, L., Raimondo, D.M. & Allgöwer, F., 2009. *Nonlinear Model Predictive Control: Towards New Challenging Applications*. Springer-Verlag Berlin Heidelberg.
- [24] MathWorks, 2011. *The MathWorks, Inc.* [Online] Available at: <http://www.mathworks.com/products/global-optimization/description4.html> [Accessed 27 January 2011].
- [25] MOBIO final report, 2010. government-funded by AiF, no. KA0607901WD8 *Abschlussbericht Projekt MOBIO*. Technical Report. Cologne University of Applied Sciences & PlanET GmbH.

- [26] Naskeo Environnement, 2009. *Biogas Renewable Energy*. [Online] Available at: [http://www.biogas-renewable-energy.info/biogas\\_composition.html](http://www.biogas-renewable-energy.info/biogas_composition.html) [Accessed 17 January 2011].
- [27] Nedjah, N., Abraham, A. & Macedo Mourelle, L.d., 2006. *Genetic Systems Programming*. 1st ed. Netherlands: Springer.
- [28] Pedersen, M.E.H., 2010. HL1002 *Good Parameters for Differential Evolution*. Technical Report. Hvass Laboratories.
- [29] Pedersen, M.E.H., 2010. HL1001 *Optimization, Good Parameters for Particle Swarm*. Technical Report. Hvass Laboratories.
- [30] Poli, R., 2007. 1744-8050 *An Analysis of Publications on Particle Swarm Optimisation Applications*. Technical Report. Essex: Department of Computer Science Unyversity of Essex.
- [31] Poli, R., Kennedy, J. & Blackwell, T., 2007. Particle swarm optimizatio An overview. *Springer Science + Business Media*, 1, p.33–57.
- [32] Price, K. & Storn, R., 2005. *Differential Evolution Toolbox*. [Online] Available at: <http://www.icsi.berkeley.edu/~storn/code.html#matl> [Accessed 7 February 2011].
- [33] Renewable Energy Association, 2009. *Renewable Energy Association*. [Online] Available at: <http://www.r-e-a.net/biofuels/biogas/anaerobic-digestion/benefits-of-ad> [Accessed 19 January 2011].
- [34] Rossiter, J.A., 2004. *Model-Based Predictive Control: A Practical Approach*. CRC Press.
- [35] Sprinkle, J., Eklund, J.M. & Sastry, S.S., 2004. Toward Design Parameterization Support for Model Predictive Control. *IEEE 4th International Conference on Intelligent Systems Design and Application*.
- [36] Tricaud, C. & Chen, Y., 2008. Linear and Nonlinear Model Predictive Control Using A General Purpose Optimal Control Problem Solver RIOTS\_95. *2008 Chinese Control and Decision Conference (CCDC 2008)*, pp.1552-57.
- [37] Wolf, C., 2009. Biogas Plant Control and Optimization Using Computational Intelligence Methods. *Oldenbourg Wissenschaftsverlag*, (DOI 10.1524/auto.2009.0809), pp.638-49.
- [38] Wolf, C., 2010. *Graphic on Anaerobic digestion diagram*. Thehnical report Anaerobic Digestion. Gummersbach: Cologne University of Applied Sciences.

# Appendix A

The tables below present the simulation results obtained by the NMPC optimization of the Sunderhook biogas plant. Each table presents how the fitness function value evolved according to different prediction and control horizon simulation times and a fixed step size.

**Table A.1: Control Horizon vs. Prediction Horizon Tests, Step size: 0.01.**

Prediction Horizon		50	100	150
Control Horizon				
3		-0.4804	-0.4820	-0.4831
7		-0.4436	-0.445	-0.4441
14		<b>-0.4146</b>	-0.4155	-0.4162
21		-0.4017	-0.4030	-0.4027

**Table A.2: Control Horizon vs. Prediction Horizon Tests, Step size: 0.025.**

Prediction Horizon		50	100	150
Control Horizon				
3		-0.4828	-0.4841	-0.4843
7		-0.4798	-0.4828	-0.4830
14		<b>-0.4675</b>	-0.4638	-0.4679
21		-0.4330	-0.4319	-0.4343

**Table A.3: Control Horizon vs. Prediction Horizon Tests, Step size: 0.05.**

Prediction Horizon		50	100	150
Control Horizon				
3		-0.4822	-0.4843	-0.4841
7		<b>-0.4847</b>	-0.4832	-0.4837
14		-0.4835	-0.4835	-0.4839
21		-0.4807	-0.4831	-0.4786

# Appendix B

The tables below present the simulation results obtained by the NMPC optimization of the Sunderhook biogas plant. Each table presents how the fitness function value evolved according to different optimization methods and the different configurations on their “population size” and “number of generations”.

**Table B.1: CMAES optimization method vs. number of generations and population size.**

Population Size \ N° Generations	4	6
Population Size	4	6
6	-0.4444	-0.4441
8	-0.4447	-0.4456
10	-0.4456	-0.4468

**Table B.2: DE optimization method vs. number of generations and population size.**

Population Size \ N° Generations	4	6
Population Size	4	6
6	-0.4420	-0.4457
8	-0.4432	-0.4460
10	-0.4442	-0.4472

**Table B.3: PSO optimization method vs. number of generations and population size.**

Population Size \ N° Generations	4	6
Population Size	4	6
6	-0.4467	-0.4469
8	-0.4480	-0.4482
10	-0.4477	-0.4484

**Table B.4: NMPC optimization - Substrate mixture initial state.**

Substrate name	Initial state n°1	Maximum substrate inlet [m <sup>3</sup> /d]	Minimum substrate inlet [m <sup>3</sup> /d]
	[m <sup>3</sup> /d]		
Maize	30	40	20
Silo seepage	1.5	3	1
Manure	15	30	10
Manure solids	3	5	0
Recirculation b/t fermenters	40	40	40

# Appendix C

The tables below present the simulation results obtained by the NMPC optimization of the Sunderhook biogas plant with or without the fitness trigger option. Each table presents how the fitness function value evolved according to different prediction and control horizon simulation times; and also, the fitness trigger option.

**Table C.1: NMPC optimization & Fitness trigger OFF.**

Prediction Horizon		50	100	150
Control Horizon				
3		-0.4804	-0.4820	-0.4831
7		-0.4436	-0.445	-0.4441
14		-0.4146	-0.4155	-0.4162
21		-0.4017	-0.4030	-0.4027

**Table C.2: Control NMPC optimization & Fitness trigger ON.**

Prediction Horizon		50	100	150
Control Horizon				
3		-0.4836	-0.4821	-0.4824
7		-0.4824	-0.4826	-0.4834
14		-0.4346	-0.4339	-0.4300
21		-0.40917	-0.4098	-0.4079

**Table C.3: Absolute error [%] of NMPC optimization with fitness trigger.**

Prediction Horizon		50	100	150
Control Horizon				
3		-0.66	-0.02	0.14
7		-8.04	-7.62	-8.12
14		-4.6	-4.24	-3.21
21		-1.82	-1.67	-1.26

**Table C.4: NMPC optimization & Fitness trigger evaluation - Substrate mixture initial state.**

Substrate name	Initial state n°1	Maximum substrate	Minimum substrate
	[m <sup>3</sup> /d]	inlet [m <sup>3</sup> /d]	inlet [m <sup>3</sup> /d]
Maize	30	40	20
Silo seepage	1.5	3	1
Manure	15	30	10
Manure solids	3	5	0
Recirculation b/t fermenters	40	40	40

# Appendix D

The tables below present the NMPC optimization settings and the simulation results obtained by the NMPC optimization of the Sunderhook biogas plant with regard to the NMPC algorithm reliability.

**Table D.1: Reliability assessment error of NMPC optimization.**

Substrate name	Fitness percentage error	Cost benefit absolute error
Test n° 1	0.19 %	-3 €d
Test n° 2	0.04 %	-1 €d
Test n° 3	0.52 %	-11 €d
Test n° 4	0.04 %	+1 €d
Test n° 5	0.08 %	-1 €d
Test n° 6	0.25 %	-1 €d
Test n° 7	0.49 %	-10 €d

**Table D.2: NMPC optimization tool settings for reliability assessment.**

NMPC parameter name	NMPC parameter value	Manipulated variable
Plant model	Sunderhook	
Optimization method	CMAES	
Population size	8	
Number of generations	4	
Prediction horizon time [d]	50	
Control horizon time [d]	7	
Change type	Percentual [%]	
Change value	5	
Number of iterations	15	
Fitness trigger	OFF	

**Table D.3: NMPC Reliability assessment - Substrate mixture initial state.**

Substrate name	Initial state n°1	Maximum substrate	Minimum substrate
	[m <sup>3</sup> /d]	inlet [m <sup>3</sup> /d]	inlet [m <sup>3</sup> /d]
Maize	30	40	20
Silo seepage	1.5	3	1
Manure	15	30	10
Manure solids	3	5	0
Recirculation b/t fermenters	40	40	40